

**THE DEGREE OF DEACETYLATION AND
THE MOLECULAR WEIGHT OF CHITOSAN
AFFECTING OSTEOLASTIC (MC3T3-E1) PHENOTYPES**

WIROJ SUPHASIRIROJ

**A THESIS SUBMITTED IN PARTIAL FULFILLMENT
OF THE REQUIREMENTS FOR
THE DEGREE OF MASTER OF SCIENCE (PERIODONTICS)
FACULTY OF GRADUATE STUDIES
MAHIDOL UNIVERSITY
2007**

COPYRIGHT OF MAHIDOL UNIVERSITY

Thesis

Entitled

**THE DEGREE OF DEACETYLATION AND
THE MOLECULAR WEIGHT OF CHITOSAN
AFFECTING OSTEOLASTIC (MC3T3-E1) PHENOTYPES**

.....
Mr. Wiroj Suphasiriroj
Candidate

.....
Assoc.Prof. Pusadee Yotnuengnit
D.D.S., Grad. Dip. in Clin. Sc.
(Periodontics), M.S.,
Cert. in Periodontics,
Dip. Thai Board of Periodontology
Major-Advisor

.....
Assoc.Prof. Rudee Surarit
B.Sc., M.S. (Biochemistry),
Ph.D. (Oral Biology)
Co-Advisor

.....
Dr. Rath Pichyangkura
B.Sc. (Biochemistry),
Ph.D. (Biochemistry)
Co-Advisor

.....
Prof.M.R. Jisnuson Svasti, Ph.D.
Dean
Faculty of Graduate Studies

.....
Assoc.Prof. Penpan Laohapand
B.Sc., D.D.S., Grad. Dip. in Clin. Sc.
(Periodontics), M.D.S. (Dental Science),
Dip. Thai Board of Periodontology
Chair
Master of Science Programme in
Periodontics, Faculty of Dentistry

Thesis
Entitled
**THE DEGREE OF DEACETYLATION AND
THE MOLECULAR WEIGHT OF CHITOSAN
AFFECTING OSTEOLASTIC (MC3T3-E1) PHENOTYPES**

was submitted to the Faculty of Graduate Studies, Mahidol University
for the degree of Master of Science (Periodontics)

on
March 26th, 2007

.....
Mr. Wiroj Suphasiriroj
Candidate

.....
Asst.Prof. Thitiwan Buranawichetkul
D.D.S., M.S., Cert. in Periodontics,
Dip. Amer. Board of Periodontology
Chair

.....
Assoc.Prof. Pusadee Yotnuengnit,
D.D.S., Grad. Dip. in Clin. Sc.
(Periodontics), M.S., Cert. in Periodontics,
Dip. Thai Board of Periodontology
Member

.....
Assoc.Prof. Rudee Surarit,
B.Sc.,
M.S. (Biochemistry),
Ph.D. (Oral Biology)
Member

.....
Dr. Rath Pichyangkura,
B.Sc. (Biochemistry),
Ph.D. (Biochemistry)
Member

.....
Asst.Prof. Suphot Tamsailom,
D.D.S., M.S. (Periodontics),
Dip. Thai Board of Periodontology
Member

.....
Prof.M.R. Jisnuson Svasti, Ph.D.
Dean
Faculty of Graduate Studies
Mahidol University

.....
Asst.Prof. Theeralaksna Suddhasthira,
B.Sc., D.D.S. (1st Class Hons.), Grad. Dip.
in Clin. Sc. (Oral surgery), Cert. in
Oral&Maxillofacial Surgery, Dip. Amer.
Board of Oral&Maxillofacial Surgery,
Ph.D. (Biomedical Science), Dip. Thai
Board of Oral&Maxillofacial Surgery
Dean
Faculty of Dentistry, Mahidol University

ACKNOWLEDGEMENT

The successful of this thesis can be attributed to the extensive support and assistance from my major advisor, Assoc.Prof. Pusadee Yotnuengnit, and my co-advisors, Assoc.Prof. Rudee Surarit and Dr. Rath Pichyangkura. I deeply thank them for their valuable advice and guidance in this research.

I would like to thank Asst.Prof. Suphot Tamsailom, member of Department of Periodontics, Faculty of Dentistry, Chulalongkorn University, for his kindness in examining the research instruments and providing suggestions for improvement, and who was the external examiner of the thesis defense.

I would like to thank Asst.Prof. Thitiwan Buranawichetkul for her kindness in examining the research instruments and providing suggestions for improvement.

I would like to thank all staffs of Research Unit, Faculty of Dentistry, Mahidol University for their advice and technical assistance.

I would like to thank all staffs of Center of NanoImaging, Faculty of Science, Mahidol University for technical assistance in scanning electron image processing.

I am grateful to all the lecturers of the Department of Oral Medicine for the knowledge in periodontology.

I am particularly indebted to the Faculty of Graduate Studies, Mahidol University for the grant which enable me to undertake this study.

Finally, I am grateful to my family for their financial support, entirely care, and love. For usefulness of this thesis, I dedicate to my father, my mother and all teachers, who taught me in childhood.

Wiroj Suphasiriroj

THE DEGREE OF DEACETYLATION AND THE MOLECULAR WEIGHT OF CHITOSAN AFFECTING OSTEOBLASTIC (MC3T3-E1) PHENOTYPES

WIROJ SUPHASIRIROJ 4836241 DTPE/M

M.Sc. (PERIODONTICS)

THESIS ADVISORS : PUSADEE YOTNUENGKIT, DIP. THAI BOARD OF PERIODONTOLOGY, RUDEE SURARIT, Ph.D.(ORAL BIOLOGY), RATH PICHYANGKURA, Ph.D.(BIOCHEMISTRY)

ABSTRACT

Chitosan, a versatile biopolymer, has good potential for utilization in periodontal tissue regeneration. However, the degree of deacetylation (DD) and the molecular weight (MW) of chitosan relating to biological properties have not previously been clearly elucidated. The aim of this study was to investigate the effects of the degree of deacetylation and molecular weight of chitosan on osteoblastic (MC3T3-E1) phenotypes. The chitosan, collagen and chitosan-collagen composite scaffolds were fabricated by freeze drying technique. Microstructure of scaffolds and growth of osteoblasts on the scaffolds were examined using scanning electron microscopes. Scanning electron images were analyzed using ImagePro[®] Plus software program to determine the pore size and area fraction of scaffolds. The studies on cell attachment, cell proliferation, alkaline phosphatase (ALP) activity and mineralized nodule formation of osteoblasts were determined according to the different degree of deacetylation and molecular weight of chitosan. The results showed that the microstructure of scaffolds had porosity and pore size ranging from 0 to 50 microns. No statistically significant difference was found on cell attachment but the low DD of chitosan had a statistically significantly ($p < 0.05$) higher proliferative effect and ALP activity than the high DD of chitosan, regardless of molecular weight. Mineralized nodule formation was not found on all test scaffolds. In conclusion, the degree of deacetylation of chitosan is a crucial factor for biological properties so it should be considered in further applications for periodontal tissue regeneration.

KEY WORDS: CHITOSAN/COLLAGEN/SCAFFOLD/DEGREE OF DEACETYLATION/
MOLECULAR WEIGHT

111 pp.

ผลของระดับการกำจัดหมู่อะเซทิลและน้ำหนักโมเลกุลของสารไคโตซานต่อการแสดงออกของ
เซลล์สร้างกระดูกหนู (THE DEGREE OF DEACETYLATION AND THE
MOLECULAR WEIGHT OF CHITOSAN AFFECTING OSTEOBLASTIC
(MC3T3-E1) PHENOTYPES)

วิโรจน์ ศุภศิริโรจน์ 4836241 DTPE/M

วท.ม. (ปริทัศน์วิทยา)

คณะกรรมการควบคุมวิทยานิพนธ์: ผศ.ดร. ชัยพร เนื่องนิสัย, อ.ท. (ปริทัศน์วิทยา), ฤดี สุราฤทธิ, Ph.D.
(Oral biology), รัฐ พิษณุวงกูร, Ph.D. (Biochemistry)

บทคัดย่อ

ไคโตซานเป็นวัสดุชีวภาพที่มีศักยภาพเหมาะสมสำหรับใช้ในการส่งเสริมให้เกิดการงอกใหม่
ของเนื้อเยื่อปริทัศน์ แต่ระดับการกำจัดหมู่อะเซทิลและน้ำหนักโมเลกุลของสารไคโตซานต่อสมบัติ
ทางชีวภาพมีรายงานที่ไม่ชัดเจน การศึกษาวิจัยนี้จึงมุ่งเน้นที่จะศึกษาผลของระดับการกำจัดหมู่อะ
เซทิลและน้ำหนักโมเลกุลของสารไคโตซานต่อการแสดงออกของเซลล์สร้างกระดูกหนู โดยโครง
เลี้ยงเซลล์ชนิดไคโตซาน คอลลาเจน และ ไคโตซาน-คอลลาเจนสร้างขึ้นจากวิธีทำแห้งด้วยความ
เย็น ศึกษาลักษณะโครงสร้างของโครงเลี้ยงเซลล์และการเจริญเติบโตของเซลล์สร้างกระดูกบนโครง
เลี้ยงเซลล์ด้วยกล้องจุลทรรศน์อิเล็กตรอนชนิดส่องกราด วิเคราะห์ภาพที่ได้ด้วยโปรแกรม
ImagePro® Plus เพื่อศึกษาขนาดรูพรุนและสัดส่วนพื้นที่ของเนื้อสารที่มีอยู่ในโครงเลี้ยงเซลล์
ศึกษาการยึดติด การงอกขยาย การแสดงค่าเอนไซม์แอลคาไลน์ฟอสฟาเตสและการสะสมก้อนแร่
ธาตุของเซลล์สร้างกระดูกต่อระดับการกำจัดหมู่อะเซทิลและน้ำหนักโมเลกุลของสารไคโตซานที่
แตกต่างกัน ผลการศึกษาพบว่าลักษณะโครงสร้างของโครงเลี้ยงเซลล์มีความเป็นรูพรุนและมีขนาดรู
พรุน 0-50 ไมครอน สำหรับการยึดติดของเซลล์ไม่พบความแตกต่างอย่างมีนัยสำคัญทางสถิติ แต่
พบว่าระดับการกำจัดหมู่อะเซทิลที่ต่ำของสารไคโตซานมีผลต่อการงอกขยายและการแสดงค่า
เอนไซม์แอลคาไลน์ฟอสฟาเตสสูงกว่าระดับการกำจัดหมู่อะเซทิลที่สูงอย่างมีนัยสำคัญทางสถิติ
($p < 0.05$) โดยไม่มีผลจากน้ำหนักโมเลกุล และไม่พบการสะสมก้อนแร่ธาตุบนโครงเลี้ยงเซลล์ที่
ทดสอบ สรุปได้ว่าระดับการกำจัดหมู่อะเซทิลของสารไคโตซานเป็นปัจจัยที่มีผลต่อสมบัติทาง
ชีวภาพ ดังนั้นควรคำนึงถึงปัจจัยดังกล่าวเมื่อนำสารไคโตซานไปประยุกต์ใช้ในการส่งเสริมให้เกิด
การงอกใหม่ของเนื้อเยื่อปริทัศน์

CONTENT

	PAGE
ACKNOWLEDGEMENT	iii
ABSTRACT	iv
LIST OF TABLES	viii
LIST OF FIGURES	ix
LIST OF ABBREVIATIONS	xii
CHAPTER	
I INTRODUCTION	1
II OBJECTIVES AND EXPECTED BENEFITS	4
III LITERATURE REVIEWS	6
IV MATERIALS AND METHODS	34
1. Preparation of chitosan solution	35
2. Preparation of collagen solution	36
3. Fabrication and sterilization of chitosan, collagen and chitosan-collagen scaffolds	36
4. Characterization of chitosan, collagen and chitosan- collagen scaffolds	37
5. Cell cultures	38
6. Determination of cell attachment and cell proliferation	38
7. Determination of alkaline phosphatase activity	39
8. Determination of cell morphology, behavior and mineralized nodule formation	40
9. Data collection and statistic analysis	41
V RESULTS	42
1. Chitosan, collagen and chitosan-collagen scaffolds characterization	42
2. The effect of chitosan, collagen and chitosan-collagen scaffolds on MC3T3-E1 cell attachment and proliferation	53

CONTENT (CON'T)

	PAGE
3. The effect of collagen and chitosan-collagen scaffolds on alkaline phosphatase activity	63
4. The effect of collagen and chitosan-collagen scaffolds on MC3T3-E1 cell morphology, behavior and mineralized nodule formation	67
VI DISCUSSION	77
VII CONCLUSION	84
REFERENCES	85
APPENDIX	101
BIOGRAPHY	111

LIST OF TABLES

TABLE	PAGE
1. Some types of collagen and their properties	12
2. Mechanical properties of human tissues	17
3. Scaffold materials for periodontal tissue regeneration	21
4. Alloplastic materials	24
5. Chitosan scaffolds characterization, frozen in -80°C refrigerator	51
6. Chitosan scaffolds characterization, frozen in -20°C refrigerator	51
7. Collagen scaffolds characterization, frozen in -20°C refrigerator	52
8. Chitosan-collagen scaffolds characterization, frozen in -20°C refrigerator	52
9. The absorbance of the MTT formazan formation after MC3T3-E1 cells attachment	54
10. The absorbance of the MTT formazan formation after MC3T3-E1 cells proliferation	56
11. The alkaline phosphatase activity of MC3T3-E1 cells on test scaffolds and control	64

LIST OF FIGURES

FIGURE	PAGE
1. The temporal gene expression of gene characteristic of osteoblast differentiation	8
2. Major types of glycosaminoglycans	10
3. Structure of collagen	11
4. Structures of cellulose, chitin and chitosan	26
5. The roles of lysozyme and N-acetyl-beta-D-glucosaminidase	31
6. Diagram of experimental research	34
7. SEM images of chitosan scaffolds, frozen in -80°C refrigerator (x 300).	44
8. SEM images of chitosan scaffolds, frozen in -20°C refrigerator (x 300).	46
9. SEM images of collagen scaffolds, frozen in -20°C refrigerator (x 300).	48
10. SEM images of chitosan-collagen scaffolds, frozen in -20°C refrigerator (x 300).	49
11. SEM image analysis by ImagePro [®] Plus software program	50
12. The absorbance of MTT formazan formation at 5 and 24 hours for cell attachment assay.	54
13. The absorbance of MTT formazan formation on day 1, 3, 5, 7, 10, and 14 for cell proliferation assay.	57
14. The absorbance of MTT formazan formation on day 1, 3, 5, 7, 10, and 14 for cell proliferation assay (Bar chart).	58
15. The absorbance of MTT formazan formation on day 1 for cell proliferation assay.	59
16. The absorbance of MTT formazan formation on day 3 for cell proliferation assay.	59

LIST OF FIGURES (CON'T)

FIGURE	PAGE
17. The absorbance of MTT formazan formation on day 5 for cell proliferation assay.	60
18. The absorbance of MTT formazan formation on day 7 for cell proliferation assay.	60
19. The absorbance of MTT formazan formation on day 10 for cell proliferation assay.	61
20. The absorbance of MTT formazan formation on day 14 for cell proliferation assay.	61
21. The effect of collagen and chitosan-collagen scaffolds on alkaline phosphatase activity of MC3T3-E1 cells	65
22. The effect of collagen and chitosan-collagen scaffolds on alkaline phosphatase activity of MC3T3-E1 cells (Bar chart)	66
23. SEM images of MC3T3-E1 cells on cover slips (control) (x 300, x 500).	69
24. SEM images of MC3T3-E1 cells on collagen scaffolds (x 300, x 500).	70
25. SEM images of MC3T3-E1 cells on 80LMW-C scaffolds (x 300, x 500).	71
26. SEM images of MC3T3-E1 cells on 80HMW-C scaffolds (x 300, x 500).	72
27. SEM images of MC3T3-E1 cells on 50LMW-C scaffolds (x 300, x 500).	73
28. SEM images of MC3T3-E1 cells on 50HMW-C scaffolds (x 300, x 500).	74
29. Mineralized nodule formation on cover slip (control)	75
30. Images of control and test scaffolds after staining with alizarin red-S	76
31. Standard curve of p-nitrophenol on day 4 and 6 (1 st experiment)	101

LIST OF FIGURES (CON'T)

FIGURE	PAGE
32. Standard curve of total protein on day 4 and 6 (1 st experiment)	101
33. Standard curve of p-nitrophenol on day 10 and 14 (1 st experiment)	102
34. Standard curve of total protein on day 10 and 14 (1 st experiment)	102
35. Standard curve of p-nitrophenol on day 18 and 22 (1 st experiment)	103
36. Standard curve of total protein on day 18 and 22 (1 st experiment)	103
37. Standard curve of p-nitrophenol on day 26 (1 st experiment)	104
38. Standard curve of total protein on day 26 (1 st experiment)	104
39. Standard curve of p-nitrophenol on day 4 and 6 (2 nd experiment)	105
40. Standard curve of total protein on day 4 and 6 (2 nd experiment)	105
41. Standard curve of p-nitrophenol on day 10 and 14 (2 nd experiment)	106
42. Standard curve of total protein on day 10 and 14 (2 nd experiment)	106
43. Standard curve of total protein on day 18 and 22 (2 nd experiment)	107
44. Standard curve of total protein on day 18 and 22 (2 nd experiment)	107
45. Standard curve of total protein on day 26 (2 nd experiment)	108
46. Standard curve of total protein on day 26 (2 nd experiment)	108
47. SEM images of chitosan-collagen scaffolds with different ratio between chitosan and collagen.	109

LIST OF ABBREVIATIONS

ACS	=	absorbable collagen sponge
AR-S	=	alizarin red-S
ALP	=	alkaline phosphatase
α	=	alpha
α -MEM	=	alpha-minimum essential medium
β	=	beta
$^{\circ}\text{C}$	=	degree of celcius
BMPs	=	bone morphogenic proteins
Da	=	dalton
DD	=	degree of deacetylation
DDI	=	distilled, deionized water
DFDBA	=	decalcified freeze dried bone allograft
DMSO	=	dimethyl sulfoxide
ECM	=	extracellular matrix
FDBA	=	freeze dried bone allograft
GAGs	=	glycosaminoglycans
γ	=	gamma
GPa	=	gigapascal
Gly	=	glycine
HA	=	hydroxyapatite
HCL	=	hydrochloric acid
HMW	=	high molecular weight
IBP	=	internal bubbling process
kDa	=	kilodalton
kPa	=	kilopascal
LMW	=	low molecular weight
mg./ml.	=	milligram per milliliter

LIST OF ABBREVIATIONS (CON'T)

min.	=	minute
M	=	molar
MPa	=	megapascal
NA	=	no available data
NaOH	=	sodium hydroxide
nm.	=	nanometer
nmol	=	nanomole
OD ₅₄₀	=	optical density values at 540 nanometers
OPN	=	osteopontin
PBS	=	phosphate buffer saline
PDGFs	=	platelet derived growth factors
PDLCS	=	periodontal ligament cells
PEC	=	polyelectrolyte complex
PGA	=	polyglycolic acid
PLA	=	polylactic acid
PLGA	=	polylactic-polyglycolic acid
PMN	=	polymorphonuclear
PMSF	=	phenylmethyl-sulfonyl fluoride
PNAC	=	partially N-acetyl chitosan
PNP	=	para-nitrophenol
PNPP	=	para-nitrophenyl phosphate
SEM	=	scanning electron microscope
TCP	=	tricalciumphosphate
TGF- β	=	transforming growth factor-beta
Ti	=	titanium
TNF	=	tumor necrosis factor
μ m	=	micron

CHAPTER I

INTRODUCTION

Periodontitis is inflammation that extends to periodontal structures beyond the gingiva, producing a loss of connective tissue attachment of the teeth (1) and accounting for the loss of the most teeth in adult (2). The development of periodontitis is the inflammation of the periodontal tissue in response to microorganisms in dental biofilms (3). Specific periodontal pathogens (4-5) may exert pathogenic effect directly by causing tissue destruction itself or indirectly by stimulating and modulating the host response (6-11). When periodontal supporting tissues were destroyed, periodontal pockets and different types of bone deformities (*e.g.*, horizontal and vertical bone loss, osseous crater, furcation involvement, etc.) were formed (12-17).

Treatment modalities available in periodontics can be broadly classified into either surgical or non-surgical approach. Purpose and goal of periodontal therapy is to clean and smooth the root, to eliminate plaque retentive area and inflammation, to create the physiologic form, and to enhance the regeneration of periodontal tissues.

Last decades, periodontal research has attempted to understand and search the new techniques and new inventive materials for periodontal tissue regeneration, for example, root conditioning agents, osteoinductive and osteoconductive grafting materials, membrane for guided tissue regeneration, and combination of these treatments (18-39). Although these procedures became widely accepted as a clinical procedure, recent clinical evaluation has indicated that the clinical improvements obtained by these procedures are highly variable. In general, existing therapies utilized in an attempt to stimulate periodontal regeneration are limited in both predictability and outcome. Regarding periodontal membranes, many biomaterials (*e.g.*, collagen, polymer such as polylactides or polyglycolides, etc.) were fabricated and utilized in guided tissue regenerative treatment. For grafting materials, numerous therapeutic grafting modalities for restoring periodontal osseous defects have been investigated. Material to be grafted can be obtained from the same person

(autografts), from a different person of the same species (allografts), or from different species (xenografts). Furthermore, many synthetic grafting materials such as calcium sulfate (plaster of paris), calcium phosphate (hydroxyapatite or tricalcium phosphate), or HTR polymer have been tried for restoration of the periodontium (40). The considerations that govern the selection of graft materials include biological acceptability, predictability, clinical feasibility, minimal operative hazard, minimal postoperative sequel and patient acceptance (41). Nevertheless, it is difficult to find a material with all these characteristics. So far, there is no ideal material for periodontal tissue regeneration.

Currently, many researchers and clinicians have the advancement in material sciences and molecular biology named in tissue engineering, including the development of scaffolding devices and the use of regenerative molecules. As a result, tissue engineering becomes an attractive procedure to apply for periodontal tissue regeneration.

Tissue engineering, defined as the reconstruction of living tissues to be used for the replacement of damaged or lost tissue/organs of living organisms, requires an interplay among three components: the implanted and cultured cells that will create the new tissue; a biomaterial to act as a scaffold or matrix to hold the cells; and biological signaling molecules that instruct the cells to form the desired tissue type (42). Ideally, the scaffold should be biodegradable, biocompatible, and highly porous with a high surface area/volume ratio, allowing the transportation of nutrients and metabolites, and permitting cell and tissue ingrowth, as well as serving as a reservoir for bioactive molecules. In periodontology, there are two basic types of scaffolds: naturally derived scaffolds (autografts, allografts and xenografts) and synthetic biomimetic scaffolds (alloplasts and other polymers). A broad range of these scaffolds is available for clinical uses; however, each of materials to be fabricated in scaffolds had both benefits and drawbacks. Many composite materials, therefore, have been considered in recent years, for example, glycosaminoglycans (GAGs)/collagen, hydroxyapatite/collagen, polymer/calcium phosphate composite scaffolds (43). In bone tissue engineering, collagen-based composite is one of the important focuses of research due to the fact that collagen constitutes approximately 95% in bone organic matrix (44). In addition, the field of polysaccharides as biomaterials is increasing interested since

polysaccharides play critical roles in modulating the activities of signaling molecules as well as mediating certain intercellular signaling directly, and can be controllable biological activity and biodegradability (45). Under circumstance, chitosan is a one of attractive polysaccharide biomaterials developing to be scaffolds owing to its versatile properties.

Chitosan, a partially or completely deacetylated chitin, is an abundant natural biopolymer. It has attracted a great interest in pharmacology and medicine as biomaterial because of its biodegradability, biocompatibility, non-toxicity and the wide range of reported positive biological responses and activities. It has been used or proposed in the fabrication of drug delivery devices, in orthopedics, in wound healing, in ophthalmology, in pharmaceuticals, in dentistry, and in the fabrication of scaffolds for tissue engineering (46). Whether solid state or solutions are considered, all the properties of chitosan depend on two fundamental parameters: degree of deacetylation and the molecular weight distribution. Many attentions to the effect of these parameters were reported in literatures; however, the relationship between these parameters and their biological properties has not been clearly elucidated.

The aim of present study, therefore, was to investigate the effects of this versatile biopolymer according to its different degree of deacetylation and molecular weight on osteoblastic (MC3T3-E1) phenotypes in order to be innovate regenerative material utilized in periodontal tissue regeneration and/or further develop in scaffolding for bone tissue engineering.

CHAPTER II

OBJECTIVES AND EXPECTED BENEFITS

Objectives

To gain the understanding of the effects of different degree of deacetylation and molecular weight of chitosan on osteoblasts (MC3T3-E1) in vitro study by

1. Measuring cell attachment and cell proliferation by MTT assay and growth curves.
2. Measuring alkaline phosphatase activity by alkaline phosphatase assay and protein assay.
3. Measuring mineralized nodule formation by mineralization assay and staining with alizarin red S.

Expected benefits

The result of this study would provide:

1. Basic knowledge in biological response of osteoblasts (MC3T3-E1) to different degree of deacetylation and molecular weight of chitosan.
2. Useful data for further development of chitosan to be used in periodontal tissue regeneration.

CHAPTER III

LITERATURE REVIEWS

General aspects of bone biology (47-50)

Bone is a specialized form of connective tissue which is characterized by its rigidity and hardness. Its four main functions are to provide mechanical support, to permit locomotion, to provide protection, and to act as a metabolic reservoir of mineral salts. Bone is composed of cells and intercellular material (bone matrices). Developing and mature bones contain four different types of cells: osteogenic (osteoprogenitor) cells, osteoblasts, osteocytes, and osteoclasts, which concerned with production, maintenance, and modeling of the osteoid.

Osteogenic cells are differentiated and pleuropotential stem cells derived from the connective tissue mesenchyme. They form a population of stem cells that can differentiate into the more specialized bone-forming cells (*e.g.*, osteoblasts and osteocytes). In mature bones, they are found in the external periosteum and in the single layer of the internal endosteum which provide a continuous supply of new osteoblasts for growth, remodeling, and repair of the bones.

Osteoblasts are the differentiated bone-forming cell. Their main function is to synthesize, secrete, and deposit the organic components of new bone matrix called osteoid. Osteoid is a collagenous support tissue of type I collagen embedded in a glycosaminoglycan gel containing specific glycoproteins (*e.g.*, osteocalcin) that strongly bind calcium.

Osteocytes are the mature cells of the bone. It is enclosed by the bone matrix that it had previously laid down as an osteoblast. The osteocytes are responsible for maintaining the bone matrix. They have the capacity to synthesize as well as resorb matrix. Such activities are important in contributing to the homeostasis of blood calcium.

Osteoclasts are large and multinucleated cells that originate from the fusion of the circulating blood monocytes. They are found along the bone surfaces where resorption, remodeling, and repair of bone take place. Their main functions are to resorb bone during remodeling.

The bone matrix consists of two major compartments: organic and inorganic compartments. Approximately 35% of the dry weight of bone is the organic matrix. Type I collagen is the principal component (about 90%) of the organic matrix; the remaining 10% consists of noncollagenous components. The inorganic matrix, also referred to as the mineralized compartment, accounts for about 60-70% of the dry weight of the bone. The hardness and rigidity of bone is due to the presence of mineral salt in the osteoid matrix. This salt is a crystallinity complex of calcium and phosphate hydroxides called hydroxyapatite ($\text{Ca}_{10}(\text{PO}_4)_6(\text{OH})_2$).

For mineralization, both collagen fibrils and ground substance within the matrix can occur and the combined local concentration of Ca^{2+} ions and PO_4^{3-} ions must be above a threshold value. A number of factors operate to bring this about:

1. A glycoprotein (osteocalcin) in osteoid binds extracellular Ca^{2+} ions, leading to a high local concentration.
2. The enzyme alkaline phosphatase, which is abundant in osteoblast, increases local Ca^{2+} and PO_4^{3-} ion concentrations.
3. Osteoblasts produce matrix vesicles, which can accumulate Ca^{2+} and PO_4^{3-} ions, and are rich in the enzyme alkaline phosphatase and pyrophosphatase, both of which can cleave PO_4^{3-} ions from larger molecules.

Bone is a dynamic tissue, being renewed, remodeled, and both in response to mineral needs of the body, mechanical stresses put on the bone, bone thinning during aging and disease, or healing during a fracture or break in the bone under the control of hormonal and physical factors.

The two main patterns of bone can be identified according to the pattern of collagen forming osteoid:

1. Woven bone is characterized by haphazard organization of collagen fibers and is mechanically weak.
2. Lamella bone is characterized by a regular parallel alignment of collagen into sheets (lamella) and is mechanically strong.

Osteoblast proliferation, differentiation, and function (51)

Osteoblasts are the bone cells that form bone. The main secreted product of osteoblasts is type I collagen, but osteoblasts secrete other noncollagenous proteins including osteopontin, osteocalcin, and bone sialoprotein. Osteoblasts form bone by facilitating mineralization but the mechanism by which is not understood. One possibility is that lipid matrix vesicles that bud off of bone cell create a microenvironment where calcium and phosphate are concentrated in a ratio allowing for optimized crystallization. These crystals then align on secreted collagen and form a nucleation site that facilitates subsequent mineralization and hydroxyapatite formation. Another possibility is that mineralization is initiated by components of the collagen molecule in a manner not requiring matrix vesicles. It is also possible that matrix vesicle-dependent and – independent mineralization occur concurrently. As a result, osteoblasts are critically important in mineralization because they both secrete collagen and produce matrix vesicles.

Osteoblastic cells arise from pluripotent mesenchymal progenitor cells. The differentiation pathway taken by the progenitor cells is regulated by tissue specific transcription factors. Once the pluripotent progenitor cells have committed to the osteoblastic lineage, they progress through three developmental stages of differentiation: proliferation, matrix maturation, and mineralization.

In general, type I collagen and histone H4 peak during the proliferation phase and decline thereafter, alkaline phosphatase peaks during the matrix formation phase and decline thereafter, while osteopontin and osteocalcin peak during the mineralization phase (Figure 1). It is important to note that this differentiation sequence may actually be more complicated.

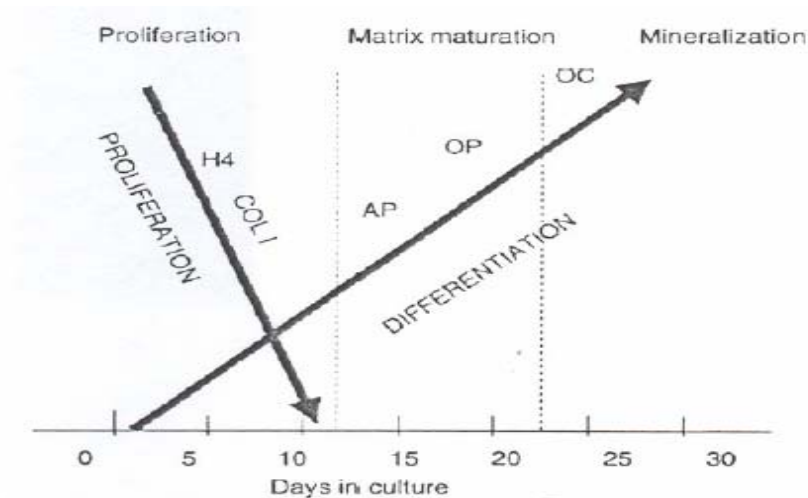


Figure 1 The temporal gene expression of gene characteristic of osteoblasts differentiation (51)

Extracellular matrix (52-53)

Tissues are not made up solely of cells. Many of the cells in tissues of multicellular organisms are embedded in an extracellular matrix consisting of a variety of secreted proteins and polysaccharides that are secreted locally and assembled into an organized meshwork in close association with the surface of the cell that produced them. The extracellular matrix in connective tissue is frequently more plentiful than the cells it surrounds, and it determines the tissue's physical properties. Variations in the relative amounts of the different types of the matrix macromolecules and the way in which they are organized in the extracellular matrix give rise to an amazing diversity of forms, each adapted to the functional requirements of the particular tissue. The matrix can become calcified to form the rock-hard structures of bone or teeth, or it can form the transparent matrix of the cornea, or it can adopt the ropelike organization that gives enormous tensile strength for tendons. In most connective tissues, the matrix macromolecules are secreted largely by cells called fibroblasts. In certain specialized types of connective tissue, such as cartilage and bone, however, they are secreted by cells of the fibroblast family that have more specific names, for example, chondroblasts form cartilage and osteoblasts form bone.

Two main classes of extracellular macromolecules that make up the matrix are glycosaminoglycans (GAGs); polysaccharide chains, which are usually found covalently linked to protein in the form of proteoglycans, and fibrous proteins;

including collagen, elastin, fibronectin, and laminin, which have both structural and adhesive function. The polysaccharide gel resists the compressive forces on the matrix while permits the rapid diffusion of nutrients, metabolites, and hormones between the blood and the tissue cells. The collagen fibers both strengthen and help organize the matrix, and the rubberlike elastin fibers give the matrix resilience. Finally, many matrix proteins help cells attach in the appropriate locations.

Glycosaminoglycans (GAGs) are unbranched polysaccharide chains composed of repeating disaccharide units. One component of the disaccharide is always a derivative of amino sugars either N-acetylglucosamine or N-acetylgalactosamine and another component of the disaccharide is usually an uronic acids *e.g.* glucuronic acid and iduronic acid. With the exception of hyaluronan, these sugars are modified by the addition of sulfate groups. As a result, GAGs are distinguished according to their sugars, the type of linkage between the sugars, and the number and location of sulfate groups: (1) hyaluronan, (2) chondroitin sulfate and dermatan sulfate, (3) keratan sulfate, and (4) heparan sulfate (Figure 2). Because there are sulfate or carboxyl groups on most of their sugars, GAGs are highly negatively charged. They are, thereby, too stiff to fold up into the compact globular structures that polypeptide chains typically form and they are strongly hydrophilic. Moreover, their high density of negative charges attract a cloud of cations, most notably Na^+ , that are osmotically active, causing large amounts of water to be sucked into the matrix. This creates a swelling pressure, or turgor, that enables the matrix to withstand compressive forces (in contrast to collagen fibrils, which resist stretching forces).

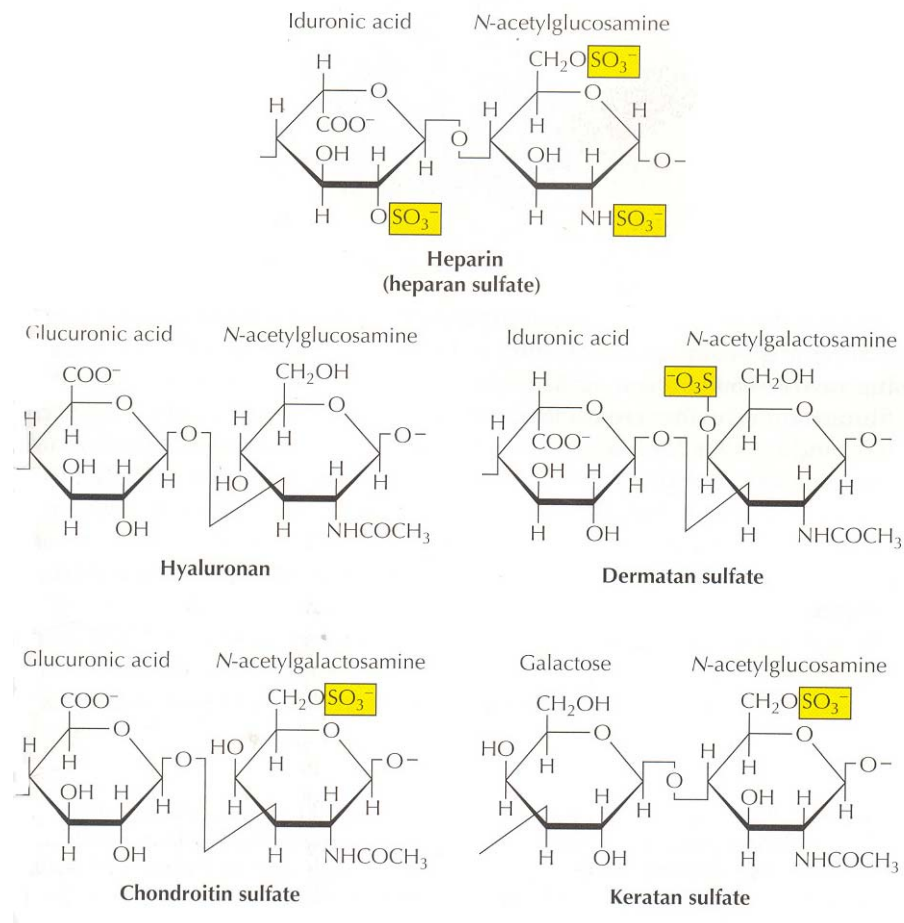
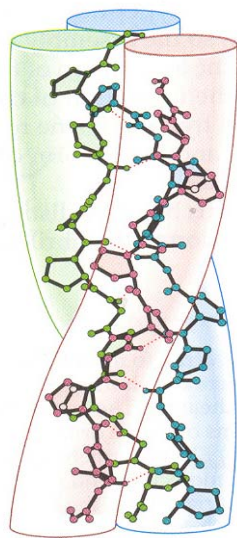


Figure 2 Major types of glycosaminoglycans (52)

The collagen, a family of fibrous proteins of extracellular matrix, is the single most abundant protein in animal tissues. Its primary feature is long, stiff, triple-stranded helical structure, in which three collagen polypeptide chains, called α -chains, are wound around one another in a ropelike superhelix. The triple helix domains of the collagen consist of repeats of the amino acid sequence Gly-X-Y. A glycine (gly), the smallest amino acid, is required in every third position in order that the polypeptide chains can pack tightly together to form the final collagen triple helix. X and Y are any amino acids but they are often proline and hydroxyproline or hydroxylysine, respectively. Because of their ring structure, these amino acids can stabilize the helical conformations of the polypeptide chains (Figure 3).

(A) Collagen triple helix



(B) Amino acid sequence

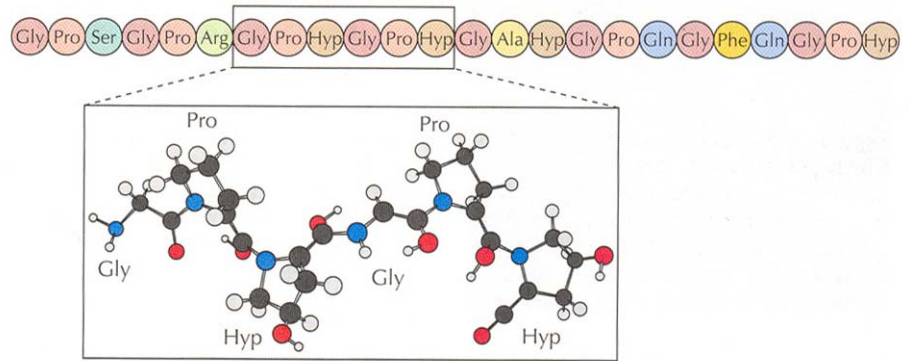


Figure 3 Structure of collagen: (A) Collagen triple helix (B) Amino acid sequence (52)

So far, about 25 types of α -chains and 20 types of collagen have been found (Table 1). The main types of collagen found in connective tissues are types I, II, III, IV, V, XI, type I being the principal collagen of skin and bone. These are the fibrillar collagens, or fibril-forming collagens, with the ropelike structure. After being secreted into the extracellular space, these collagen molecules assemble into the higher-order polymers called collagen fibrils. Collagen types IX and XII are called fibril-associated collagens because they decorate the surface of collagen fibrils. They are thought to link these fibrils to one another and to other components in the extracellular matrix. Types IV and VII are network-forming collagens. Type IV molecules assemble into a feltlike sheet or meshwork that constitutes a major part of mature basal laminae, while type VII molecules form dimers that assemble into specialized structure called anchoring fibrils. Anchoring fibrils help the basal lamina of multilayered epithelia attach to the underlying connective tissue. In addition, there are a number of collagen-like proteins, including type XVII, which has a transmembrane domain and is found in hemidesmosomes, and type XVIII, which is located in basal laminae of blood vessels.

Table 1 Some types of collagen and their properties (53)

	Type	Polymerized form	Tissue distribution
Fibril-forming (Fibrillar)	I	fibril	bone, skin, tendons, ligaments, cornea, internal organs (90% of body collagen) cartilage, intervertebral disc, notochord, vitreous humor of the eye skin, blood vessels, internal organs as for type I as for type II Cartilage
	II	fibril	
	III	fibril	
	V	fibril (with type I)	
	XI	fibril (with type II)	
Fibril-associated	IX	lateral association with some type II fibrils	Tendons, ligaments, some other tissues
	XII	lateral association with some type I fibrils	
Network-forming	IV	sheetlike network	basal lamina
	VII	anchoring fibrils	Beneath stratified squamous epithelia
Transmembrane	XVII	not known	hemidesmosomes
Others	XVIII	not known	basal lamina around blood vessels

Tissue engineering (51, 54)

Tissue engineering is a term originally used to describe construction in the laboratory of a device containing viable cells and biological mediators (*e.g.*, growth factors and adhesins) in a synthetic or biological matrix that could be implant in patients to facilitate regeneration of particular tissue. Recently, the definition has broadened to refer to any attempt to regenerate tissues in the body, whether accomplished in the laboratory or directly in the patient, by adding appropriate biological mediators and matrices.

Tissues are composed of cells, insoluble extracellular matrix (ECM), and soluble molecules that serve as regulators of cell function; therefore, a requirement for tissue regeneration is composed of three necessary components:

1. Cells: It is necessary to increase the number of cells that constitute the tissues as well as reconstruct the structure to support the cells. In the adult, tissues composed of labile cells (*e.g.* epithelial tissue) and stable cells (*e.g.* connective tissue including bone) can regenerate.
2. Scaffolds: The material to be use for fabrication of matrix can serve as scaffold for migration and proliferation of cells. In addition, scaffolds can be designed as drug delivery carrier to control a site- and time-specific release to protect growth factors. The materials included synthetic and

natural calcium phosphate, synthetic polymers (*e.g.*, polylactic acid and polyglycolide), and natural polymers (*e.g.*, collagen, fibrin and chitosan).

3. Growth factors: These are required to promote cell differentiation and proliferation including polypeptides and eicosanoids.

Tissue-engineered implant is a biological/biomaterial combination in which some component of tissue has been combined with biomaterials to create a device for the restoration or modification of tissue or organ function.

In recent years, the contemporary concepts in tissue engineering principles, “cell-based tissue engineering”, was proposed by Muschler *et al.* (42). They highlight a transition from the historically materials-based tissue-level approach, with which mechanically durable, bioinert or biocompatible materials were preferred, to a focus on cell-based or bioactive materials and stimuli. This evolving approach focuses on the function of cells and the role of materials, implants, and biophysical stimuli in modulating cell function. There are four major types of cell-based tissue engineering:

1. Targeting connective tissue progenitors in situ

Targeting strategies are designed to promote desired tissue formation by stimulating the activation, migration, proliferation, and/or differentiation of local connective tissue progenitor cells. Implantation of acellular tissue scaffolds (*e.g.*, allograft bone, ceramics, hyaluronic acid, and synthetic polymers) is an example of this strategy. The strategy relies on a sufficient local population of connective tissue progenitor cells. Tissue scaffolds provide a surface on which cells and connective tissue progenitor cells can attach and migrate as well as a protected void space in which new tissue can form and be distributed throughout the region where new tissue desired. When these properties promote bone healing, they are referred to as osteoconduction. In addition, locally delivered growth factors (*e.g.*, bone morphogenic proteins, fibroblast growth factors, and vascular endothelial growth factors) also target local cells. The capacity of some growth factors to selectively activate bone-forming connective tissue progenitor cells and/or enhance the probability that their progeny will differentiate into bone has been defined as osteoinduction.

2. Transplantation of autogenous connective tissue progenitors

Transplantation of connective tissue progenitors can improve the outcome of both conductive and inductive grafts. Autogenous cancellous bone grafting has long been the most prevalent and relatively effective example of cell transplantation, although only a small fraction of the transplanted cells actually survive.

3. Transplantation of cultured-expanded or modified connective tissue progenitors

Culture-expanded cells in vitro offer the potential to generate a large number of progenitor cells. However, culture expansion also adds substantial cost and some risks, such as contamination with bacteria or viruses or depletion of the proliferative capacity of the connective tissue progenitors prior to implantation. In vitro selection of the most rapidly proliferating cells may also select cells with mutations or epigenetic changes that might confer a tumor-forming potential.

Transplantation of genetically modified cells, new or modified genes is usually accomplished with use of vectors that are created by modifying naturally occurring viruses such as a retrovirus, lentivirus, adenovirus or adeno-associated virus. The intrinsic biological potential and performance of connective tissue progenitors can be genetically modified with a variety of means that either transiently or permanently alter the genes that a cell expresses. The biological risk associated with genetic manipulation is greater than that associated with the alternatives.

4. Transplantation of fully formed tissue (Ex vivo tissue generation and transplantation)

Fully organized and mature tissues are created outside of the body (ex vivo) and followed by functional transplantation and integration. However, this strategy involves three great challenges: generation of functional tissues, transplantation in a manner that preserved the viability and function of cells, and biological/mechanical fixation and integration with surrounding tissue.

In many tissues such as bone, the number and mitotic activity of precursor cells are so high. In most circumstance, matrices alone can serve as scaffold to facilitate regeneration. Exogenous cell and mitogenic factors may only be necessary in special cases. It is of interesting to note that one approach in bone engineering has been to employ matrices that serve as analogues of the extracellular matrix of the tissue to be engineered. A matrix can play several roles during the process of regeneration:

1. The matrix can structurally reinforce the defect size so as to maintain the shape of the defect and prevent distortion of surrounding tissue.
2. The matrix can serve as a scaffold for attachment, migration, proliferation and differentiation of cells in vivo or for cells seeded in vitro.
3. The matrix provides a void volume in which vascularization, new tissue formation, and remodeling can occur.
4. The matrix can serve as a vehicle for delivery of cells or growth factors into a graft site, facilitating their retention and distribution throughout the region where new tissue is desired.
5. The matrix can serve as a barrier to the ingrowth of surrounding tissue that may impede the process of regeneration.
6. The matrix can serve as an insoluble regulator of cell function through its interaction with certain integrins and other cell receptors.

Because of these versatile functions, a broad range of scaffolds is available for clinical use, and many new scaffolds are under development. From this point of view, numerous critical variables related to the design and the selection of scaffolds should be also considered (42, 55-56). These variables can be categorized into six factors.

1. Bulk materials

Current clinical scaffolds are made from a broad range of bulk materials. These include tissue-derived materials (*e.g.*, allograft bone matrix, skin, and intestinal submucosa), biological polymers (*e.g.*, collagen, hyaluronan, fibrin, alginate, and chitosan), synthetic polymers (*e.g.*, polylactide, polyglycolide, and polycaprolactone), ceramics or mineral-based matrices (*e.g.*, tricalcium phosphate, hydroxyapatite, and calcium sulfate), metals (*e.g.*, titanium, tantalum, and other alloys), and composites of two or more materials.

2. Three-dimensional architecture and porosity

Matrix architecture defines the mechanical structure of the scaffold, but it also defines the initial void space (porosity and pore size) that is available for cell seeding, attachment, growth, ECM production, new blood vessels, as well as, the pathways for mass transport (convection and diffusion). A large surface area favors cell attachment and growth, whereas a large pore volume is required to accommodate and subsequently deliver a cell mass sufficient for tissue regeneration. Highly porous scaffolds are also desirable for the easy diffusion of nutrients to and waste products from the implants and for vascularization which are major requirements for the regeneration of highly metabolic organs. Most scaffolds are designed to have an internal porous structures of void space that are interconnected through pores or channels on the scale of 50 to 1000 μm . Nevertheless, the diameter of cells in suspension dictates the minimum pore size, which varies from one cell to another (56-57). The effect of implant pore size on tissue regeneration is emphasized by experiments demonstrating optimum pore size of 5 μm for neovascularization, 5-15 μm for fibroblast ingrowth, close to 20 μm for the ingrowth of hepatocytes, 40-100 μm for osteoid ingrowth, and 100-350 μm for regeneration of bone. In addition, the void spaces between packed particles are generally an order of magnitude larger than the stated microstructure or pore size of most granules themselves.

Another important consideration is the continuity of pores within a synthetic matrix. Materials transport and cell migration will be inhibited if the pores are not interconnected even if the matrix porosity is high. Large scale cell transplantation in open structures is presently limited by inadequate nutrient delivery. Cells more than approximately 200 μm from a blood supply are either metabolically inactive or necrotic due to low oxygen tension. It is for this reason that cartilage, with its very low metabolic activity, has been one of the few cell types successfully engineered into large tissue structures.

A further concern is the changes in the effective pore size over time in vivo. If the matrices are biodegradable, as in the case with polylactide or polyglycolide matrices, the average pore size will increase and bottlenecks in

the continuity of the pore structure will open. Alternatively, if the matrix does not degrade, its effective pore size may be reduced by in vivo events such as the invasion of fibrous tissue into the pores.

3. Mechanical properties

The scaffold should have the mechanical strength needed for the creation of a macroporous scaffold that will retain its structure after implantation, particularly in the reconstruction of hard, load-bearing tissues, such as bones and cartilages. A scaffold's mechanical properties (*e.g.*, strength, modulus, toughness, and ductility) are determined both by the material properties of the bulk materials and by its structure. Matching the mechanical properties of a scaffold to the graft environment is critically important so that progression of tissue healing is not limited by mechanical failure of the scaffold prior to successful tissue regeneration. Mechanical properties of human tissue are shown in Table 2 (56).

Table 2 Mechanical properties of human tissues (NA = no available data)

	Tensile strength (MPa)	Compressive strength (MPa)	Youngs' modulus (GPa)	Fracture toughness (MPa.m^{1/2})
Cancellous bone	NA	4-12	0.02-0.5	NA
Cortical bone	60-160	130-180	3-30	2-12
Cartilage	3.7-10.5	NA	0.7-15.3 (MPa)	NA
Ligament	13-46	NA	0.065-0.541	NA
Tendon	24-112	NA	0.143-2.31	NA

One of the greatest challenges in scaffold designs is the control of the mechanical properties of the scaffold over time. Scaffolds that do not degrade (metals and ceramics) can simplify this problem and provide excellent and durable function. However, these materials can also compromise tissue repair and function. It is obvious that persistence of a scaffold or implant precludes the formation of new tissue in the space that it occupies. Therefore, the development of resorbable materials (*e.g.*, tricalcium phosphate, natural or synthetic polymers) to be fabricated in scaffolds are increasingly interesting.

Nevertheless, the degradation or resorption processes appear to be concerned in these performances: the rate at which the matrix loses its mechanical properties, the rate at which the matrix is removed from the site, and the nature and concentration of the soluble products that are released into the site as the material is broken down.

4. Surface chemistry

Interactions between cells and scaffolds occur at the surface and are direct result of the unique chemical environment that is created. The surface chemistry depends on the properties of the bulk material but is not defined by the bulk materials. This is due to the fact that almost all implanted materials rapidly become coated with proteins and lipids, and these adsorbed biomolecules are the principal mediators of the cellular response to most materials. So, the net effect involves an interaction between a given surface and available biomolecules that adsorb to the surface. For example, fibronectin is more active adhesion molecule on hydrophilic surfaces (*e.g.*, glass) than on hydrophobic surfaces (*e.g.*, teflon or polyethylene). Like other implanted materials, allograft bone matrices (both mineralized and demineralized) rapidly accumulate biomolecules on their surface, which have biological effects on local cells. However, allograft bone already contains many embedded adhesion molecules and growth factors. These include the bone morphogenic proteins (BMPs), although the concentration is far lower than that delivered with use of purified recombinant BMPs products and release is much slower, requiring matrix degradation by local cells. Furthermore, the concentration and presentation of bioactive molecules in allograft bone may vary widely depending on age, gender, and genetics of the donor.

5. Initial scaffold environment: Osmolarity and pH

A scaffold must provide and maintain an environment with physiological pH and osmolarity. For most scaffolds, simple hydration with normal saline solution prior to exposing them to cells avoids cell injury. However, some matrices do not allow an isotonic condition, they can be expected to induce osmotic injury, reducing or precluding cell viability. Example include many

bone matrix materials that are prepared with use of solutions containing high concentrations of low molecular weight materials to improve handling (*e.g.*, glycerol) and materials that dissolve rapidly in water, releasing hyperosmolar concentrations of local ions (*e.g.*, calcium sulfate). In contrast, matrices containing high molecular weight carriers (*e.g.*, cellulose, starch, and hyaluronan) may be acceptable due to their less osmotic pressure.

6. Late scaffold environment: Degradation products

All degradable matrices release degradation products into the graft site environment that must be further degraded or cleared. The effect that these degradation products react on the cells within the graft site depends on their concentration, their effect on local pH, and their relative biological toxicity.

Polyesters, such as polylactides and polyglycolides, are currently synthetic degradable surgical materials. The degradation of these materials can be controlled over a range of weeks to years. However, the degradation products of these products (lactic acid and glycolic acid) are not ideal for tissue regeneration. They are degraded by hydrolysis in a process that first randomly degrades the bulk polymer, progressively reducing the molecular weight and the mechanical properties of the material but leaving the total mass of polymer essentially the same until the molecular weight of the fragments that are created is small enough to make them soluble. When this occurs, soluble material is generated rapidly, liberating the bulk polymer into solution but creating a profound local decrease in pH. In some setting, the polymer can crystallize as it degrades, creating particles that persist in the graft site for years.

In highly porous devices, the effects of degradation products may be less pronounced because the volume fraction of the bulk polymer in the graft site is smaller and the degradation products that are released are cleared more readily through a boarder surface of contact with local extracellular fluids and vascular perfusion.

Options for the structural design of tissue scaffolds are almost infinite. The macrostructures include regular geometric shapes (*e.g.*, blocks, pellets, and dowels), amorphous structures (*e.g.*, granules, or fibers), randomly integrated

structures (*e.g.*, foams, or freeze-dried materials), and formally designed regular structure (*e.g.*, machined, printed, woven, or assembled structures). Gel or putty preparations can also be made from powders or fibers, by mixing them with plasticizing agents (*e.g.*, glycerol, cellulose, and hyaluronan) or by conducting in situ polymerization with use of chemical, photochemical, or enzymatic methods.

For the last decades, the methods for scaffold processing and fabrication techniques have been proposed (42, 56, 58-60). The choice of the correct technique is critical because the fabrication can significantly alter the properties of the implant and its degradation characteristics. Most methods for fabricating porous scaffolds were reported *i.e.*, freeze-drying, particulate leaching, gas infusion, phase separation, high pressure processing, etc.

Scaffolding in periodontal tissue regeneration (57)

During 1960s, resective surgical therapy, with or without osseous recontouring was considered in the belief that attainment of shallow pocket depths was a worthwhile goal. Subsequently, clinical and scientific research was focusing on a number of approaches for periodontal regeneration. Several procedures have been performed surgically including root-conditioning agents, osteoinductive and osteoconductive grafting materials, guided tissue regeneration, and combination of these treatments. In general, existing therapies utilized in an attempt to stimulate periodontal tissue regeneration are limited in both predictability and extent of outcome. Currently, researchers have used advances made in material science and molecular biology including the development of scaffolding devices, the use of regenerative molecules, for example, platelet-derived growth factors (PDGFs) or bone morphogenic proteins (BMPs), to treat periodontal defects.

The management of periodontal defects has been an ongoing challenge in clinical periodontics. This is a mainly result of the fact that the tissue which comprise periodontium, the periodontal ligament, cementum, and alveolar bone, representing three unique tissues in their own right. Thus, reconstruction of the periodontium is not just a simple matter of regenerating one tissue but involves at least three quite diverse and unique tissues. Furthermore, the challenges in regenerating periodontal tissue

include several limiting factors such as the lack of blood supply on the diseased root surface, a complex microbiota that can contaminate wounds at the soft-hard tissue interface, and occlusal forces on the tooth complex in transverse and axial planes.

The use of scaffolds serves not only as space maintainers, but also as delivery vehicles or targeting bioactive molecules to the wound site. A list of scaffolds utilized in periodontal tissue regenerative procedures was shown in Table 3 (57).

Table 3 Scaffold materials for periodontal tissue regeneration

Biomaterials	Tradename
Allografts	
Calcified freeze dried bone, decalcified freeze dried bone	Grafton®, Lifenet®, Musculoskeletal Transplant Foundation®
Xenografts	
Bovine mineral matrix, bovine derived HA	Bio-Oss®, Osteograft®, Pep-Gen P-15®
Alloplasts	
Hydroxyapatite dense HA, porous HA, resorbable HA	Osteogen®, Periograft®, ProOsteone®
Tricalciumphosphate (TCP), calcium phosphate cement	Synthograft®, α -BSM®
Hard tissue replacement polymers	Biopiant®
Bioactive glass	PerioGlas®, BioGran®
Coral-derived calcium carbonate	Biocoral®
Polymers & Collagens	
Collagen	Helistat®, Collacote®, Colla-Tec®, Gelfoam®
Poly(lactide-copolyglycolide)	
Methylcellulose	
Hyaluronic acid ester	Hy®
Chitosan	
Enamel matrix derivative	Emdogain®

These scaffolds may function as osteoconductive and/or osteoinductive devices depending on the type of material used. There are two basic types of scaffolds used in periodontology: naturally derived scaffolds and synthetic biomimetic scaffolds.

Grafting materials for periodontal tissue regeneration

Bone graft materials are generally evaluated based on their osteogenesis (osteogenic), osteoinductive, or osteoconductive potential. Osteogenesis refers to the formation or development of new bone by cells contained in the graft; osteoinductive is a chemical process by which molecules contained in the graft (*e.g.*, bone morphogenetic protein or BMPs) convert the neighboring cells into osteoblast which in turn form bone; osteoconductive is a physical effect by which the matrix of the graft forms a scaffold that favors outside cells to penetrate the graft and form new bone (61-64).

The various graft and implant materials used so far can be placed into four categories: (65)

1. Autogenous grafts: Grafts transferred from one position to another within the same individual. This type of graft comprises of cortical bone or cancellous bone and marrow; and is harvested either from intraoral or external donor sites.
2. Allogenic grafts: Grafts transferred between genetically dissimilar member of the same species. The type of grafts used are frozen iliac cancellous bone and marrow, mineralized freeze dried bone grafts (FDBA) and decalcified freeze dried bone grafts (DFDBA)
3. Xenogenic grafts: Grafts taken from a donor of another species.
4. Alloplastic materials: Synthetic or inorganic implant materials which are used as substitutes for bone grafts.

Autogenous grafts

Autogenous bone grafts are the gold standard of grafting materials. They may retain some cell viability and are considered to promote bone healing mainly through osteogenesis and/or osteoconduction. They are gradually resorbed and replaced by new viable bone. In addition, potential problems of histocompatibility and disease transmission are eliminated (66).

Allogenic grafts

Allogenic bone grafts were utilized in attempts to stimulate bone formation in intrabony defects in order to avoid the additional surgical insult associated with the use of autogenous bone grafts. Although the grafts are usually pretreated by freezing, radiation, or chemicals in order to suppress foreign body reactions, the use of allogenic grafts involves a certain risk regarding antigenicity (67-68).

FDBA is a mineralized bone graft, which through the manufacturing process loses cell viability, and is supposed to promote bone regeneration through osteoconduction (65). The freeze drying also markedly reduced the antigenicity of the material (69). In contrast, DFDBA enhances its osteogenic potential by exposing bone morphogenic protein (BMPs) which presumably have the ability to induce host cells to differentiate to osteoblasts (25, 70). However, the controversial results regarding the effect of DFDBA on the regeneration of periodontal intraosseous defects along with great differences in the osteoinductive potential (ranging from high to no osteoinductive effect) of commercially available DFDBA (71-72).

Xenogenic graft

Boplant[®] is calf bone, treated by detergent extraction, sterilized, and freeze dried has been used for the treatment of osseous defects (73).

Kiel bone[®] is calf or ox bone denatured with 20% hydrogen peroxide, dried with acetone, and sterilized with ethylene oxide (74).

Anorganic bone is ox bone from which the organic material has been extracted by means of ethylenediamine and then sterilized by autoclaving.

These materials have been tried and discarded for various reasons (40). Recently, new processing and purification methods have been utilized which make it possible to remove all organic components from a bovine bone source and leave a non-organic bone matrix in an unchanged inorganic form. However, the differences in the purification and manipulation methods of bovine bone exist, leading to commercially available products with different chemical properties and possibly different biological behavior. Furthermore, these materials are available in different particle sizes (65).

Alloplastic materials

Alloplastic materials are synthetic, inorganic, biocompatible and/or bioactive bone graft substitutes which are claimed to promote bone healing through osteoconduction. Several alloplastic implant materials have been used in an attempt to improve clinical conditions and regenerate bone in periodontal bony defect (Table 4) (65).

Table 4 Alloplastic materials.

Plaster of Paris
Polymers
Calcium carbonate
Ceramics
Resorbable
Tricalcium phosphate
Resorbable hydroxyapatite
Nonresorbable
Dense hydroxyapatite
Porous hydroxyapatite
Bioglass

Early studies using calcium phosphate materials focused on the principle that local release of calcium ions would stimulate bone formation at the site (75). These studies with soluble calcium powders yielded equivocal results and led to further studies with tricalcium phosphate (76-77) and modified forms of hydroxyapatite (28, 78-79).

Until now, there are four kinds of alloplastic materials: hydroxyapatite (HA), beta-tricalcium phosphate (β -TCP), polymers and bioactive glasses (Bio-glasses), which are frequently used in regenerative periodontal surgery (65). The most

successful of these materials have been ceramics of either bioresorbable or nonresorbable type (75).

Consequently, in an effort to eliminate periodontal osseous defects, several kinds of grafting materials have been used in the past with the varying degrees of technical difficulty, postoperative morbidity, and success. For these reasons, the considerations that govern the selection of graft materials are crucial regarding biological acceptability, predictability, clinical feasibility, minimal operative hazard, minimal postoperative sequel and patient acceptance (41).

Chitin and Chitosan

Chitin, discovered by H. Braconnot in 1811, was first identified and named by A. Odier in 1823 (80, 81). It has a widespread distribution amongst invertebrates and the lower forms of plant life. It is in the external skeletons of arthropods, the largest phylum of the animal kingdom. This group includes the insects, arachnids (spiders, scorpions, etc.), and crustaceans (crabs, lobsters, shrimps, etc.). Chitin is also found in the internal organs of some classes of mollusks and annelids but has never been found in the tissue of vertebrates. Among plants, it has been identified in the cell walls of some fungi (81-82).

Chitin, a naturally abundant mucopolysaccharides and the second most universally abundant biopolymer next to cellulose, is well known to consist of 2-acetamido-2-deoxy- β -D-glucopyranose (N-acetyl-D-glucosamine) through a β (1 \rightarrow 4) linkage (Figure 4). It may thus be regarded as a derivative of cellulose, in which the C2 hydroxyl groups (-OH) in the pyranose ring are replaced by the amido group (-NHCOCH₃). The crystallographic structure present 3 different polymorphs including alpha (α), beta (β) and gamma (γ), which tend to adapt to helix form. It can be α helix in shrimp, β helix in squid and cuttlefish, or in a mixed form of α and β helices (80, 82).

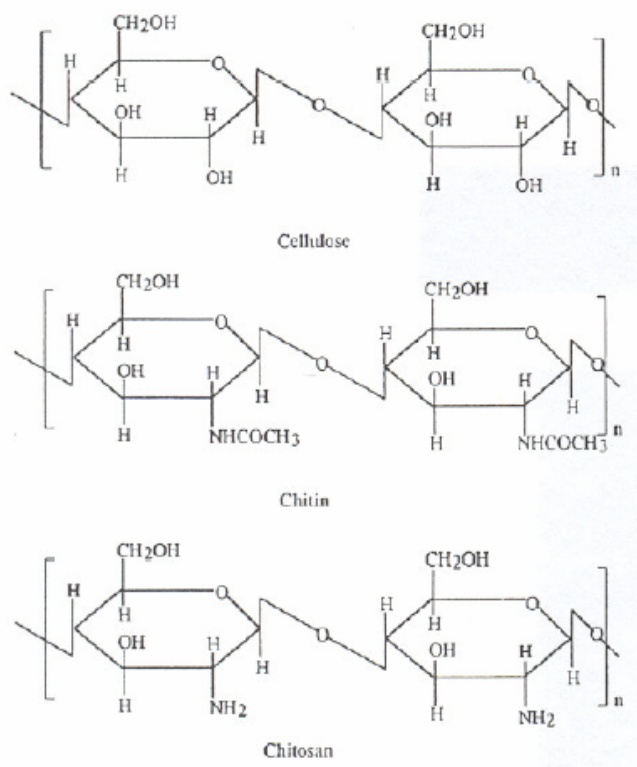


Figure 4 Structures of cellulose, chitin and chitosan (46)

Chitin usually forms a part of very complex systems and never occurs pure in nature; it is always contaminated with calcium carbonate and/or protein. Insect exoskeletons are largely composed of chitin-protein complexes, whereas crustacean shells usually contain large proportions of calcium carbonate and protein. Such these complexes, the drastic procedures required for isolation of chitin. Shells of crabs, lobsters, or shrimps may be extracted directly, but it is preferable to grind the shells to a size that will pass a 6 mm. screen and be retained on a 1 mm. screen. Then demineralization and deproteinization were treated respectively. The demineralization is to treat the ground shell with 5% hydrochloric acid solution for 24 hours to remove the calcium carbonate and to reduce the ash content of the shell. The next processing step, deproteinization, is accomplished by treating the demineralized shells with proteolytic enzymes such as pepsin or trypsin to remove protein. Alkaline deproteinization may be used and is preferred when the final product is to be deacetylated chitin (chitosan). Alkaline deproteinization is accomplished by stirring the

demineralized ground shells with three successive quantities of 5% sodium hydroxide solution at 85-90° C. Each treatment is 30-45 minutes in duration and is followed by a brief water wash to remove partially solubilized residual (82-84). Chitin at this stage may be light pink, caused by remaining pigment. These are solubilized and removed by a mild oxidation with acidified hydrogen peroxide solution for 6-7 hours at ambient temperature to bleaching (82).

The pure chitin is insoluble in water, dilute acids, dilute and concentrated alkalis, and all organic solvents. It is soluble in anhydrous formic acid, hypochlorite solutions, and concentrated mineral acids (81, 84).

When chitin is treated with concentrated alkali at high temperature, either by 40% aqueous sodium hydroxide for 2 hours at 135-140°C or 24 hours at 50-60°C, it undergoes various degrees of deacetylation and degradation, to give a product called chitosan (81).

Chitosan, a partially or completely deacetylated chitin, is consisting of $\beta(1\rightarrow4)$ linked 2-amino-2-deoxy-D-glucopyranose (N-glucosamine) (Figure 4) Structurally, chitosan resembles glycosaminoglycans especially hyaluronic acid, which are natural components of human tissues (85-86). In solubility, chitosan resembles chitin in being insoluble in water, concentrated alkali, alcohol and other organic solvents but differs from chitin in being soluble in dilute acids such as acetic acid and formic acid (81, 84, 87). Chitosan is only soluble at acidic pH (<6.5) when the free amino group ($-\text{NH}_2$) become protonated to form cationic amine group ($-\text{NH}_3^+$). At this pH, chitosan has been identified as a linear polycation with an intrinsic pKa value of 6.5 (46, 85-86, 88). Cationicity of chitosan allows the formation of polyelectrolyte complexes (PEC) by electrostatic interactions with water soluble anionic macromolecules like DNA, glycosaminoglycans, proteins, or synthetic anionic polymers (polyacrylic acid) (46, 89).

The term of chitosan refers in fact to a series of deacetylated chitins with different molecular weight (50kDa to 2000 kDa), viscosity, and degree of N-deacetylation (40 to 98%) (46).

Scant attention has been paid to chitin, in spite of its structural similarity to cellulose, primarily due to its inertness. Chitin is a highly insoluble material and possesses a low chemical reactivity. On the other hand, chitosan has three kinds of

reactive functional groups, at C-2, C-3, and C-6 positions. When functional groups of chitosan were chemically modified, their physical, mechanical, chemical, and biological properties may change. However, these modifications can provide numerous materials and many possibilities to a chemist, bioengineer and health care professions (46, 86).

Chitosan can be easily fabricated into powders, fibers, films, membranes, sponges, porous scaffolds, hydrogels, beads and micro- and nanospheres, which are highly interesting for manufacturing many different medical devices (46, 90-96).

Fundamental parameter

All the properties of chitin and chitosan depend on two fundamental parameters: the degree of deacetylation (DD) and molecular weight distribution. Physical and chemical properties of chitosan such as rheological properties, antimicrobial activity, immunoadjuvant activity, enzyme-binding capacity, metal-binding capacity, film and gel forming properties, mechanical and porosity of the membrane depend on its degree of deacetylation and molecular weight (80, 90, 97). In the same appearance, these fundamental parameters also influence on biological properties: biocompatibility, cell attachment and cell proliferation, the biodegradation by lysozyme, the wound healing, and the osteogenesis enhancement (98-103). As a consequence, no rigorous work is possible without a perfect knowledge of these parameters. However, the relationship between these parameters and their biological properties has not been clearly elucidated.

Biological and physiological properties of chitin and chitosan

Biocompatibility and non-toxicity

Many studies have been investigated in vitro and in vivo. The results conclude that chitosan and its derivative are biocompatibility such as non-toxic, non-allergenic, non-carcinogenic and non-inflammation.

In vitro study, Prasitsilp *et al.* recommended that the percentage of degree of deacetylation of chitosan has a very important effect on the biocompatibility (98). The photocrosslinkable chitosan were determined that it has not showed any cytotoxicity in cell culture tests on human skin fibroblasts, coronary endothelial cells and smooth muscle cells (104). Furthermore, Zhu *et al.* reported that phosphorylated chitosan has excellent cytocompatibility compared to the chitosan without phosphorylated modifications (105).

In animal study, chitosan film in toxicity tests indicated that it is non-toxic and free of pyrogen (106). Phosphorylated chitosan reinforced calcium phosphate cement also indicated that no adverse effects were found in tissues around the holey bone defects in rabbit tibias (107).

In human study, Muzzarelli *et al.* implanted methylpyrrolidinone chitosan in surgical wound from wisdom tooth avulsion and reported that none of the patient have an adverse effects over one year of observation (108).

Cell attachment and cell proliferation

Fakhry *et al.* determined two commercial chitosans, Chitosan-H and Protasan CL212, on osteoblast and fibroblast cell attachment. The results suggest that these two commercial chitosans supported the initial attachment and spreading of osteoblasts preferentially over fibroblasts (109).

Howling *et al.* and Chatelet *et al.* demonstrated that highly deacetylated chitosans strongly stimulated fibroblast proliferation while lower degree of deacetylated chitosan showed less activity (99-100). In contrast to the previous report by Mori *et al.*, they suggested that chitin and its derivatives showed almost no acceleratory effect on the proliferation of cultured fibroblasts (110).

Ohara *et al.* cultured an osteoblastic cell line (NOS-1) with water-soluble and low molecular chitooligosaccharide. They suggested that a super-low concentration of chitooligosaccharide could moderate the activity of osteoblastic cells through mRNA levels and that the genes concerning cell proliferation and differentiation can be controlled by water-soluble chitosan (111).

Cell migration and wound healing

In the early phase of wound healing, there are two stages as major components of wound healing. The first stage is the inflammatory stage, and the second is the stage of new tissue formation. At the inflammatory stage, infiltrating neutrophils clean foreign agents in the area, chitosan, which has been reported as wound healing accelerator, accelerates the infiltration of inflammatory cells, consequently accelerating wound cleaning. At the new tissue formation stage, fibroplasia begins by the formation of granulation tissue within the wound space. Ueno *et al.* suggested chitosan to be having a function in the acceleration of infiltration of PMN cells at the early stage of wound healing. In addition, they suggested that chitosan stimulate infiltrating PMN to synthesize the osteopontin, which plays the role of regulating the evolution of wound healing (112-113). Indirectly, chitosan induce fibroblast to secrete interleukin-8, which attracted migration of PMN cells into the wound area (110).

Macrophage also plays an important role in the process of wound healing. Activated macrophage releases many growth factors which upregulate the ECM production. In previous studies, chitosan stimulates macrophage to produce interleukin-1, transforming growth factor- beta (TGF- β), and platelet-derived growth factor (PDGF) (114-115). Furthermore, chitin and chitosan has been reported that activated complement via the alternative pathway (116-117).

Bone formation and bone substitution

The osteogenic potential of chitosan is controversial. Klokkevold *et al.* suggested that chitosan has potential to accelerate the differentiation of osteoprogenitor cells derived from fetal Swiss Webster mice calvariae and may facilitate the formation of bone (118). On the other hand, Muzzarelli *et al.* implanted methylpyrrolidinone chitosan in surgical wound from wisdom tooth avulsion and

suggested that methylpyrrolidinone chitosan promoted osteoconduction and the space left avulsion was filled with newly formed bone (108). A similar view is found in the report by Kawakami *et al*, who pointed out that chitosan-bonded hydroxyapatite paste has the osteoconductive properties (119). When the chitosan reconstituted with absorbable collagen sponge (ACS), the results suggested that it has a significant potential to accelerate the regeneration of bone (120).

Regarding degree of deacetylation of chitosan, Hidaka *et al*. reported that membranes prepared with 65, 70 and 80% deacetylated chitin initially elicited marked inflammatory reactions that subside in time with granulation tissue formation and osteogenesis, on the other hand, membranes prepared with 94 and 100% deacetylated chitin showed mild inflammation and minimal osteogenesis (101).

Biodegradation

Chitosan can be enzymatically degraded by chitinases, chitosanases and lysozymes. The main enzyme involved in the degradation of chitin derivatives in the body is lysozyme. In addition, as with all polysaccharides, depolymerization may occur by acid hydrolysis and by an oxidative-reductive depolymerization reaction (102, 121). Figure 5 summarizes the role of lysozyme and N-acetyl-beta-D-glucosaminidase as described by Muzzarelli (122).

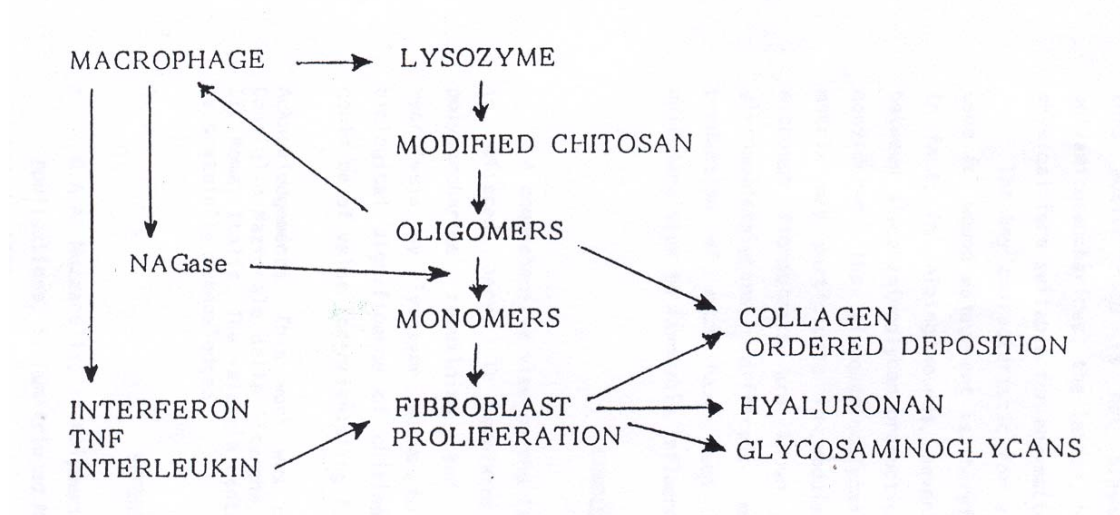


Figure 5 The roles of lysozyme and N-acetyl-beta-D-glucosaminidase (122)

Lysozyme, normally produced by macrophages, hydrolyzed susceptible modified chitosan to oligomers which activate macrophages to produce interferon, tumor necrosis factor (TNF) and interleukin-1. Activated macrophages also produce N-acetyl-beta-D-glucosaminidase, which catalyses production of D-glucosamine, N-acetyl glucosamine and substitute glucosamines from oligomers.

The degradation rate of chitosan can be controlled by changing its polymer composition (*i.e.*, the co-polymerization ratio of glucosamine to N-acetylglucosamine or the length of acryl side-chain on N-acetylglucosamine) and/or its molecular weight. Tomihata and Ikada suggested that high deacetylated chitin showed slower biodegradation and milder tissue response than low deacetylated chitin (103). Furthermore, the degraded products of chitosan are non-toxic, non-immunogenic and noncarcinogenic (123).

For application, chitosan has attracted a great interest as in pharmacology and medicine as biomaterial because of its biodegradability, biocompatibility, non-toxicity and the wide range of reported positive biological responses and activities. It has been used or proposed in the fabrication of drug delivery devices, in orthopedics, in wound healing, in adhesive formulation for surgical applications, in ophthalmology, in pharmaceuticals, in dentistry, and in the fabrication of scaffolds for tissue engineering.

Application in dental and periodontal surgery

Muzzarelli *et al.* implanted methylpyrrolidinone chitosan in surgical wound from wisdom tooth avulsion and suggested that methylpyrrolidinone chitosan promoted osteoconduction and the space left avulsion was filled with newly formed bone (108). In another study, Muzzarelli *et al.* used chitosan ascorbate gel for the reduction of the periodontal pockets in surgical intervening in advanced periodontitis patients. The clinical improvements satisfied with the reduction of tooth mobility and periodontal pocket depths (124).

Gerentes *et al.* studied in different parameters of the chitin-based hydrogel to develop this hydrogel as injectable material in periodontal surgery (125).

Application in controlled drug delivery

Due to its unique polymeric cationic character and its gel and film forming properties, chitosan has been extensively examined in the pharmaceutical industry for its potential in the development of drug delivery system (126).

Chitosan itself has been proposed as carrier for drugs (aspirin, heparin, etc.), antibiotics (tetracycline, ampicillin, etc.), protein (gelatin, vaccine, etc.), polysaccharides (alginate, chondroitin sulfate, etc.), DNA, degradable polymer (polylactide, polyglycolide, poly- ϵ -caprolactone) and synthetic hydrophilic polymers (polyethylene glycol, polyvinylpyrrolidone, polyvinylalcohol), mainly for oral and mucosal administration (46, 127-131).

CHAPTER IV

MATERIALS & METHODS

The processes of experimental researches were summarized in Figure 6.

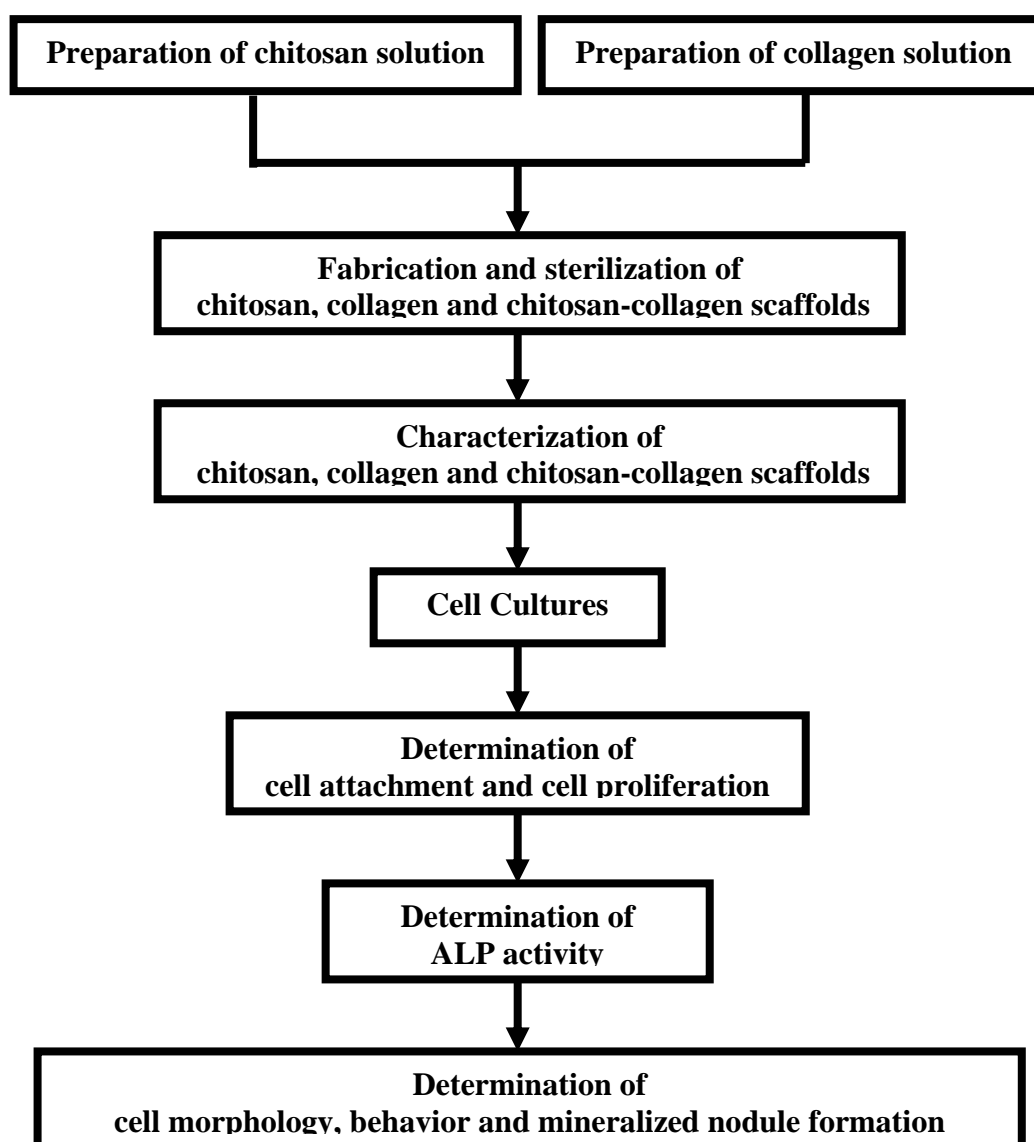


Figure 6 Diagram of experimental research

Preparation of chitosan solution

Chitosan, 80% degree of deacetylation (DD), was prepared by conventional methods. Low molecular weight of 80% DD chitosan was prepared by enzymatic hydrolysis of chitosan by chitosanase produced from *Bacillus sp.* PP-8. Chitosan solution (1% w/v) was made by solubilizing chitosan powder in 1 % acetic acid.

Partially N-acetyl chitosan (PNAC), 50% degree of deacetylation, was prepared by solubilizing chitin in NaOH and allowed the chitin solution to deacetylate slowly at 4°C overnight. The solution was checked for optimum PNAC production by addition of 1 N HCl to 1 ml aliquot of the solution to neutralize this solution to pH 7.0. When no precipitation was formed, the whole reaction was neutralized. PNAC was precipitated by addition of equal volume of acetone; the precipitant was washed with deionized water and then vacuum dried. Low molecular weight of PNAC was prepared by sonication of the PNAC solution for 15 minutes. PNAC solution (1% w/v) was made by solubilizing powder PNAC in 1 % acetate buffer (pH 4.5).

These materials were contributed by Dr. Rath Pichyangkura, Biochemistry department, Faculty of Science, Chulalongkorn University, Thailand.

In this experiment, chitosan were divided into four groups according to their degree of deacetylation (80% and 50% degree of deacetylation) and molecular weight (Low = 100,000 Dalton and High = 1,000,000 Dalton) as follow:

Group 1 80% degree of deacetylation and low molecular weight (**80LMW**).

Group 2 80% degree of deacetylation and high molecular weight (**80HMW**).

Group 3 50% degree of deacetylation and low molecular weight (**50LMW**).

Group 4 50% degree of deacetylation and high molecular weight (**50HMW**).

Preparation of collagen solution

According to O'Leary *et al.* (132) with slightly modification, type I collagen was extracted from rat-tail tendon by incubation in sterile 17 mM acetic acid, with mechanical stirring for 48 hours at 4°C. Undissolved tendon pieces were removed by centrifugation at 17,500 revolutions/min. at 4°C in Beckman centrifugation (Model J2-21, Belgium) for 60 minutes. The pH of collagen solution was adjusted to 7.0 with sterile 0.1 M NaOH and the precipitated collagen collected by centrifugation at 8,000 revolutions/min at 4°C in universal 32 rotor of a Hettich centrifugation (D-78532 Tuttlingen, Germany) for 20 minutes. The collagen pellet was dissolved in sterile 17 mM acetic acid by stirring at 4°C for 48 hours and then was dialyzed by molecular porous membrane (Spectra/Por® CE, MWCO:10,000, USA) for 48 hours. The pH of collagen solution was adjusted to 7.0 with sterile 0.1 M NaOH and the precipitated collagen collected by centrifugation at 8,000 revolutions/min at 4°C in universal 32 rotor of a Hettich centrifugation for 20 minutes. The resulting collagen pellet was frozen at -80°C for 24 hours prior to lyophilize for 48 hours. Collagen solution (1% w/v) was made by solubilizing collagen pellet in 1 % acetic acid.

Fabrication and sterilization of chitosan, collagen and chitosan–collagen scaffolds.

Chitosan solution (1% w/v) was diluted in 1% acetic acid for preparing in three concentration; 0.33%, 0.25% and 0.20%. One hundred microlitres in each concentration of chitosan solution were pipetted on the cover slips (cultured grade, Common groups). The samples were frozen at -80°C or -20°C for 24 hours prior to lyophilize for 6 hours to generate chitosan scaffolds. These chitosan scaffolds were tested in scaffold characterization, with the exception of 0.25% chitosan scaffolds were tested on cell attachment and cell proliferation.

Collagen solution (1% w/v) was diluted in 1% acetic acid for preparing in three concentrations; 1.0%, 0.25% and 0.10%. One hundred microlitres in each concentration of collagen solution were pipetted on the cover slips. The samples were frozen at -80°C or -20°C for 24 hours prior to lyophilize for 6 hours to generate

collagen scaffolds. These collagen scaffolds were tested in scaffold characterization, with the exception of 0.25% collagen scaffolds were tested in all experiments.

To obtain 0.25% chitosan-collagen solution, chitosan solution (0.50%) and collagen solution (0.50%) were stirred in homogeneous blending for 1 hour. One hundred microlitres of homogeneous chitosan-collagen solution were pipetted on the cover slips. The samples were frozen at -80°C or -20°C for 24 hours prior to lyophilize for 6 hours to generate chitosan-collagen scaffolds. These chitosan-collagen scaffolds were tested in all experiments and were divided into four groups according to degree of deacetylation (80% and 50% degree of deacetylation) and molecular weight (Low = 100,000 Dalton and High = 1,000,000 Dalton) of chitosan as follow:

- Group 1 80% degree of deacetylation and low molecular weight of chitosan blended with collagen (**80LMW-C**).
- Group 2 80% degree of deacetylation and high molecular weight of chitosan blended with collagen (**80HMW-C**).
- Group 3 50% degree of deacetylation and low molecular weight of chitosan blended with collagen (**50LMW-C**).
- Group 4 50% degree of deacetylation and high molecular weight of chitosan blended with collagen (**50HMW-C**).

For sterilization, the lyophilized test scaffolds were radiated by ultraviolet lamp within biological safety cabinet (Gelaire BBSB3A, Sydney, Australia) for 6 hours.

Charaterization of chitosan, collagen and chitosan-collagen scaffolds

After test scaffolds were fabricated, microstructure of lyophilized scaffolds was visualized by sputter coating with platinum-palladium (Sputter coater, Hitachi E-120, Japan) and viewing on scanning electron microscope (Hitachi S-2500, Japan) at a magnification of 300. Scanning electron images were used to qualitatively compare the pore structure and pore distribution of the tested scaffolds. ImagePro Plus® software program version 3.0 for Windows (Media Cybernetics, USA) was used to quantitatively compare the pore size and area fraction of the tested scaffolds after scanning electron images were scanned by a scanner (Nikon Scantouch 210, Taiwan)

with scale 6.93% and 4800 resolution. Pore size was categorized in three pore diameter ranges (micropore : smaller than 20 μm , medium pore size : 20-50 μm , and macropore : larger than 50 μm). The area fraction represented porosity and calculated in this equation:

$$\text{Area fraction (\%)} = \frac{\text{Area of bulk material (mass)}}{\text{Area of bulk material (mass)} + \text{Area of pore}} \times 100$$

Cell cultures (133)

MC3T3-E1 cells (ATCC number Lot No. 3225550), a clonal pre-osteoblast cell line derived from new born mouse calvaria, were grown in alpha-minimum essential medium (α -MEM, available from Gibco[®], New York, USA) containing 10% fetal bovine serum (Hyclone[®], Logan, USA) and antibiotic-antimycotic (10,000 unit/ml penicillin G, 10 mg/ml streptomycin and 25 $\mu\text{g/ml}$ amphotericin B, available from Gibco[®], New York, USA) and were incubated at 37°C in humidified air with 5% CO₂. The culture medium was changed at selected time interval (every 2-3 days). After reaching confluence, adherent cells were enzymatically detached by 0.1% Trypsin-EDTA (Gibco[®], New York, USA) and then were subcultured. The third to eighth passages were then used in the following experiment.

Cultures were characterized for cell growth parameters (cell attachment and cell proliferation), cell morphology and functional activities (ALP activity and ability to form calcium-phosphate deposits). Following experiment, the tested scaffolds were divided into 5 groups, composed of collagen, 80LMW-C, 80HMW-C, 50LMW-C and 50HMW-C scaffolds, comparing cover slips which comprised the control group.

Determination of cell attachment and cell proliferation

MTT assay (reduction of 3-(4,5-dimethylthiazol-2-yl)-2,5-diphenyltetrazolium bromide to a purple formazan product) was used to estimate cell attachment and cell proliferation as previously described by Mosmann T. (134). MC3T3-E1 cells were plated at a density of 2×10^4 cells/well in twenty-four well plates which containing with test scaffolds and cover slips. At 5 and 24 hours after cell attachment (135) and on day 1, 3, 5, 7, 10 and 14 after cell proliferation (136), cells were rinsed with phosphate

buffer saline solution (PBS), and then incubated with 500 μ l/well of MTT (0.5 mg/ml, available from Sigma[®], USA) for 2 hours. This time period permitted the cellular conversion of MTT to insoluble formazan salts, which were dissolved with 500 μ l/well of dimethylsulfoxide (DMSO, available from Sigma[®], USA). The absorbance was measured by spectrophotometer at 540 nm. on a scanning multiwell (Elisa reader model ceres 900 Hdi, USA). The optical densities were calculated and presented in mean \pm standard deviation. Data were derived from triplicate wells for each assay point and all samples were made in triplicate.

Determination of alkaline phosphatase activity

Alkaline phosphatase activity was determined in cell lysate by measuring the release of p-nitrophenol (PNP) from disodium p-nitrophenyl phosphate (PNPP). (137)

Cells were plated at a density of 2×10^4 cells/well in twenty-four well plates which containing with test scaffolds and cover slips. After reaching confluence (Day 3), cells were cultured in α -MEM containing 10 mM β -glycerophosphate (Sigma[®], USA) and 50 μ g/ml of ascorbic acid (Sigma[®], USA). On day 4, 6, 10, 14, 18, 22 and 26, cells were washed twice with phosphate buffer saline solution, then cells were lysed by adding lysis buffer (200 μ l/well) for 15 minutes. Lysis buffer was prepared by mixing of Phenylmethyl-sulfonyl Fluoride (PMSF, available from Sigma[®], USA) and CelLytic M (Sigma[®], USA). An aliquot of cell lysate (200 μ l) were collected, centrifuged at 14,000 g for 15 minutes at 4°C and stored in -80°C. For alkaline phosphatase enzyme assay, an aliquot of cell lysate (20 μ l) was added by 40 μ l of Tris buffer (pH 10.3) and incubated for 5 minutes at 37°C. Subsequently, the reaction was started by adding 50 μ l of 2mM freshly prepared p-nitrophenyl phosphate (PNPP, available from Sigma[®], USA). After incubation at 37°C for 30 minutes, the reaction was stopped by adding 50 μ l of ice cold NaOH (EKA, Nobel, Sweden). The absorbance was measured by spectrophotometer at 405 nm. and was calculated from a standard curves which were prepared from p-nitrophenol reagent (PNP, available from Sigma[®], USA). Data were derived from triplicate wells for each assay point and all samples were made in duplicate.

The results of alkaline phosphatase activities were expressed in nanomols p-nitrophenol per mg of protein per minute (nmol PNP/mg. of protein/min) by using the

Bio-Rad protein assay as previously described by Bradford (138). Firstly, following manuscript, dye reagent was prepared by diluting 1 part Dye Reagent Concentrate (Bio-Rad®, CA, USA) with 4 parts distilled, deionized (DDI) water and protein standard (bovine serum albumin, available from Sigma®, USA) was also prepared in three to five dilutions, which is representative of the protein solution to be tested. Secondly, 10 µl of each standard and sample solution were pipetted into separate micotiter plate wells and 200 µl of diluted dye reagent was added to each well. The sample and reagent were mixed thoroughly by using a plate shaker and incubated at room temperature for 10 minutes. Finally, the absorbance was measured by spectrophotometer at 595 nm. Protein concentrations of each sample were calculated from a standard curves which were prepared from bovine serum albumin.

Determination of cell morphology, behavior and mineralized nodule formation (133, 139-142)

Cells were plated at a density of 2×10^4 cells/well in twenty-four well plates which containing with test scaffolds and cover slip. After reaching confluence (day 3), cells were cultured in α -MEM containing 10 mM β -glycerophosphate and 50 µg/ml of ascorbic acid. Cell morphology, behavior and mineralized nodule formation were checked routinely by phase contrast microscope and examined by scanning electron microscope on day 4, 10 and 18. The samples were fixed in 2.5% glutaraldehyde (EM grade, USA), 4% osmium tetroxide (Electron Microscopy Science, USA) and dehydrated in a graded ethanol (analytical grade, ACS, Spain) series to 100% ethanol, respectively. Then the samples were dried by critical point dryer (Hitachi HCP-2, Japan) before sputter coated with platinum-palladium for viewing on scanning electron microscope (Hitachi S-2500, Japan) at a magnification of 300 and 500. The presence of mineralized nodules were determined by staining with alizarin red-S (AR-S, available from Sigma, USA) to identify calcium. The mineralized nodules were washed with PBS and fixed with ice-cold methanol for 10 minutes. The dye solution was then added in each well for 2-3 minutes. Data were derived from triplicate wells for each assay point. The samples were repeated twice.

Data collection and statistic analysis

Scaffolding characteristics, cell morphology and behavior, and mineralized nodule formation, the data were analyzed by descriptive analysis. For cell attachment, cell proliferation and alkaline phosphatase activity, the data were analyzed using the statistical package SPSS for Windows version 11.5. The data distribution was checked by the Komogorov-Smirnov test for normal distribution. One-way analysis of variance (ANOVA) or Kruskal-Wallis test was applied to detect difference among groups after test of homogeneity of variance was done by Levene median test. Multiple comparisons with Scheffe or Mann-Whitney test were done where variances were homogeneous or heterogeneous, respectively. The level of statistical significant was determined at $p < 0.05$.

CHAPTER V

RESULTS

Chitosan, collagen and chitosan-collagen scaffolds characterization.

In this experiment, test scaffolds were characterized according to concentration, freezing temperatures before lyophilizing and materials to be used. These test scaffolds are divided into 4 major groups as follow:

- Group 1 **Chitosan scaffolds** were prepared by chitosan solution in three concentrations (0.33%, 0.25% and 0.20%) and were frozen in -80°C refrigerator before lyophilizing.
- Group 2 **Chitosan scaffolds** were prepared by chitosan solution in three concentrations (0.33%, 0.25% and 0.20%) and were frozen in -20°C refrigerator before lyophilizing.
- Group 3 **Collagen scaffolds** were prepared by collagen solution in three concentrations (1.00%, 0.25% and 0.10%) and were frozen in -20°C refrigerator before lyophilizing.
- Group 4 **Chitosan-collagen scaffolds** were prepared by 0.25% chitosan solution and 0.25% collagen solution, and were frozen in -20°C refrigerator before lyophilizing.

After test scaffolds were fabricated, microstructure of lyophilized scaffolds was visualized by sputter coating with platinum-palladium and viewing on scanning electron microscope at a magnification of 300. Visual inspection reveals that lyophilizing of all frozen test scaffolds produced porous structure with interconnectivity. The test scaffold surface appearance had bulk materials and pore distribution as shown in Figure 7-10. The SEM photographs demonstrated that different concentration, degree of deacetylation and molecular weight of chitosan scaffolds, different concentration of collagen scaffolds, and chitosan-collagen

scaffolds had unique porous microstructure and pore distribution. In addition, freezing temperatures before lyophilizing also affect to porous microstructure and pore distribution of chitosan scaffolds (Figure 7-8). The results indicated that chitosan scaffolds prepared at low freezing temperatures (-80°C) exhibited less porous microstructure and porous distribution than chitosan scaffolds prepared at high freezing temperatures (-20°C).

The area fraction and pore size were determined by SEM image analysis with ImagePro[®] Plus software program version 3.0 for Windows (Figure 11). Data were summarized in Table 5-8.

All test scaffolds had more percentage in micropore than medium pore size and macropore, regardless of different concentration, degree of deacetylation and molecular weight of chitosan scaffolds, different concentration of collagen scaffolds, and chitosan-collagen scaffolds. When the freezing temperature before lyophilizing are considered (Table 5-6), the results demonstrated that chitosan scaffolds prepared at high freezing temperatures (-20°C) had more medium pore size and macropore than chitosan scaffolds prepared at low freezing temperatures (-80°C). In addition, the macropore were not available in chitosan scaffolds prepared at low freezing temperatures (-80°C). From this point of view, it is interesting to note that freezing temperatures before lyophilizing was the critical factor affecting the pore size.

Moreover, all test scaffolds had percentage of area fraction according to their concentrations. The higher concentration had more percentage of area fraction than the lower concentration (Table 5-8). For chitosan scaffolds, the results indicated that low molecular weight had more percentage of area fraction than high molecular weight, regardless of degree of deacetylation and freezing temperatures before lyophilizing. With this regard, it was interesting to note that concentration and molecular weights of chitosan within the test scaffolds were the critical factors affecting the area fraction.

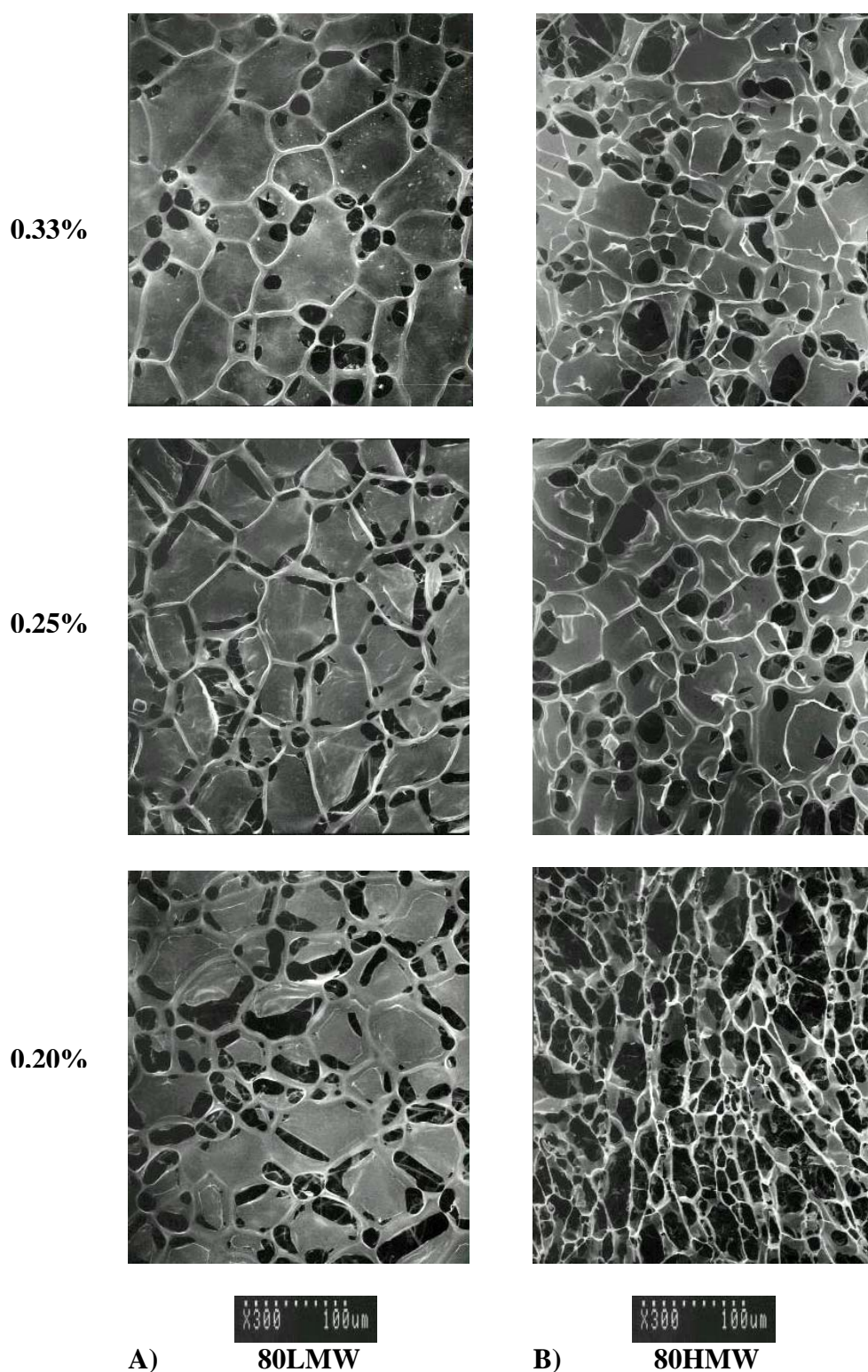
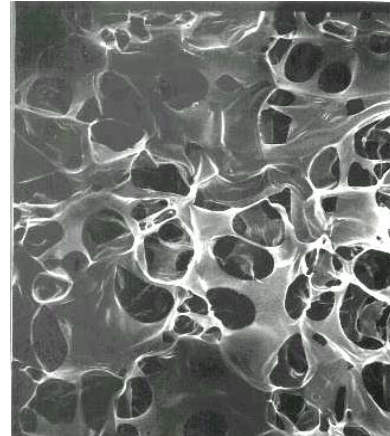
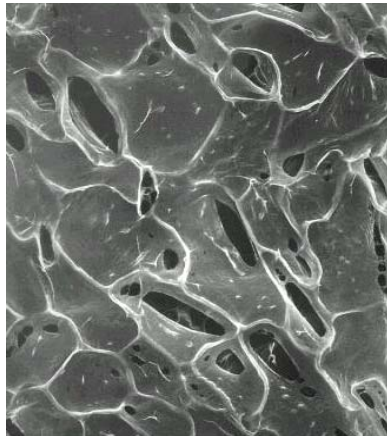


Figure 7 SEM images of chitosan scaffolds, frozen in -80°C refrigerator (x 300).

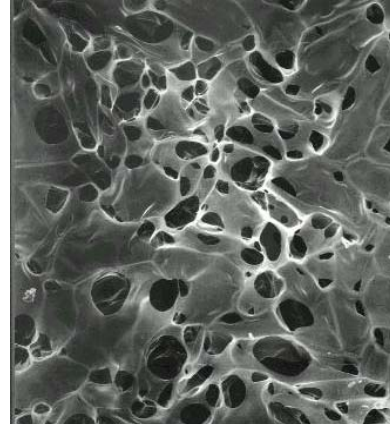
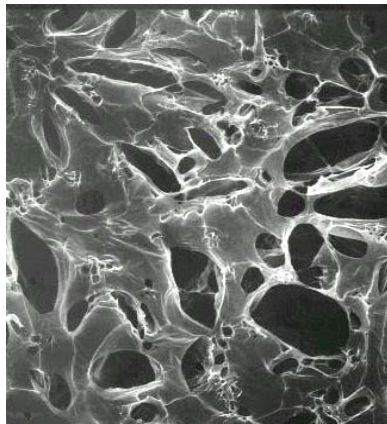
A) 80LMW chitosan scaffolds with 0.33%, 0.25% and 0.20% in concentration.

B) 80HMW chitosan scaffolds with 0.33%, 0.25% and 0.20% in concentration.

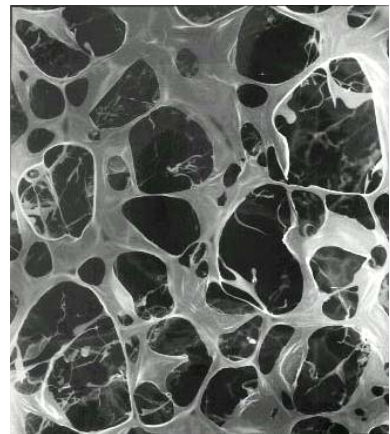
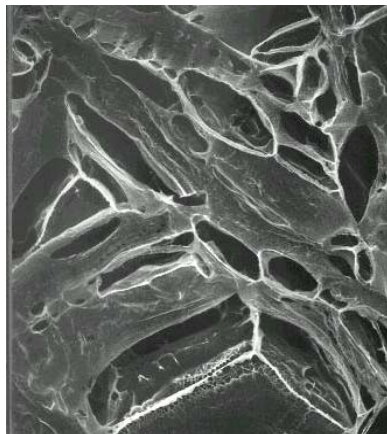
0.33%



0.25%



0.20%



X300 100um

C) 50LMW

X300 100um

D) 50HMW

Figure 7 (con't) SEM images of chitosan scaffolds, frozen in -80°C refrigerator

(x 300). C) 50LMW chitosan scaffolds with 0.33%, 0.25% and 0.20% in concentration. D) 50HMW chitosan scaffolds with 0.33%, 0.25% and 0.20% in concentration.

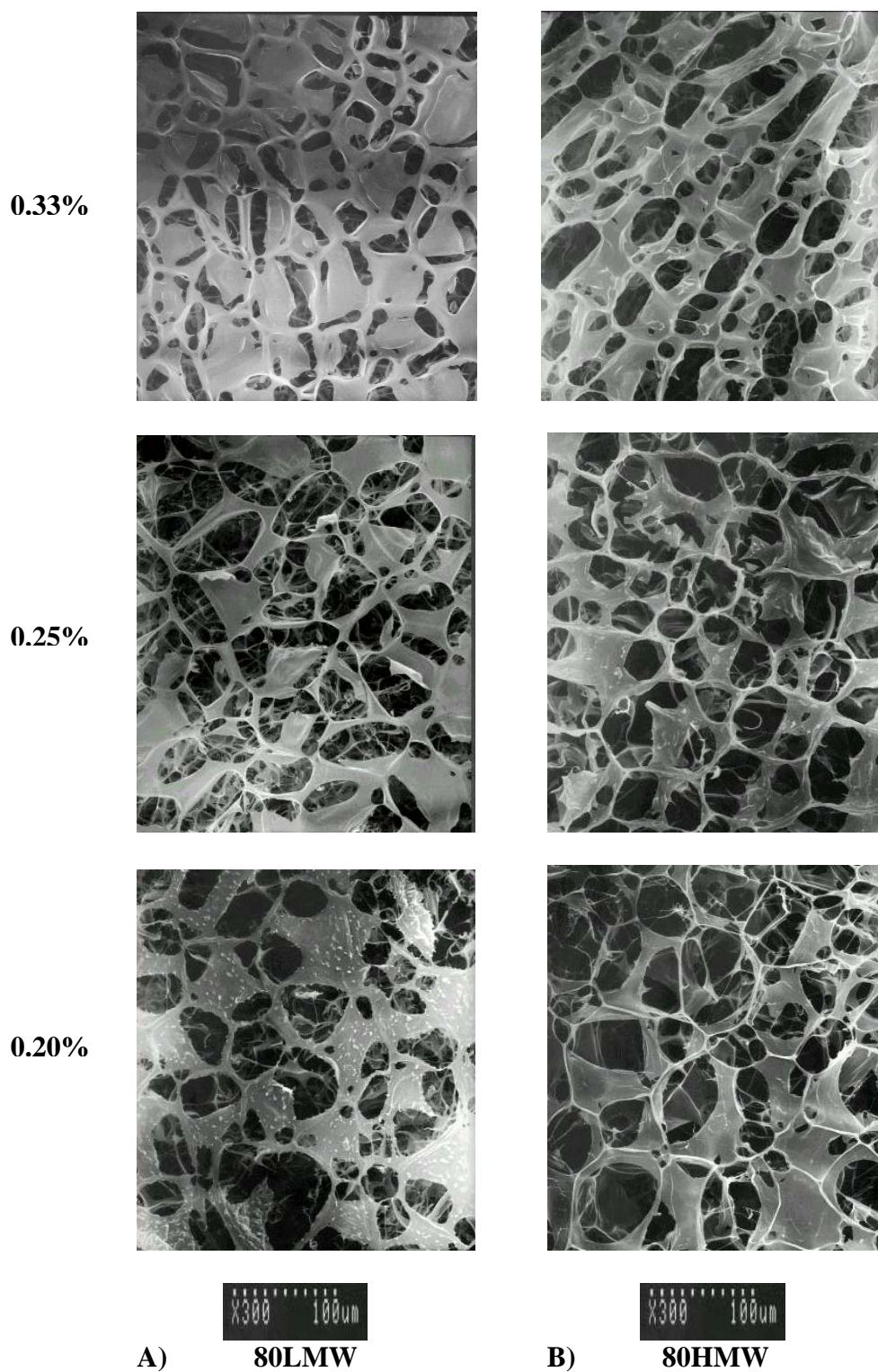


Figure 8 SEM images of chitosan scaffolds, frozen in -20°C refrigerator (x 300).

A) 80LMW chitosan scaffolds with 0.33%, 0.25% and 0.20% in concentration.

B) 80HMW chitosan scaffolds with 0.33%, 0.25% and 0.20% in concentration.

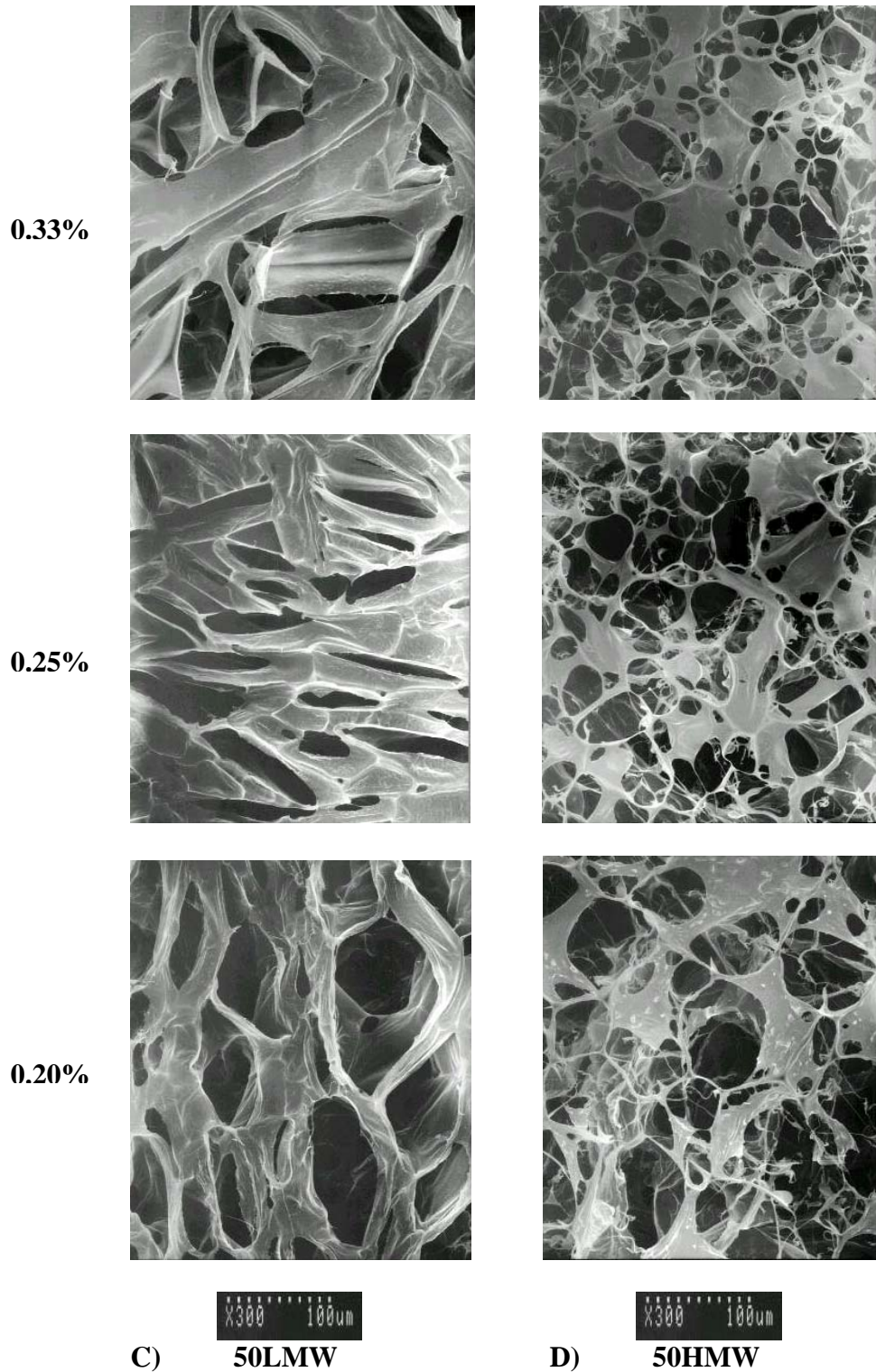


Figure 8 (con't) SEM images of chitosan scaffolds, frozen in -20°C refrigerator (x 300). C) 50LMW chitosan scaffolds with 0.33%, 0.25% and 0.20% in concentration. D) 50HMW chitosan scaffolds with 0.33%, 0.25% and 0.20% in concentration.

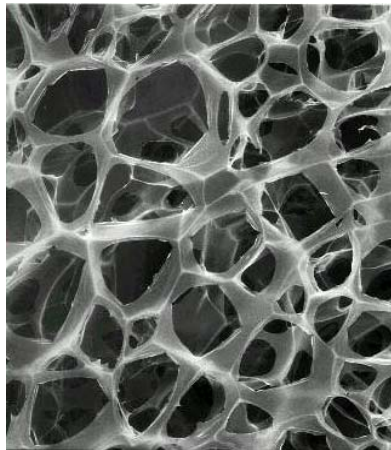
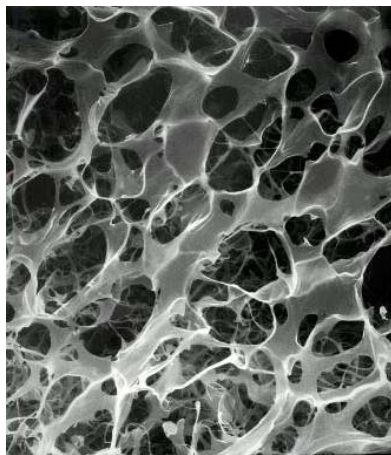
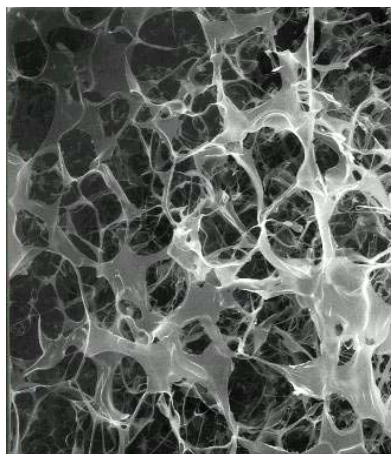
1.00%**0.25%****0.10%****Collagen**

Figure 9 SEM images of collagen scaffolds, frozen in -20°C refrigerator (x 300).
Collagen scaffolds with 1.00%, 0.25% and 0.10% in concentration.

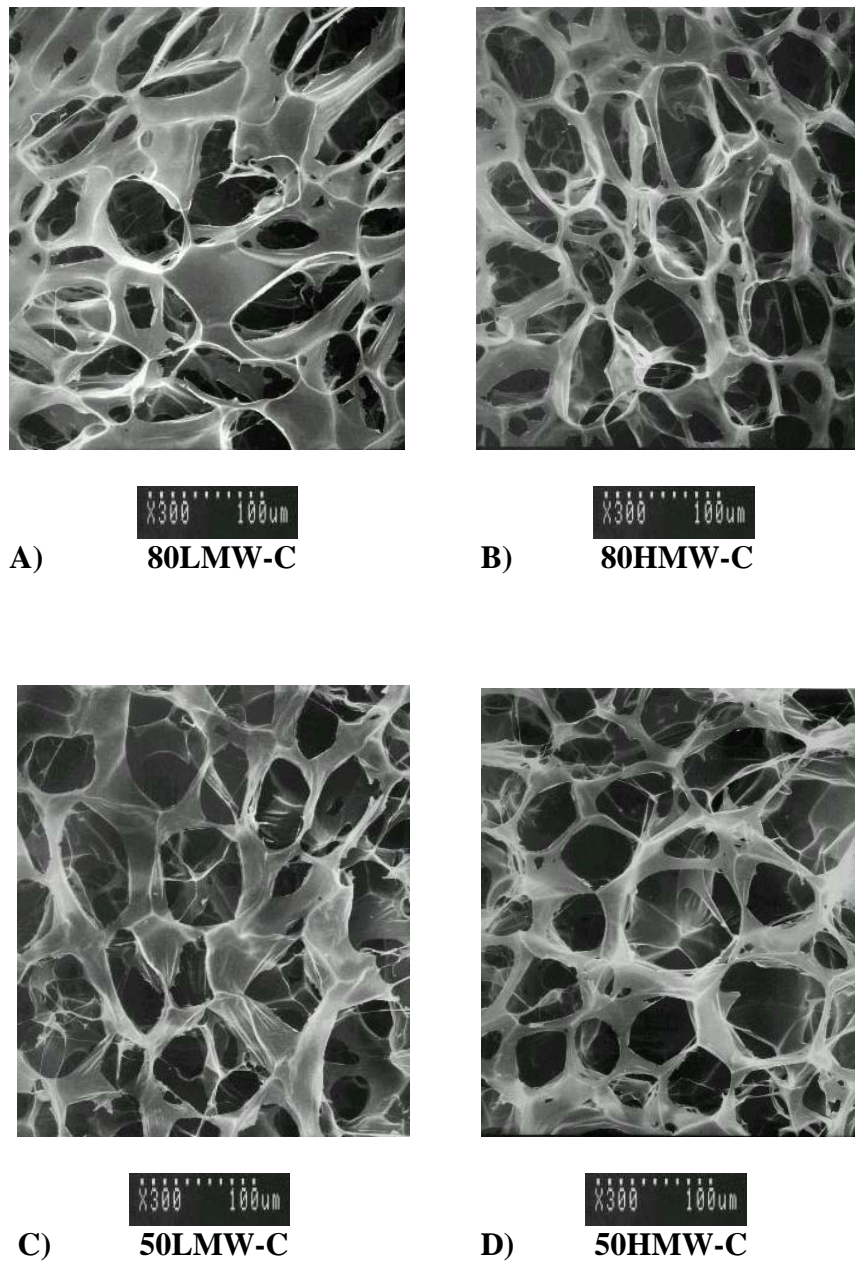


Figure 10 SEM images of chitosan-collagen scaffolds, frozen in -20°C refrigerator (x 300).

A) 80LMW-C chitosan-collagen scaffolds B) 80HMW-C chitosan-collagen scaffolds
C) 50LMW-C chitosan-collagen scaffolds D) 50HMW-C chitosan-collagen scaffolds

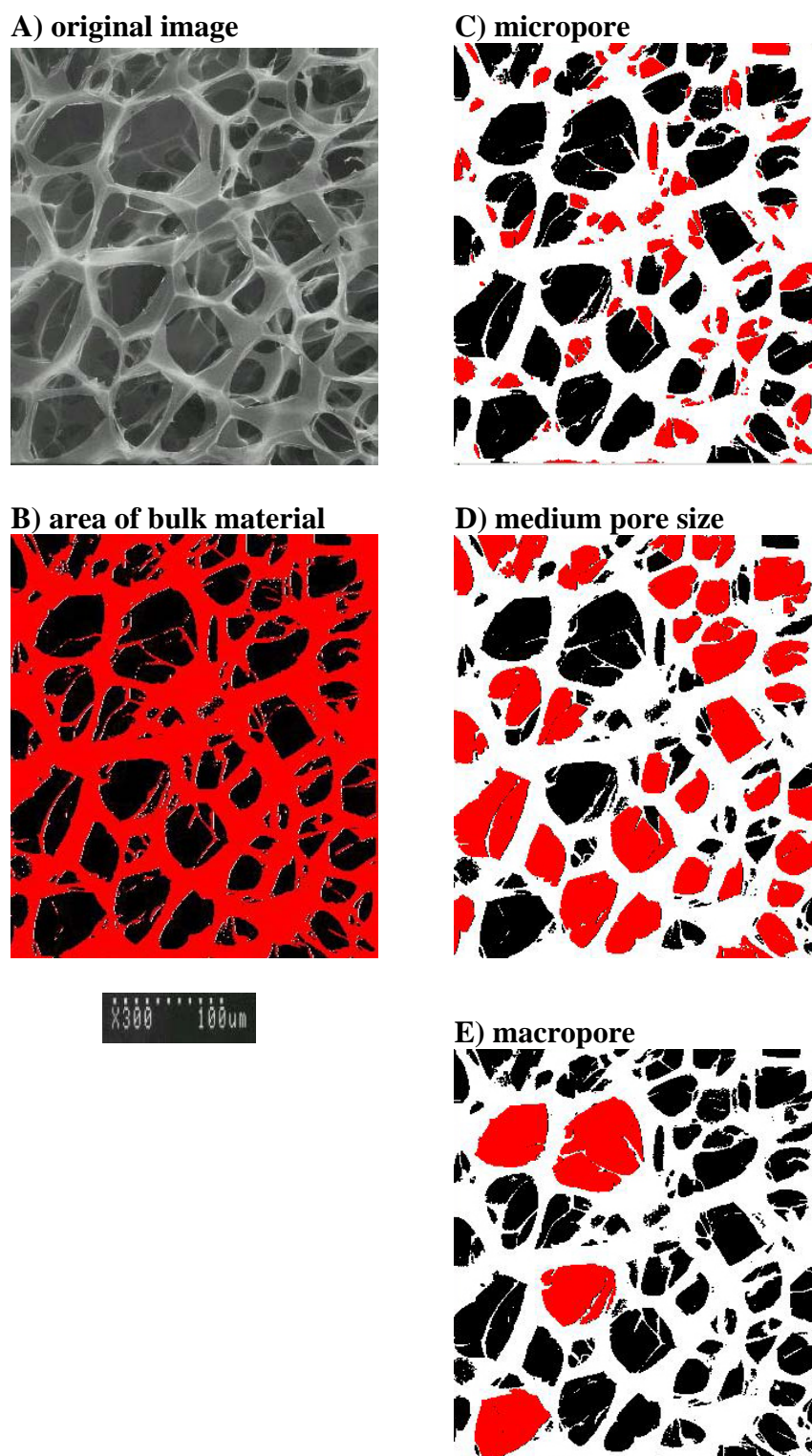


Figure 11 SEM image analysis by ImagePro[®] Plus software program

A) original scaffold B) area of bulk material C) micropore ($<20\ \mu\text{m}$)

D) medium pore size ($20\text{-}50\ \mu\text{m}$) E) macropore ($>50\ \mu\text{m}$)

Table 5 Chitosan scaffolds characterization, frozen in -80°C refrigerator

(NA = no available data)

Samples	Concentration	pore size in diameter (% average)			Area fraction (%)
		<20 μm	20-50 μm	>50 μm	
80LMW	0.33%	97.37	2.63	NA	84.69
	0.25%	98.92	1.08	NA	81.36
	0.20%	97.94	2.06	NA	81.26
80HMW	0.33%	95.56	4.44	NA	78.78
	0.25%	94.72	5.28	NA	78.65
	0.20%	96.30	3.70	NA	59.42
50LMW	0.33%	97.16	2.84	NA	79.54
	0.25%	93.86	6.14	NA	58.76
	0.20%	96.23	3.77	NA	54.61
50HMW	0.33%	96.05	3.95	NA	76.10
	0.25%	95.26	4.74	NA	56.37
	0.20%	90.12	9.88	NA	56.37

Table 6 Chitosan scaffolds characterization, frozen in -20°C refrigerator

(NA = no available data)

Samples	Concentration	pore size in diameter (% average)			Area fraction (%)
		<20 μm	20-50 μm	>50 μm	
80LMW	0.33%	95.83	4.17	NA	82.28
	0.25%	95.31	4.69	NA	58.82
	0.20%	94.13	5.59	0.28	58.04
80HMW	0.33%	93.83	5.88	0.29	67.36
	0.25%	89.82	9.58	0.60	55.64
	0.20%	92.41	7.34	0.25	58.62
50LMW	0.33%	91.95	6.04	2.01	79.89
	0.25%	85.50	12.21	2.29	71.32
	0.20%	90.91	7.36	1.73	66.64
50HMW	0.33%	95.48	4.52	NA	71.55
	0.25%	93.94	5.33	0.73	60.04
	0.20%	93.19	5.26	1.55	55.89

Table 7 Collagen scaffolds characterization, frozen in -20°C refrigerator

Samples	Concentration	pore size in diameter (% average)			Area fraction (%)
		<20 μm	20-50 μm	>50 μm	
Collagen	1.00%	81.73	16.34	1.93	60.19
Collagen	0.25%	92.91	6.04	1.05	54.30
Collagen	0.10%	92.54	6.22	1.24	48.86

Table 8 Chitosan-collagen scaffolds characterization, frozen in -20°C refrigerator

Samples	Concentration	pore size in diameter (% average)			Area fraction (%)
		<20 μm	20-50 μm	>50 μm	
80LMW-C	0.25%	90.20	7.84	1.96	70.73
80HMW-C	0.25%	82.51	14.21	3.28	51.32
50LMW-C	0.25%	87.45	10.34	2.21	46.10
50HMW-C	0.25%	86.86	11.86	1.28	62.32

The effect of chitosan, collagen and chitosan-collagen scaffolds on MC3T3-E1 cells attachment and proliferation.

After seeding and culturing MC3T3-E1 cells (2×10^4 cells/ml.) on test scaffolds, the MTT assay was performed to assess the effects of chitosan, collagen, and chitosan-collagen scaffolds on cell attachment (at 5 and 24 hours) and on cell proliferation (on day 1, 3, 5, 7, 10, 14). The optical density values at 540 nm. (OD_{540}) of MTT were calculated from nine samples in triplicate and presented in Mean \pm standard deviation. Statistical significance was accepted at $p\text{-value} < 0.05$. In these experiments, the test scaffolds were divided into 9 groups composed of collagen, 80LMW, 80HMW, 50LMW, 50HMW, 80LMW-C, 80HMW-C, 50LMW-C and 50HMW-C scaffolds, comparing cover slips which comprised the control group. During the experimental periods, the lower degree of deacetylation of chitosan scaffolds (50LMW and 50HMW) were excluded from the study because these scaffolds detached from cover slips. Thus, the test scaffolds were determined in 7 groups.

For cell attachment, the OD_{540} of MTT of each test scaffolds are shown in Table 9. All test scaffolds showed no statistically significant difference from the control at 5 and 24 hours. In comparison to collagen scaffolds, both chitosan and chitosan-collagen scaffolds showed no statistically significant difference from them at 5 and 24 hours. When comparing chitosan scaffolds to chitosan-collagen scaffolds in each degree of deacetylation and molecular weight, also no statistically significant difference was found at 5 and 24 hours. Thereby, it was obvious that MC3T3-E1 cells can attach well whether on chitosan and chitosan-collagen scaffolds, irrespective of degree of deacetylation and molecular weight of chitosan (Figure 12).

Table 9 The absorbance of the MTT formazan formation after MC3T3-E1 cells attachment (Mean \pm SD.). Statistical significance was accepted at p -value < 0.05 .

Samples \ Times	5 hrs. (Mean \pm SD.)	24 hrs. (Mean \pm SD.)
Control	0.063 \pm 0.004	0.072 \pm 0.009
Collagen	0.062 \pm 0.006	0.078 \pm 0.010
80LMW	0.062 \pm 0.004	0.067 \pm 0.006
80HMW	0.060 \pm 0.005	0.077 \pm 0.010
80LMW-C	0.061 \pm 0.006	0.068 \pm 0.007
80HMW-C	0.065 \pm 0.006	0.076 \pm 0.007
50LMW-C	0.070 \pm 0.003	0.074 \pm 0.008
50HMW-C	0.066 \pm 0.004	0.079 \pm 0.007

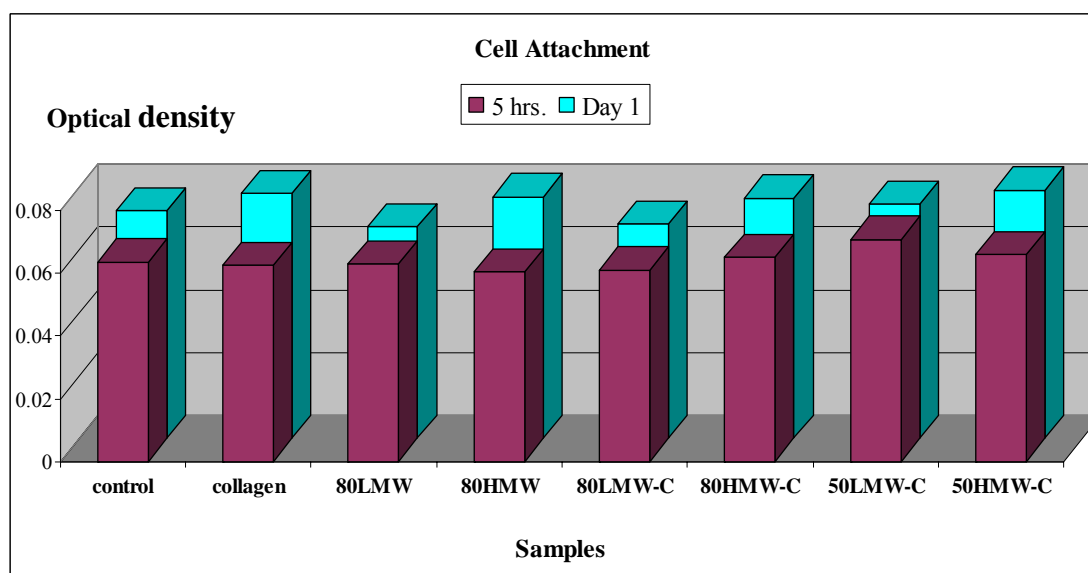


Figure 12 The absorbance of MTT formazan formation at 5 and 24 hours for cell attachment assay. Each value was calculated from nine samples and presented in Mean \pm SD. Statistical significance was accepted at p -value < 0.05 .

For cell proliferation, the OD₅₄₀ of MTT of each test scaffolds are shown in Table 10. The results showed that the MC3T3-E1 cells increasingly proliferated on all test scaffolds and control after cell attachment, however, the cell proliferation rates were different in each test scaffold throughout the experimental periods (Figure 13-14). On day 1 (Figure 15), all test scaffolds showed no statistically significant difference from the control but a statistically significant difference was found among the test scaffolds and control on the following days. On day 3 (Figure 16), the MC3T3-E1 cells proliferated well on control, collagen, and 50LMW-C scaffolds, respectively. The OD₅₄₀ values of MTT on collagen, 80HMW-C and 50LMW-C scaffolds showed a statistically significant difference from the other test scaffolds. In contrast, no statistically significant difference was found from the control. On day 5 (Figure 17), the MC3T3-E1 cells proliferated well on 50LMW-C, control and collagen scaffolds, respectively. The OD₅₄₀ values of MTT on collagen and 50LMW-C scaffolds showed a statistically significant difference from the other test scaffolds whereas only the OD₅₄₀ values of MTT on 50LMW-C scaffolds showed no statistically significant difference from the control. On day 7 (Figure 18), the MC3T3-E1 cells proliferated well on control, 50LMW-C and collagen scaffolds, respectively. The OD₅₄₀ values of MTT on collagen and 50LMW-C scaffolds showed a statistically significant difference from the other test scaffolds. In contrast, no statistically significant difference was found from the control. On day 10 (Figure 19), the MC3T3-E1 cells proliferated well on the control, collagen, and 50LMW-C scaffolds, respectively. The OD₅₄₀ values of MTT on collagen, 50LMW-C and 50HMW-C scaffolds showed a statistically significant difference from the other test scaffolds. In contrast, no statistically significant difference was found from the control. On day 14 (Figure 20), the MC3T3-E1 cells proliferated well on the control, 50LMW-C and collagen scaffolds, respectively. The OD₅₄₀ values of MTT on collagen and 50LMW-C scaffolds showed a statistically significant difference from the other test scaffolds and control.

Table 10 The absorbance of the MTT formazan formation after MC3T3-E1 cells proliferation (Mean \pm SD.).Statistical significance was accepted at $p\text{-value} < 0.05$.

* statistically significant difference from the control, # statistically significant from 50LMW-C

Times Samples	Day 1 (Mean \pm SD.)	Day 3 (Mean \pm SD.)	Day 5 (Mean \pm SD.)	Day 7 (Mean \pm SD.)	Day 10 (Mean \pm SD.)	Day 14 (Mean \pm SD.)
Control	0.072 \pm 0.009	0.163 \pm 0.038	0.289 \pm 0.019	0.409 \pm 0.049	0.603 \pm 0.027	0.860 \pm 0.031#
Collagen	0.078 \pm 0.010	0.151 \pm 0.013	0.264 \pm 0.010*#	0.362 \pm 0.011	0.590 \pm 0.059	0.817 \pm 0.024*
80LMW	0.067 \pm 0.006	0.114 \pm 0.018*#	0.175 \pm 0.024*#	0.210 \pm 0.038*#	0.337 \pm 0.048*#	0.537 \pm 0.064*#
80HMW	0.077 \pm 0.010	0.121 \pm 0.020*#	0.176 \pm 0.009*#	0.238 \pm 0.027*#	0.358 \pm 0.036*#	0.538 \pm 0.053*#
80LMW-C	0.068 \pm 0.007	0.100 \pm 0.021*#	0.182 \pm 0.029*#	0.255 \pm 0.026*#	0.434 \pm 0.047*#	0.733 \pm 0.061*#
80HMW-C	0.076 \pm 0.007	0.150 \pm 0.047	0.234 \pm 0.026*#	0.267 \pm 0.024*#	0.429 \pm 0.049*#	0.743 \pm 0.074*#
50LMW-C	0.074 \pm 0.008	0.150 \pm 0.006	0.309 \pm 0.030	0.362 \pm 0.050	0.585 \pm 0.031	0.818 \pm 0.034*
50HMW-C	0.079 \pm 0.007	0.125 \pm 0.028*	0.239 \pm 0.023*#	0.312 \pm 0.016*#	0.567 \pm 0.038	0.780 \pm 0.059*

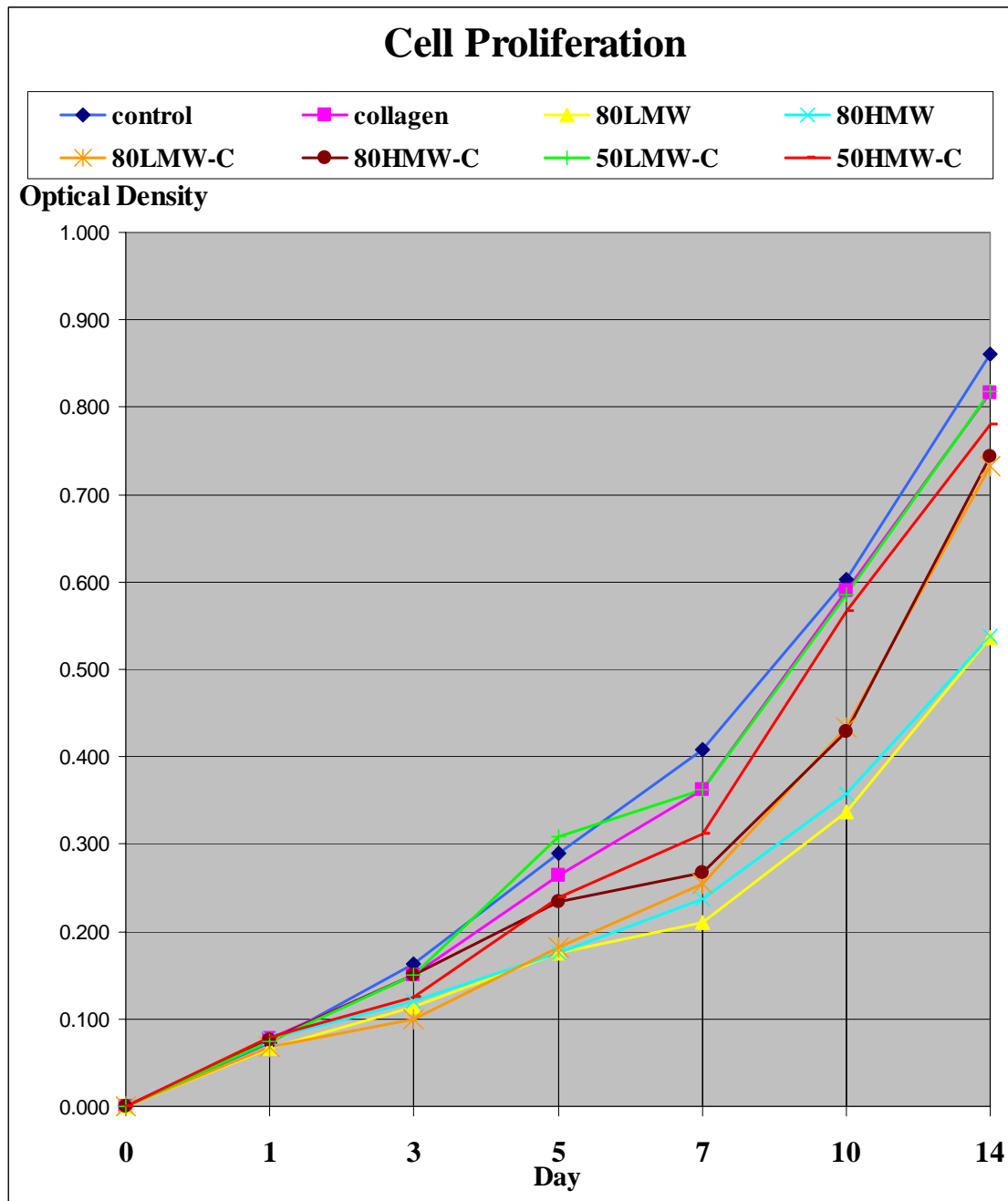


Figure 13 The absorbance of MTT formazan formation on day 1, 3, 5, 7, 10 and 14 for cell proliferation assay. Each value was calculated from nine samples and presented in Mean \pm SD. Statistical significance was accepted at p -value < 0.05 .

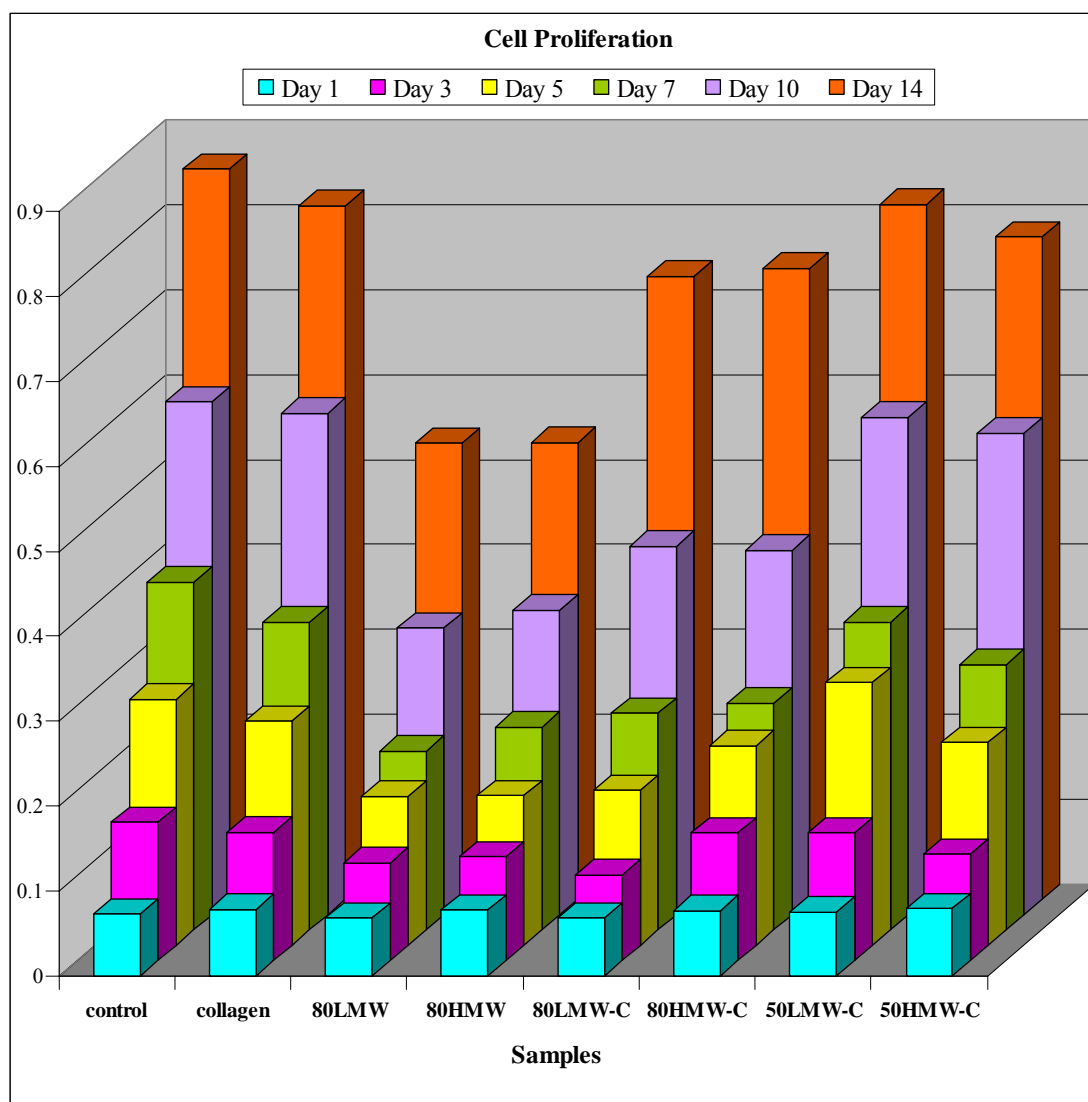


Figure 14 The absorbance of MTT formazan formation on day 1, 3, 5, 7, 10 and 14 for cell proliferation assay (Bar chart). Each value was calculated from nine samples and presented in Mean \pm SD. Statistical significance was accepted at *p-value* < 0.05 .

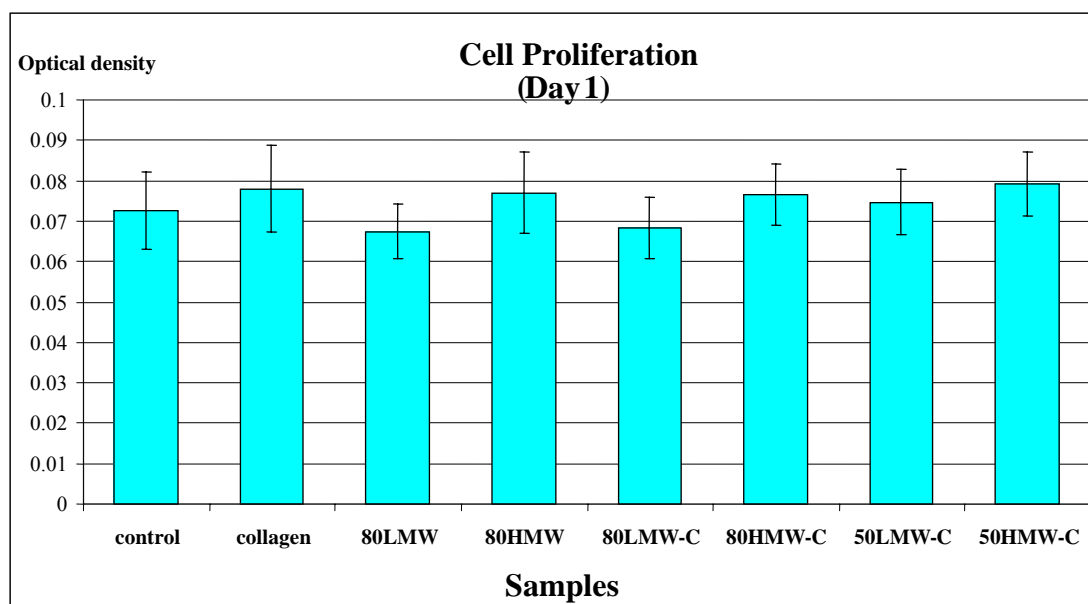


Figure 15 The absorbance of MTT formazan formation on day 1 for cell proliferation assay. Each value was calculated from nine samples and presented in Mean \pm SD. Statistical significance was accepted at p -value < 0.05 .

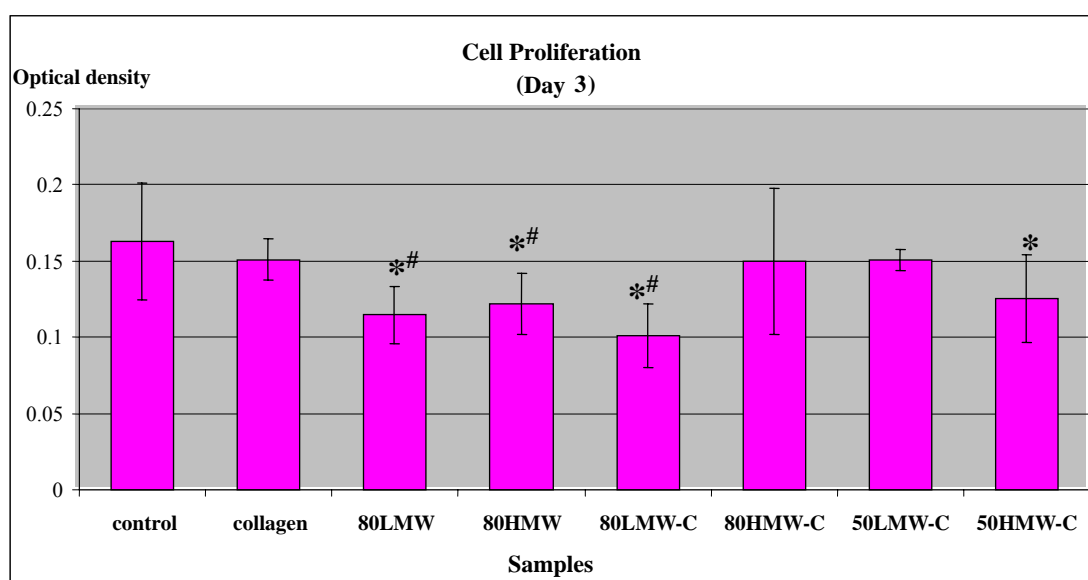


Figure 16 The absorbance of MTT formazan formation on day 3 for cell proliferation assay. Each value was calculated from nine samples and presented in Mean \pm SD. Statistical significance was accepted at p -value < 0.05 .

* statistically significant difference from the control, # statistically significant from 50LMW-C

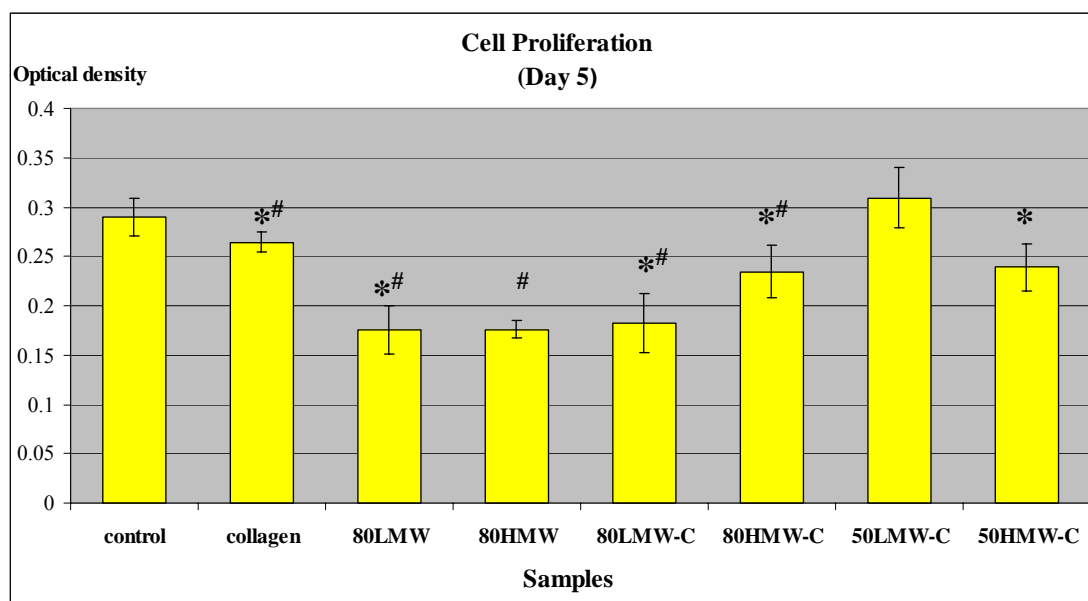


Figure 17 The absorbance of MTT formazan formation on day 5 for cell proliferation assay. Each value was calculated from nine samples and presented in Mean ± SD. Statistical significance was accepted at $p\text{-value} < 0.05$.

* statistically significant difference from the control, # statistically significant from 50LMW-C

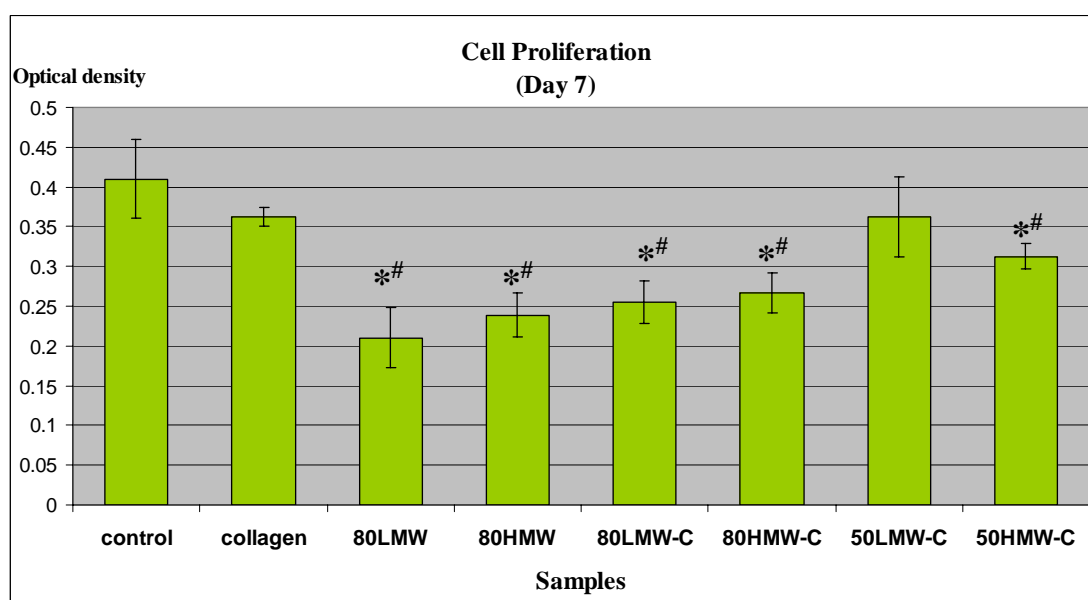


Figure 18 The absorbance of MTT formazan formation on day 7 for cell proliferation assay. Each value was calculated from nine samples and presented in Mean ± SD. Statistical significance was accepted at $p\text{-value} < 0.05$.

* statistically significant difference from the control, # statistically significant from 50LMW-C

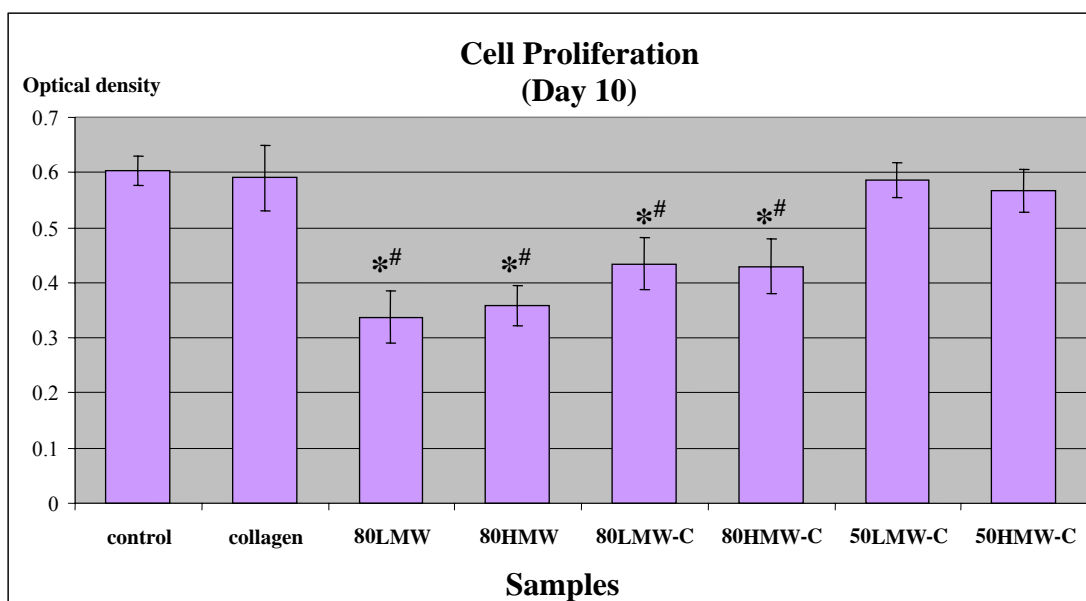


Figure 19 The absorbance of MTT formazan formation on day 10 for cell proliferation assay. Each value was calculated from nine samples and presented in Mean ± SD. Statistical significance was accepted at $p\text{-value} < 0.05$.

* statistically significant difference from the control, # statistically significant from 50LMW-C

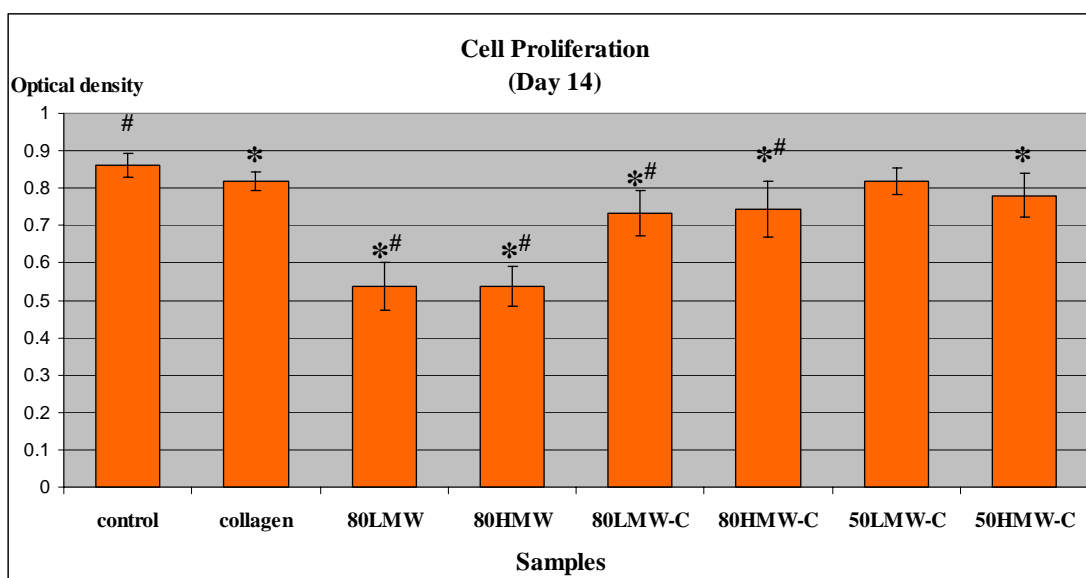


Figure 20 The absorbance of MTT formazan formation on day 14 for cell proliferation assay. Each value was calculated from nine samples and presented in Mean ± SD. Statistical significance was accepted at $p\text{-value} < 0.05$

* statistically significant difference from the control, # statistically significant from 50LMW-C

When the effect of collagen on cell proliferation was considered, collagen scaffolds were chosen to be compared with chitosan-collagen scaffolds for each different degree of deacetylation and molecular weight. The results showed that the effect of collagen and chitosan-collagen scaffolds on cell proliferation was diverse (Table 10, Figure 15-20). In spite of the fact that the concentration of collagen both in the collagen and chitosan-collagen scaffolds were equal to 0.25% weight by volume (w/v), only 50LMW-C scaffolds on day 3, 7, 10 and 14 and 50HMW-C scaffolds on day 3, 5, 10 and 14 had a proliferation effect corresponding to collagen scaffolds. On the other hand, 80LMW-C and 80HMW-C scaffolds had a less proliferative effect than collagen scaffolds throughout experimental periods.

Regarding the high degree of deacetylation of chitosan, the results showed that the high degree of deacetylation of chitosan, either with or without collagen, had a less proliferative effect on MC3T3-E1 cells in comparison with the other test scaffolds.

The effect of collagen and chitosan-collagen scaffolds on alkaline phosphatase activity.

MC3T3-E1 cells (2×10^4 cells/ml.) were seeded and cultured on test scaffolds for 26 days. After reaching confluence (day 3), cells were cultured in α -MEM containing 10 mM β -glycerophosphate and 50 μ g/ml of ascorbic acid. The alkaline phosphatase activity was determined in cell lysate by measuring the release of p-nitrophenol (PNP) from disodium p-nitrophenyl phosphate (PNPP), and was expressed in nmol/mg.of protein/min. Each value was calculated from twelve samples in duplicate and presented in Mean \pm standard deviation. Statistical significance was accepted at *p-value* < 0.05. In this experiment, the test scaffolds were divided into 5 groups, composed of collagen, 80LMW-C, 80HMW-C, 50LMW-C and 50HMW-C scaffolds, comparing cover slips which comprised the control group. The level of alkaline phosphatase activity in test scaffolds and control are shown in Table 11. Figure 21-22 showed that all test scaffolds increased alkaline phosphatase activity in the same pattern as the control throughout the experimental periods. The alkaline phosphatase activity increased during differentiation, reaching a maximum on day 4 for all test scaffolds and control but a statistically significant difference was found among all test scaffolds and control. Collagen scaffolds showed a statistically significant difference from the chitosan-collagen scaffolds, with the exception of 50LMW-C, no statistically significant difference was found. Regarding the low degree of deacetylation of chitosan in chitosan-collagen scaffolds, no statistically significant difference was found between low and high molecular weights. Afterwards, the alkaline phosphatase activity gradually decreased between day 6 and day 10, and maintained this plateau level on the following days for all test scaffolds and control. From this point of view, the results suggested that all test scaffolds had the same pattern of alkaline phosphatase activity as control during differentiation, albeit the control had more the alkaline phosphatase activity in the early stage of differentiation. In addition, the results indicated that chitosan-collagen scaffolds with the low degree of deacetylation of chitosan had more alkaline phosphatase activity than chitosan-collagen scaffolds with high degree of deacetylation of chitosan, regardless of molecular weight.

Table 11 The alkaline phosphatase activity of MC3T3-E1 cells on test scaffolds and control The alkaline phosphatase activity were expressed in nmol PNP/mg of protein/min. Each value was calculated from twelve samples in duplicate and presented in Mean \pm standard deviation. Statistical significance was accepted at p -value < 0.05

* statistically significant difference from the control, # statistically significant from 50LMW-C

Samples	Day 4 (Mean \pm SD.)	Day 6 (Mean \pm SD.)	Day 10 (Mean \pm SD.)	Day 14 (Mean \pm SD.)	Day 18 (Mean \pm SD.)	Day 22 (Mean \pm SD.)	Day 26 (Mean \pm SD.)
Control	5.00 \pm 0.82#	3.62 \pm 1.71#	0.94 \pm 0.10	1.04 \pm 0.03#	0.89 \pm 0.20#	0.99 \pm 0.17	0.91 \pm 0.05
Collagen	2.86 \pm 0.63*	1.62 \pm 0.738*#	0.84 \pm 0.08*#	0.93 \pm 0.04*	0.92 \pm 0.19	1.00 \pm 0.19	0.89 \pm 0.04
80LMW-C	1.98 \pm 0.38*	1.41 \pm 0.36*#	0.91 \pm 0.07	0.89 \pm 0.06*	0.90 \pm 0.10	0.99 \pm 0.13	0.83 \pm 0.05*
80HMW-C	1.42 \pm 0.36*#	1.25 \pm 0.25*#	0.88 \pm 0.10*#	0.90 \pm 0.07*	0.87 \pm 0.13#	0.96 \pm 0.16	0.83 \pm 0.04*
50LMW-C	2.41 \pm 0.79*	2.13 \pm 0.61*	0.95 \pm 0.12	0.93 \pm 0.06*	0.98 \pm 0.19	0.98 \pm 0.22	0.86 \pm 0.06
50HMW-C	2.26 \pm 0.54*	1.61 \pm 0.47*#	0.99 \pm 0.15	0.95 \pm 0.07*	0.91 \pm 0.18	1.00 \pm 0.24	0.88 \pm 0.06

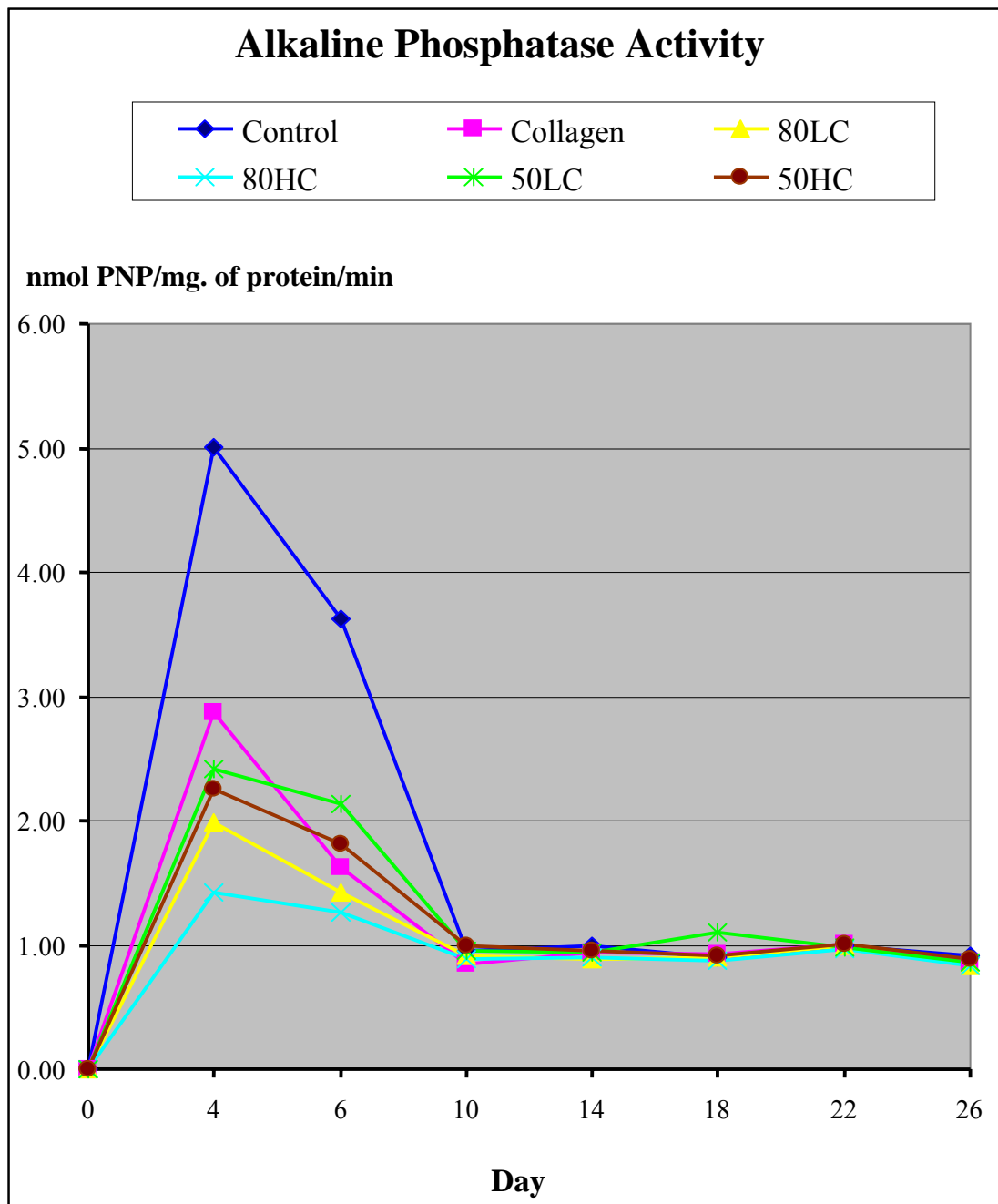


Figure 21 The effect of collagen and chitosan-collagen scaffolds on alkaline phosphatase activity of MC3T3-E1 cells. The alkaline phosphatase activity were expressed in nmol/mg.of protein/min. Each value was calculated from twelve samples in duplicate and presented in Mean \pm SD. Statistical significance was accepted at p -value < 0.05 .

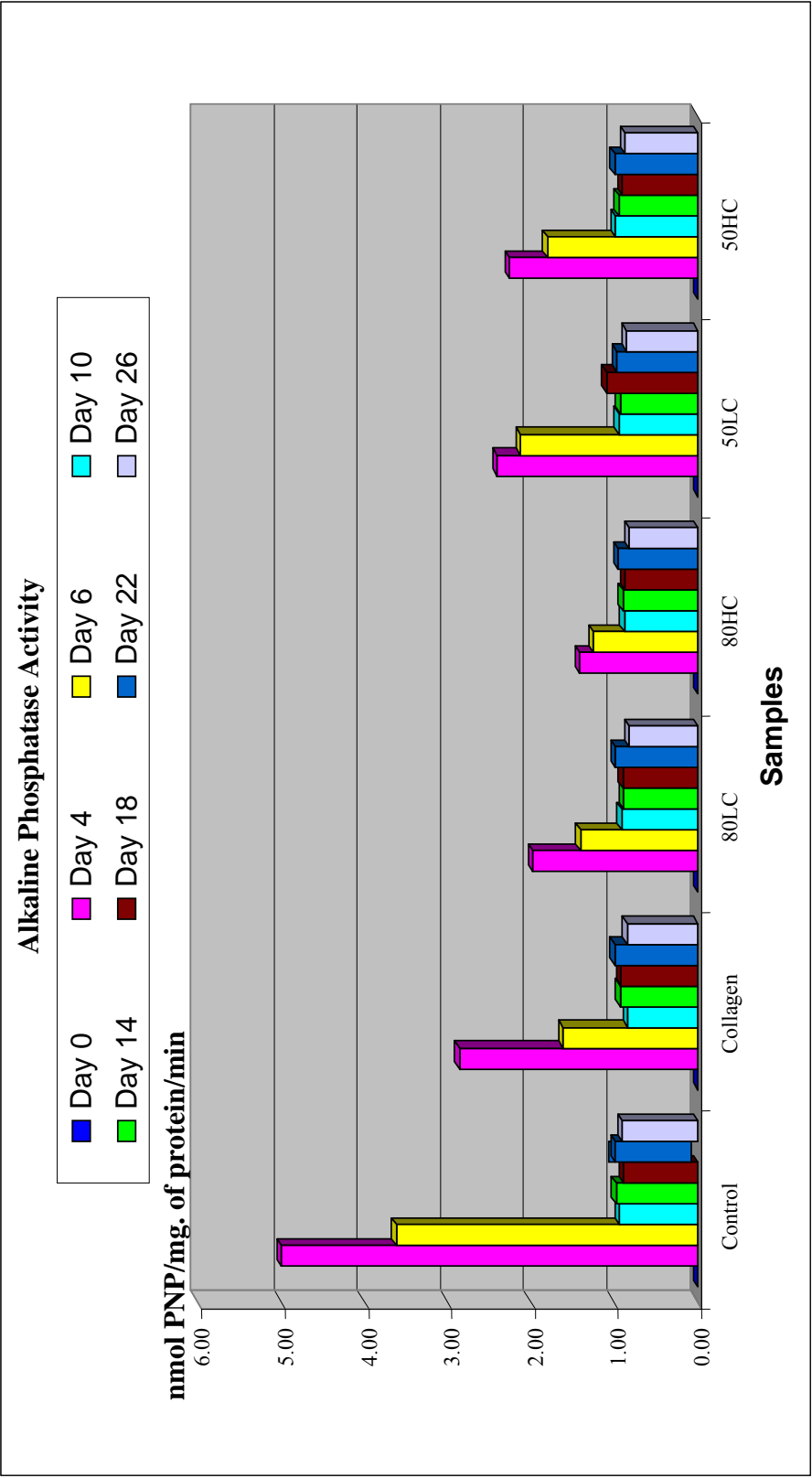


Figure 22 The effect of collagen and chitosan-collagen scaffolds on alkaline phosphatase activity of MC3T3-E1 cells (Bar chart)
The alkaline phosphatase activity were expressed as nmol PNP/mg. of protein/min. Each value was calculated from twelve samples in duplicate and presented in Mean \pm SD. Statistical significance was accepted at $p\text{-value} < 0.05$.

The effect of collagen and chitosan-collagen scaffolds on MC3T3-E1 cell morphology, behavior and mineralized nodule formation.

MC3T3-E1 cells (2×10^4 cells/ml.) were seeded and cultured on test scaffolds for 26 days. After reaching confluence (day 3), cells were cultured in α -MEM containing 10 mM β -glycerophosphate and 50 μ g/ml of ascorbic acid. Cell morphology, behavior and mineralized nodule formation were checked routinely by phase contrast microscope and examined by scanning electron microscope on day 4, 10 and 18 after plating. In this experiment, the test scaffolds were divided into 5 groups, composed of collagen, 80LMW-C, 80HMW-C, 50LMW-C and 50HMW-C scaffolds, comparing cover slips which comprised the control group. Before cell seeding, the distribution of interconnected micropore structure of each test scaffolds were previously characterized in the first part of this research thesis.

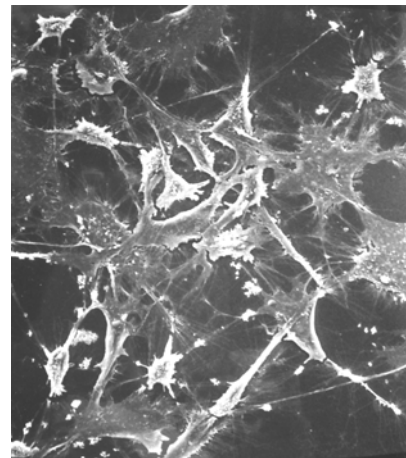
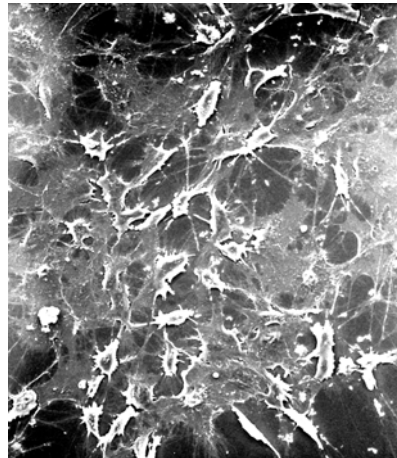
Regarding cell morphology and behavior, the MC3T3-E1 cells on the control and test scaffolds were fixed, stained, dehydrated and examined by scanning electron microscope at various time points. SEM images demonstrated that the porous structure of all test scaffolds promoted intercellular contact and accumulation of extracellular matrix comparing to the control (Figure 23-28). MC3T3-E1 cells attached, spread and sprouted their cytoplasmic process, filopodia, on the test scaffold surface and grew well on these test scaffolds, although growth rate of cells are different. On day 4, the results showed that chitosan-collagen scaffolds with lower degree of deacetylation of chitosan were covered with overlying cell layer and extracellular matrix more than chitosan-collagen scaffolds with high degree of deacetylation of chitosan. Nevertheless, overlying cell layer did not reach confluence, the bulk of test scaffolds in the background and the overlying cell layer and extracellular matrix could be observed. On day 10, cells were spread and grew in multilayers. Intercellular connections were maintained through cytoplasmic elongations. Many anchoring processes were observed extending from cells to biomaterial surface as well to the other cells. The results showed that chitosan-collagen scaffolds with lower degree of deacetylation of chitosan were fully covered by MC3T3-E1 cells. In contrast, chitosan-collagen scaffolds with high degree of deacetylation of chitosan, overlying cell layer did not reach confluence, the bulk of test scaffolds in the background and the overlying cell layer with extracellular matrix

could be observed. On day 18, all test scaffolds had multilayer cells and deposited matrix throughout the entire scaffolds. The matured MC3T3-E1 cells grew in the same direction and arranged in parallel. Some areas in SEM images suggested that MC3T3-E1 cells accumulated in nodule-like structure and tended to be calcification.

For mineralized nodule formation, MC3T3-E1 cells were checked routinely with phase contrast microscope. In the control cells, opaque regions appeared on day 14 of culture. The mineralized nodules became progressively more opaque and enlarged between day 14 and day 22 of culture. The mineralized nodules formations were determined by staining with alizarin red-S (Figure 29-30). In contrast, the appearance of opaque regions and mineralized nodule formation did not occur in test scaffolds (Figure 30).

In conclusion, it is interesting to note that chitosan-collagen scaffolds with low degree of deacetylation of chitosan promote MC3T3-E1 cell attachment, proliferation and differentiation more favorable than chitosan-collagen scaffolds with high degree of deacetylation of chitosan, regardless of molecular weight of chitosan. However, chitosan-collagen scaffolds either low or high degree of deacetylation of chitosan did not enhance mineralized nodule formation.

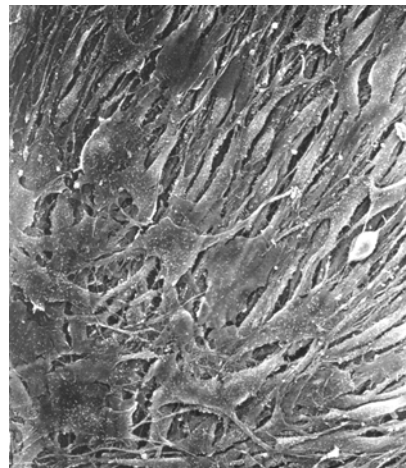
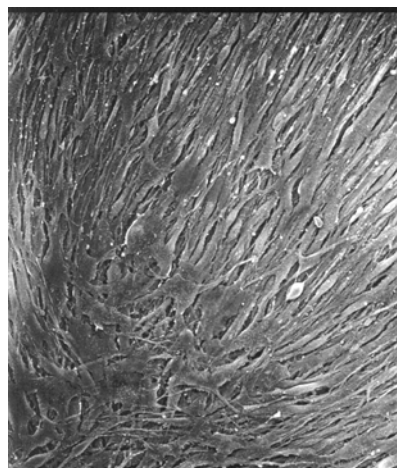
A) Day 4



B) Day 10



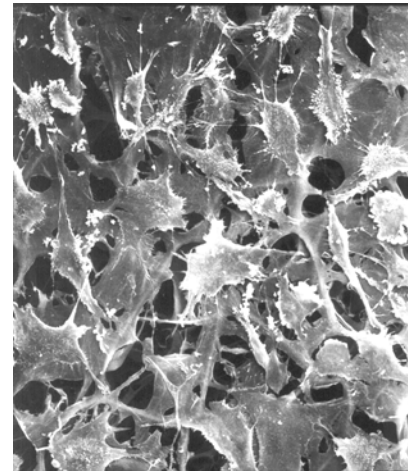
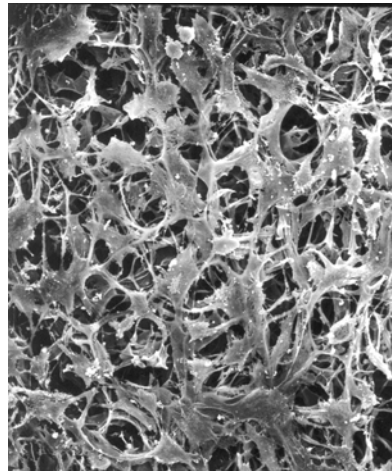
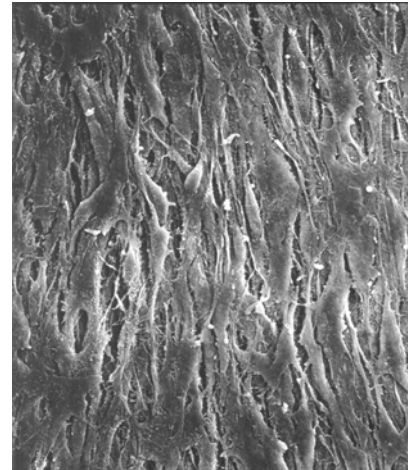
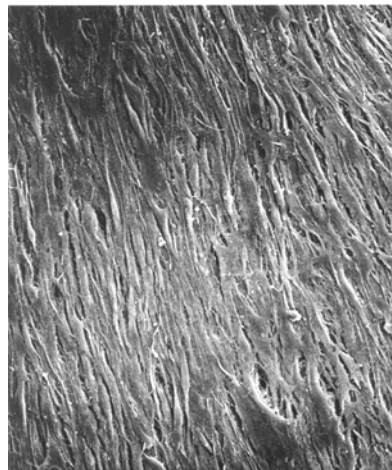
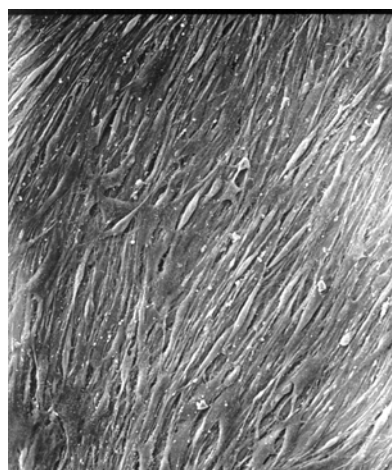
C) Day 18



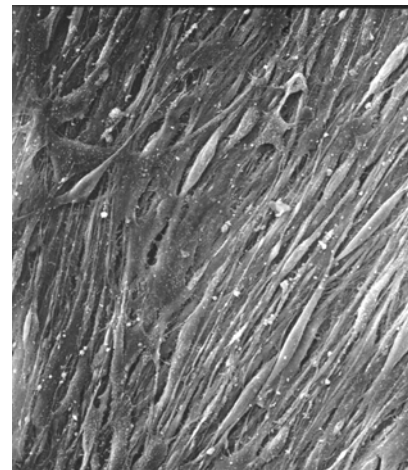
X300 100μm

X500 60μm

**Figure 23 SEM images of MC3T3-E1 cells on cover slips (control) (x 300, x 500).
A) Day 4 B) Day 10 C) Day 18**

A) Day 4**B) Day 10****C) Day 18**

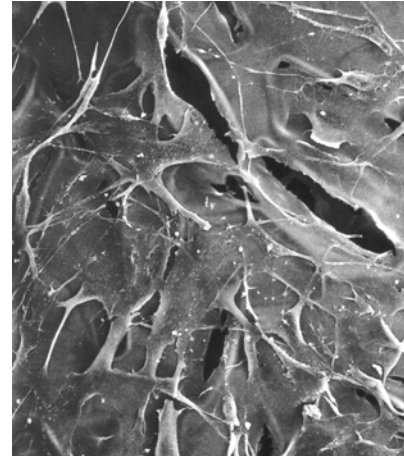
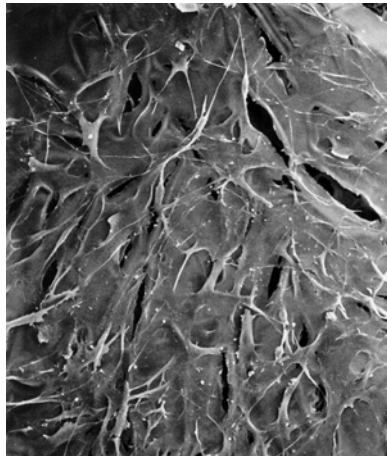
X300 100um



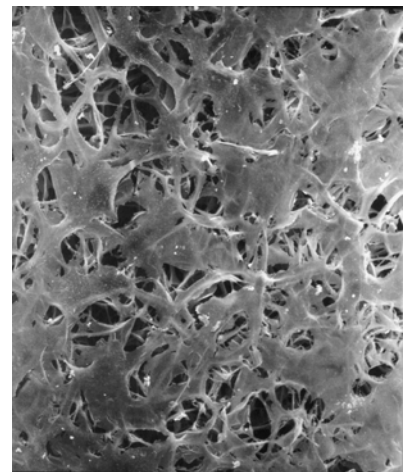
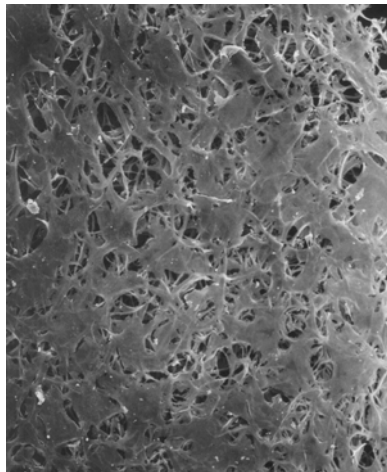
X500 60um

Figure 24 SEM images of MC3T3-E1 cells on collagen scaffolds (x 300, x 500).
A) Day 4 B) Day 10 C) Day 18

A) Day 4



B) Day 10

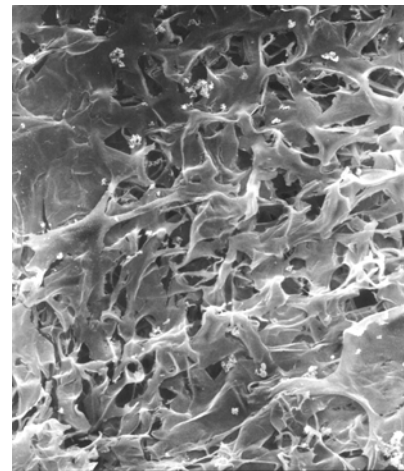
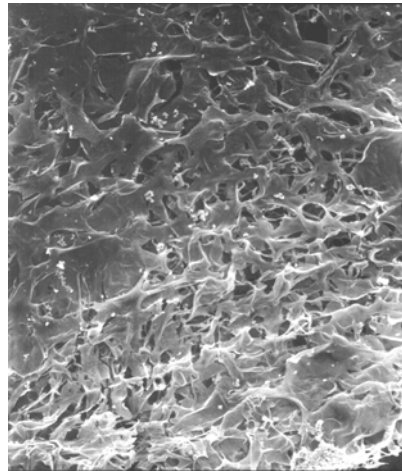


C) Day 18

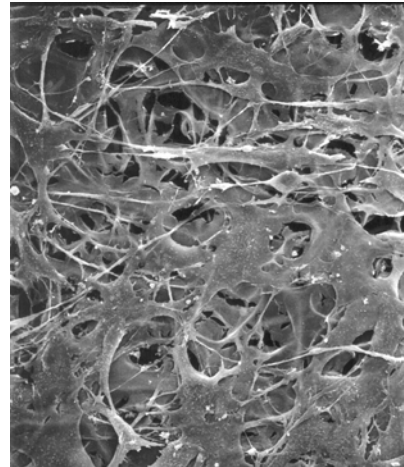
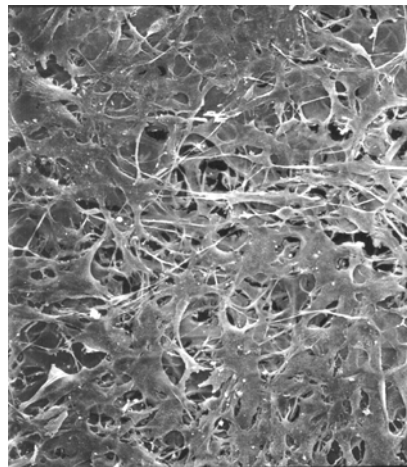


**Figure 25 SEM images of MC3T3-E1 cells on 80LMW-C scaffolds (x 300, x 500).
A) Day 4 B) Day 10 C) Day 18**

A) Day 4



B) Day 10



C) Day 18

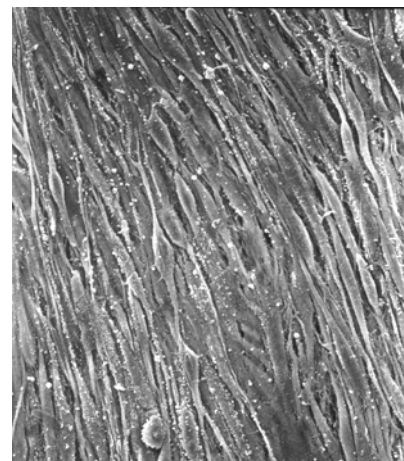
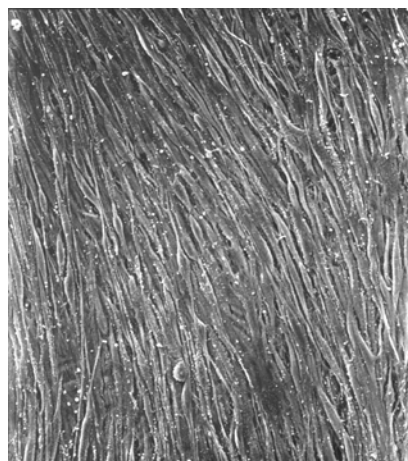
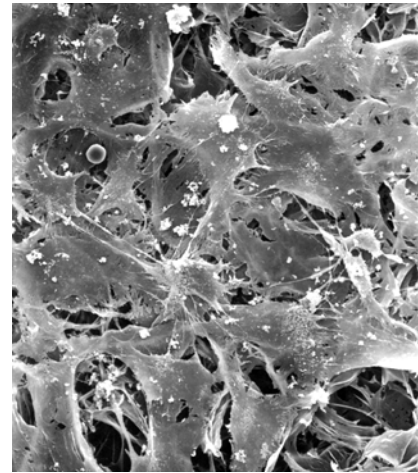
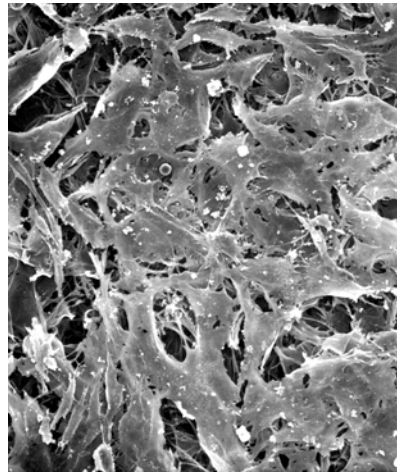
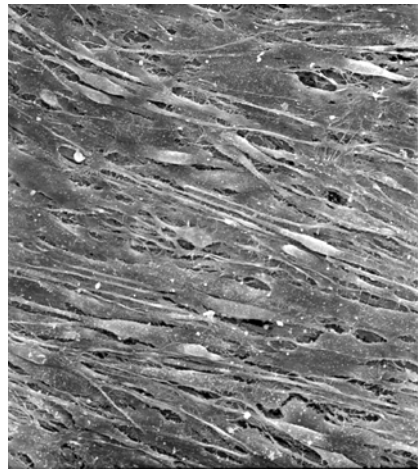
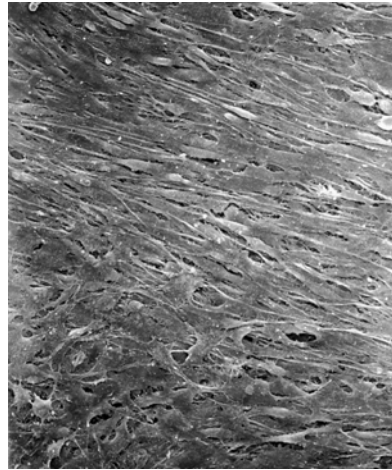


Figure 26 SEM images of MC3T3-E1 cells on 80HMW-C scaffolds (x 300, x 500).
 A) Day 4 B) Day 10 C) Day 18

A) Day 4



B) Day 10



C) Day 18

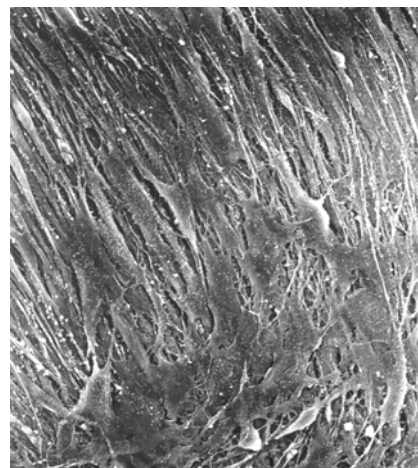
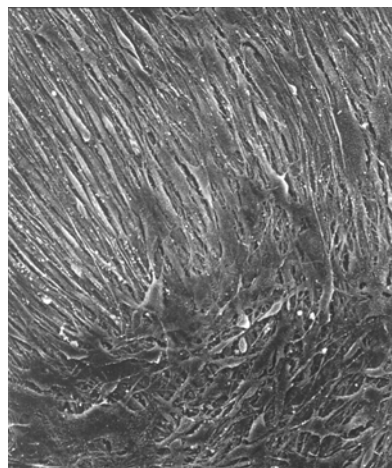
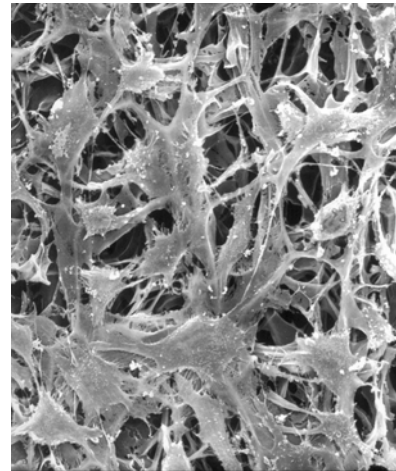
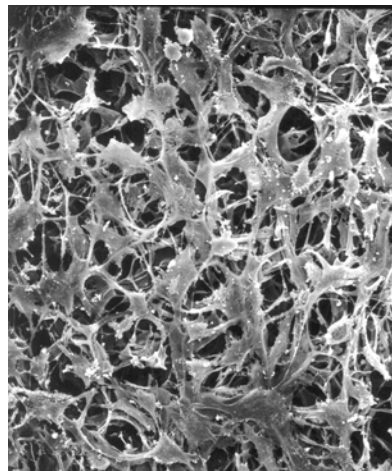
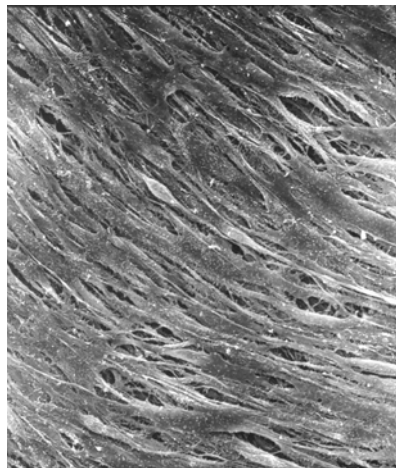
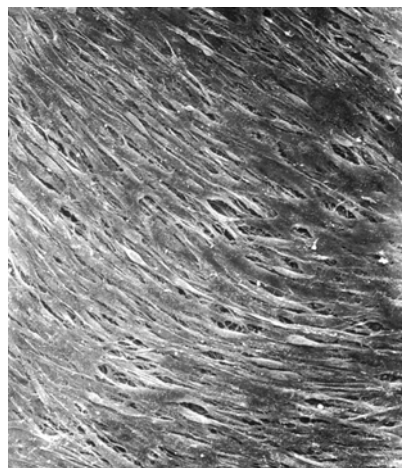


**Figure 27 SEM images of MC3T3-E1 cells on 50LMW-C scaffolds (x 300, x 500).
A) Day 4 B) Day 10 C) Day 18**

A) Day 4



B) Day 10



C) Day 18



X300 100um

X500 60um

**Figure 28 SEM images of MC3T3-E1 cells on 50HMW-C scaffolds (x 300, x 500).
A) Day 4 B) Day 10 C) Day 18**

A) Day 14



B) Day 18



C) Day 22

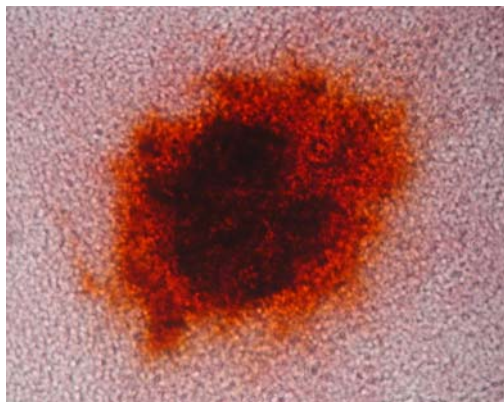
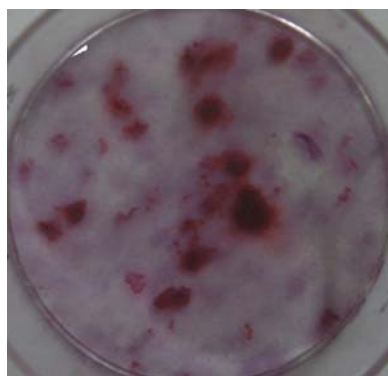
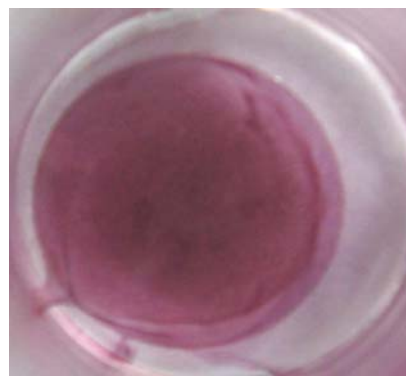


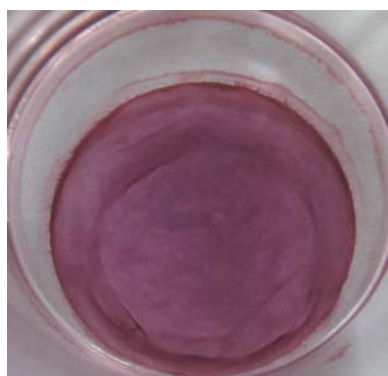
Figure 29 Mineralized nodule formation on cover slip (control).
A) Day 14 B) Day 18 C) Day 22



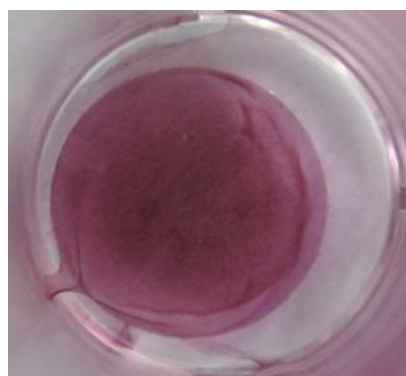
A) Control



B) Collagen



C) 80LMW-C



D) 80HMW-C



E) 50LMW-C



F) 50HMW-C

Figure 30 Images of control and test scaffolds after staining with alizarin red-S
A) control B) collagen C) 80LMW-C D) 80HMW-C E) 50LMW-C F) 50HMW-C

CHAPTER VI

DISCUSSION

Tissue engineering has been defined as the application of biological, chemical and engineered principles toward the repair, restoration or regeneration of living tissues using biomaterials as scaffolds, cells and growth factors alone or in combination. The development of scaffolding devices and the use of regenerative molecules were applied to periodontal tissue regeneration. The use of scaffolds serves not only as space maintainers, but also as delivery vehicles for targeting bioactive molecules to the wound site. Three dimensional scaffolds act as template that guide and accelerate new tissue formation. Candidate bone scaffold materials are hydroxyapatite (HP), tri-calcium phosphate (TCP), polylactic acid (PLA), polyglycolic acid (PGA) and polylactic-polyglycolic acid copolymers (PLGA), including polysaccharides such as chitosan and glycosaminoglycans (GAGs) (45, 143).

Chitosan has been extensively used in bone tissue engineering since its biocompatibility (98, 104-107) and biodegradability (102-103, 121-123), and it can be developed in various forms (91-96) and controlled release of cytokines and growth factors (144-147). Degree of deacetylation and molecular weight are two important fundamental parameters which influence physicochemical properties (90, 103) and biological properties (98, 99-100, 110).

Scaffolds used for tissue engineering must have a porous architecture to allow ingrowth of cells, nutrient and waste transport. The effect of pore size on tissue regeneration is emphasized by experiments demonstrating optimum pore size of 5 μm for nutrient transportation and vascularization, larger than 20 μm for soft tissue ingrowth, 40-100 μm for osteoid ingrowth, and 100-350 μm for regeneration of bone (56, 148). Chitosan can be molded into porous scaffolds with interconnectivity (144, 149-150). SEM photographs in Figure 7-8 demonstrated that chitosan scaffolds had unique porous microstructure and pore distribution according to different concentration, degree of deacetylation and molecular weight of chitosan. The mean

pore size of all test scaffolds was mostly micropore and medium pore size ranging from 0 to 50 μm , allowing nutrient and waste transportation, vascularization and soft tissue ingrowth. In addition, the pore size in this range was suitable for applying to fabricate periodontal membrane in guided tissue regeneration.

Interestingly, freezing temperature of lyophilized chitosan scaffolds had the influence on mean pore size. The results demonstrated that chitosan scaffolds prepared at high freezing temperature (-20°C) had more medium pore size and macropore than those prepared at low freezing temperature (-80°C). In general, ice crystals nucleate from solution and grow along the lines of thermal gradients during the freezing process. The freezing temperature has a role on controlling the cooling rate. The high freezing temperature generates ice crystal with slower cooling rate than the low freezing temperature. Additionally, ice removal by lyophilization generates a porous materials, the mean pore size can be controlled by varying the freezing temperature (45). Madihally *et al.* demonstrated the mean pore diameter of cylindrical chitosan scaffolds could be controlled within the range of 40 to 250 μm , by varying the freezing temperature and the cooling rate (148). Additionally, the structure of scaffolds produced using the constant cooling rate technique ($0.9^{\circ}\text{C}/\text{min}$) appears significantly more homogeneous throughout the entire scaffold than the scaffold structure produced using the original quenching technique ($4.1^{\circ}\text{C}/\text{min}$) (151). Yin *et al.* suggested that the different morphology of chitosan-gelatin/ β -tricalcium phosphate scaffolds were established by growth rate of ice crystals formed in the process of freezing composite suspensions at different temperatures (152). In an attempt to extend the upper pore size limit of chitin matrices obtained by lyophilization, the novel method designed as an internal bubbling process (IBP) was proposed by Khor *et al.* (152). This was achieved by adding CaCO_3 to the chitin solution, casting into a mold to give a CaCO_3 -chitin gel, which was submerge in 1N HCL solution to generate gaseous CO_2 creating IBP throughout the gel. In addition, several scaffold processing and fabrication techniques have been proposed, for example, phase separation, particular leaching, laser sintering, stereolithography apparatus, etc (42, 56, 58-60, 153). However, the choice of correct technique is crucial because the fabrication can significantly alter the properties of the biomaterials and its degradation characteristics. Furthermore, porosity could not be determined by mercury porosimetry method due to

limitation of test scaffolds (spongy-like structure), therefore, the area fraction represented porosity was used in this study.

For improving the mechanical or biological properties, chitosan blended with other polymers is widely investigated. In this experiment, pore size and area fraction analysis showed more percentage of macropore and less percentage of area fraction in chitosan-collagen scaffold than those in chitosan scaffolds (Figure 8-10). In that respect, it is indicated that the incorporation of chitosan into collagen matrices tends to increase the pore size and decrease the density of composite matrix. Moreover, Taravel *et al.* reported that addition of chitosan into collagen scaffolds can considerably modify the mechanical properties of the collagen scaffolds; increased the mechanical strength of the scaffolds and reduced the biodegradation rate against collagenase (155). Tan *et al.* also reported that the addition of chitosan greatly influenced the ultrastructure of collagen, changed the fiber crosslink and increased pore size (156). A similar view is found in the reported by Lee *et al.*, who point out that mechanical properties of collagen composite scaffolds were enhanced significantly after blending with chitosan. The collagen/chitosan/glycosaminoglycan scaffolds showed an increased compressive modulus of 145.4 kPa compared to the collagen/ glycosaminoglycan scaffolds (15.8 kPa) (157). Additionally, chitosan composite scaffolds were combined with other polymers, for example, chitosan/ glycosaminoglycan (151, 157), chitosan-gelatin (158), chitosan/hydroxyapatite (159-160), chitosan/tricalcium phosphate (107, 152), etc.

Chitosan has a wide range of report in positive biological responses and activities; however, there are currently very few published data on the effect of degree of deacetylation and molecular weight of chitosan on osteoblastic phenotypes and bone formation especially in vitro study. To obtain this basic knowledge, it is an essential to study the effect of these important parameters to cell morphology, cell growth, cell behavior, and functional activities of osteoblasts. Initially, the results of cell attachment in this work suggested that no statistically significant difference among all test scaffolds at 5 and 24 hours. MC3T3-E1 cells can attach well to chitosan scaffolds (high degree of deacetylation), collagen scaffolds and chitosan-collagen scaffold, regardless of degree of deacetylation and molecular weight of chitosan. Fakhry *et al.* demonstrated that MC3T3-E1 cells can attach to Chitosan-H

(MW : 1,400,000; DD : 80%) and Protasan CL212 (MW : 270,000; DD : 70%). at 1 and 24 hours (109). The results also suggested that these two commercial chitosan support the initial attachment and spreading of osteoblasts preferentially over fibroblasts (3T3). In modification, chitosan has been used to modify the surface properties of PLLA matrices for enhancing the attachment of osteoblasts (146) or coated titanium (Ti) surface via silane-glutaraldehyde chemistry for exhibiting increased osteoblast attachment (161). In cartilage tissue engineering, chitosan was used to improve chondrocytes attachment by modified surface of poly(L-lactic acid) membrane with chitosan (162). Iwasaki *et al.* indicated that the alginate-based chitosan hybrid polymer fibers showed much improved adhesion capacity with chondrocytes in comparison with alginate polymer fiber (163).

For cell proliferation, MC3T3-E1 cells proliferated well on low degree of deacetylation of chitosan with collagen, high degree of deacetylation of chitosan with collagen and chitosan scaffolds, respectively. Concerning about degree of deacetylation, it is interesting to note that low degree of deacetylation of chitosan within composite scaffolds had more osteoblast proliferation than high degree of deacetylation of chitosan in those scaffolds. Corresponding to SEM image as in Figure 22-27 demonstrated that chitosan-collagen scaffolds with low degree of deacetylation of chitosan were covered with overlying layer and extracellular matrix more than those scaffolds with high degree of deacetylation of chitosan. Fibroblast and keratinocyte proliferation appeared to be dependent on degree of deacetylation. Howling *et al.* (99) reported that chitosan with relatively high degree of deacetylation strongly stimulated fibroblast proliferation while samples with lower levels of deacetylation showed less activity. In contrast to the stimulatory effects on fibroblasts, chitosan with high degree of deacetylation inhibited human keratinocytes. From this point of view, it can be conclude that degree of deacetylation of chitosan is a critical factor to determine cell proliferation albeit the effect of collagen on proliferation should be considered in this study.

When the effect of collagen within chitosan-collagen scaffolds is considered, it is possible to indicate that the degree of deacetylation of chitosan within chitosan-collagen scaffolds had an influence on MC3T3-E1 cell proliferation more than collagen. In this regard, the results showed that the low degree of deacetylation of

chitosan within chitosan-collagen scaffolds had more proliferative effect than the high degree of deacetylation of chitosan within those scaffolds despite with the same collagen concentrations (0.25% w/v). Alternatively, it is hypothesized that the high degree of deacetylation of chitosan within chitosan-collagen scaffolds may hinder the effect of collagen on MC3T3-E1 cell proliferation.

When chitosan scaffolds are considered, only high degree of deacetylation of chitosan was determined in this study since the low degree of deacetylation of chitosan scaffolds detached from the cover slip after culturing. In addition, the results indicated pure chitosan scaffolds had poor osteoblast proliferation in comparison with other test scaffolds. It is recommended that chitosan should be combined with other biomaterials for developing the scaffolds in bone tissue engineering. As a result, chitosan was blended with collagen to fabricate in chitosan-collagen scaffolds in this study, however, the ratio of chitosan to collagen solution appeared to be an important factor to allow these scaffold attach to cover slips. From the preliminary study, only the ratio of chitosan to collagen solution was 50:50, which was able to attach on cover slips after culturing (data not shown). For periodontal tissue engineering, Peng *et al.* (164) also found that the adherence and growth of human periodontal ligament cells (PDLs) cultured within chitosan-collagen scaffolds were better than on single chitosan scaffolds. Recently, Arpornmaeklong *et al.* (165) reported that chitosan sponges tended to promote growth of MC3T3-E1 cells to a greater level than collagen and chitosan-collagen sponges even though growth of cells on chitosan sponges was lower than other sponges during culture-days 3 and 6.

When molecular weight of chitosan is concerned, no statistically significant difference was found on osteoblast proliferation among all test scaffolds in each degree of deacetylation of chitosan as presented in Table 10. The molecular weight of chitosan in this study ranges from 100,000 to 1,000,000 daltons. As a result, it can be concluded that molecular weight of chitosan in this range did not influence on osteoblast proliferation. However, the molecular weight is a crucial factor for physiochemical properties of chitosan. Several publications reported that mechanical properties (tensile strength, modulus of elasticity, chain flexibility, etc.), chemical bonding, solubility and degradability depended on molecular weight (90, 144, 148, 152).

MC3T3-E1 cells, grown in the presence of serum and ascorbic acid, differentiate into osteoblasts and produce extensive collagenous extracellular matrix that can be mineralized by the addition of β -glycerophosphate. Alkaline phosphatase (ALP), an early marker of osteoblast differentiation, was expressed at high levels during the period of extracellular matrix deposition and down-regulated after the mineralization stage (166). Figure 20-21 showed that all test scaffolds increased alkaline phosphatase activity in the same pattern as the control throughout the experimental periods, albeit the control had more the alkaline phosphatase activity in the early stage of differentiation. The alkaline phosphatase activity increased during differentiation, reaching a maximum on day 4 for all test scaffolds and the control. Afterwards, the alkaline phosphatase activity gradually decreased between day 6 and day 10, and maintained this plateau level on the following days for all test scaffolds and the control. According to the report by El-Ghanuam *et al* (167), the ALP activity exhibited the maximum at the 10th day, while it was gradually increased until the 21st day according to report by Arpornmaeklong *et al* (165). On day 4, a maximum ALP activity, the results suggested that the composite scaffolds with low degree of deacetylation of chitosan had more ALP activity than those with high degree of deacetylation of chitosan. Thereby, it is conclude that the degree of deacetylation of chitosan influence on ALP activity.

Moreover, the results demonstrated that all test scaffolds had less ALP activity than the control during the early stage of differentiation (on day 0-6), including collagen scaffolds. It is hypothesized that collagen in collagen scaffolds and chitosan-collagen composite scaffolds might be lysed into aliquot of lysis buffer during ALP assay. Lysis buffer was prepared from CellLytic M[®] which is cell lysis/extraction reagent enabled efficient and rapid cell lysis and solubilization of proteins. Additionally, polycationicity ($-\text{NH}_3^+$) of chitosan was able to form polyelectrolyte complex with most of proteins, its cationic might bind to protein or albumin comprised of fetal bovine serum (46). As a result of this phenomenon, all test scaffolds which contain collagen and chitosan caused of increased total protein content values, affecting to reduce ALP activity. Nevertheless, all test scaffolds could be compared with each other since the concentration of chitosan and collagen in each scaffold are equal (0.5% chitosan solution blended with 0.5% collagen solution).

Regarding cell morphology and behavior, MC3T3-E1 cells attached, spread and sprouted their cytoplasmic process on the test scaffold surface and grew well on these test scaffolds although growth rate of cells are different. Many anchoring processes were observed extending from cells to biomaterial surface as well to the other cells. Subsequently, all test scaffolds had multilayer cells and deposited matrix throughout the entire scaffolds. The matured MC3T3-E1 cells grew in the same direction and arranged in parallel. Some areas in SEM images (Figure 23-28) suggested that MC3T3-E1 cells accumulated in nodule-like structure and tended to be calcification. However, only the control enabled MC3T3-E1 cells to form mineralized nodules after staining with alizarin red- S. The reason why all test scaffolds was not able to enhance MC3T3-E1 cells on mineralized nodule formation in spite of the fact that MC3T3-E1 cells had a capacity to grow and differentiate on these test scaffolds, one explanation is the low level of ALP activity of test scaffolds in comparison with the control. Alkaline phosphatase enzymes played an important role in cleavage a phosphate from β -glycerophosphate in culture. The free phosphates entered to the cells, resulting in the up-regulation of osteopontin (OPN) RNA levels. Osteopontin, a late marker of osteoblast differentiation, is a phosphorylated glycoprotein secreted to the mineralizing extracellular matrix by osteoblasts during bone development and may control mineralization. If the ALP activity is too low or inactive, the expression of osteopontin is not induced (168). The mineralized nodule formation did not occur. To confirm this result, further study in relation to the effect of test scaffolds to osteopontin expression is needed.

When lyophilized chitosan-collagen scaffolds were applied in periodontology, a variety of useful applications can be performed. The chitosan-collagen scaffolds with micropore and medium pore size suitable in casting the membrane for guided tissue regeneration. Additionally, these composite materials can be further developed in many forms such as microgranules, fibers, chips, etc. for utilizing in bone grafting materials or local drug delivery. In tissue engineering, if these chitosan-collagen composite scaffolds enlarge the pore size, allowing osteoblasts to penetrate into the scaffolds, or deliver cells, growth factors and genes, it appears to be the utilization in periodontal tissue regeneration.

CHAPTER VII

CONCLUSION

Chitosan scaffolds had unique porous microstructure and pore distribution according to different concentration, degree of deacetylation and molecular weight of chitosan. Interestingly, the freezing rate of lyophilized chitosan scaffolds had the influence on the mean pore size. MC3T3-E1 cells attached well on all test scaffolds, regardless of degree of deacetylation and molecular weight of chitosan. The proliferation and differentiation of osteoblasts depend on the degree of deacetylation of chitosan within the chitosan-collagen composite scaffolds. Conversely, the molecular weight of chitosan did not have the effect on osteoblastic phenotypes. SEM images demonstrated that MC3T3-E1 cells grew in multilayer, deposited matrix and accumulated in nodule-like structure on test scaffolds. However, only the control enabled MC3T3-E1 cells to form mineralized nodules.

Within limitation of our study, the degree of deacetylation of chitosan is a crucial factor that determines biological characteristics as well as microstructure characteristics. In the future, the microstructure of these composite scaffolds could be improved through the fabrication processes in accordance with the further applications.

REFERENCES

1. Ranney RR. Classification of periodontal diseases. *Periodontology* 2000. 1993;2: 13-25.
2. Oliver RC, Brown LJ. Periodontal diseases and tooth loss. *Periodontology* 2000. 1993;2:117-27.
3. Costerton JW, Lewandowski Z, Debeer D, Caldwell D, Korber D, James G. Biofilms, the customized microniche. *J Bacteriology*. 1994;176:2137-42.
4. Haffajee AD, Socransky SS. Microbial etiology agents of destructive periodontal disease. *J Periodontol*. 2000;5:78-111.
5. Socransky SS, Haffajee AD, Cugini MA, Smith C, Kent RL. Microbial complexes in subgingival plaque. *J Clin Periodontol*. 1998;25:134-44.
6. Socransky SS, Haffajee AD. Evidence of bacterial etiology: a historical perspective. *Periodontology* 2000. 1994;5:7-25.
7. Haake SK, Newman MG, Nisengard RJ, Sanz M. Periodontal microbiology. In: Newman MG, Takei HT, Carranza FA, editors. *Carranza's Clinical Periodontology*. 9th ed. Pennsylvania : W.B. Saunders; 2002 p. 96-112.
8. Haake SK, Nisengard RJ, Newman MG, Miyasaki KT. Microbial interactions with the host in periodontal diseases. In: Newman MG, Takei HT, Carranza FA, editors. *Carranza's Clinical Periodontology*. 9th ed. Pennsylvania : W.B. Saunders; 2002 p. 132-52.
9. Academy report. The pathogenesis of periodontal disease. *J Periodontol*. 1999;70: 457-70.
10. Genco RJ. Host responses in periodontal disease: current concept. *J Periodontol*. 1992;63:338-55.
11. Greenstien G, Lamster I. Changing periodontal paradigms: therapeutic implication. *Int J Perio & Rest Dent*. 2000;20:336-57.
12. Larato DC. Intrabony defects in the dry human skull. *J Periodontol*. 1970;41:496-8.

13. Larato DC. Furcation involvements: incidence and distribution. *J Periodontol.* 1970;41:499-501.
14. Manson JD, Nocholson K, The distribution of bone defects in chronic periodontitis. *J Periodontol.* 1974;45:88-92.
15. Nielsen IM, Glavind L, Karring T. Interproximal periodontal intrabony defects. Prevalence, localization and etiologic factors. *J Clin Periodontol.* 1980;7:187-98.
16. Vrotsos JA, Parashis AO, Theofanatos GD, Smulow JB. Prevalence and distribution of bone defects in moderate and advanced adult periodontitis. *J Clin Periodontol.* 1999;26:44-8.
17. Carranza FA. Bone loss and patterns of bone destruction. In: Newman MG, Takei HT, Carranza FA, editors. *Carranza's Clinical Periodontology.* 9th ed. Pennsylvania : W.B. Saunders; 2002 p. 354-70.
18. Renvert S, Egelberg J. Healing after treatment of periodontal intraosseous defects. II. Effect of citric acid conditioning of the root surface. *J Clin Periodontol.* 1981;8:459-73.
19. Isidor F, Karring T, Nyman S, Lindhe J. New attachment formation on citric acid treated roots. *J Periodont Res.* 1985;20:421-30.
20. Wikesjö UME, Claffey N, Christersson LA, Franzetti LC, Genco RJ, Terranova VP, Egelberg J. Repair of periodontal furcation defects in beagle dogs following reconstructive surgery including root surface demineralization with tetracycline hydrochloride and topical fibronectin application. *J Clin Periodontol.* 1988;15:73-80.
21. Shallhorn RG, Hiatt WH, Boyce W. Iliac transplants in periodontal therapy. *J Periodontol.* 1970;41:566-80.
22. Froum SJ, Ortiz M, Witkin RT, Thaler R, Scopp IW, Stahl SS. Osseous autografts. III. Comparison of osseous coagulum-bone blend implants with open curettage. *J Periodontol.* 1976;47:287-94.
23. Sanders JJ, Sepe WW, Bowers GM, et al. Clinical evaluation of freeze-dried bone allografts in periodontal osseous defects. Part III. Composite freeze-dried bone allografts with and without autogenous bone graft. *J Periodontol.* 1983;54:1-8.

24. Yukna RA. Clinical evaluation of HTR polymer bone replacement grafts in human mandibular class II molar furcations. *J periodontol.* 1994;65:342-9.
25. Mellonig JT. Decalcified freeze-dried bone allograft as an implant material in human periodontal defects. *Int J Perio & Rest Dent.* 1984;4:41-55.
26. Strub JR, Gaberthuel TW, et al. Comparison of tricalcium phosphate and frozen allogenic bone implants in man. *J Periodontol.* 1979;50:624-9.
27. Busschop J, DeBoever J. Clinical and histological characteristics of lyophilized allogenic dura mater in periodontal bony defects in humans. *J Clin Periodontol.* 1983;10:399-411.
28. Meffert RM, Thomas JR, Hamilton KM, et al. Hydroxyapatite as an alloplastic graft in the treatment of human periodontal osseous defects. *J Periodontol.* 1985; 56:63-73.
29. Froum SJ, Kushner L, Scopp W, Stahl SS. Human clinical and histologic response to durapatite implants in intraosseous lesions. *J Periodontol.* 1982;53:719-25.
30. Tanner MG, Solt CW, Vuddhaknok S. An evaluation of new attachment formation using a microfibrillar collagen barrier. *J Periodontol.* 1988;59:524-30.
31. Karring T, Nyman S, Lindhe J. Healing following implantation of periodontitis affected roots into bone tissue. *J Clin Periodontol.* 1980;7:96-105.
32. Karring T, Isidor F, Nyman S, Lindhe J. New attachment formation on teeth with a reduced but healthy periodontal ligament. *J Clin Periodontol.* 1985;12:51-60.
33. Caton J, Nyman S, Zander H. Histomeric evaluation of periodontal surgery. II. Connective tissue attachment levels after four regenerative procedures. *J Clin Periodontol.* 1980;7:224-31.
34. Nyman S, Gottlow J, Karring T, Lindhe J. The regenerative potential of the periodontal ligament. An experimental study in monkey. *J Clin Periodontol.* 1982;9:257-65.
35. Gottlow J, Nyman S, Karring T, Lindhe J. New attachment formation as the result of controlled tissue regeneration. *J Clin Periodontol.* 1984;11:494-503.

36. Rutherford RB, Niekrash CE, Kennedy JE, Charlette MF. Platelet-derived and insulin-like growth factor stimulate regeneration of periodontal attachment in monkeys. *J Periodont Res.* 1992;27:285-90.
37. Sigurdsson TJ, Lee MB, Kubota K, et al. Periodontal repair in dogs : Recombinant human bone morphogenic protein-2 significantly enhances periodontal regeneration. *J Periodontol.* 1995;66:131-8.
38. Tatakis DN, Wikesjo UME, Razi SS, et al. Periodontal repair in dogs : effect of transforming growth factor- β 1 on alveolar bone and cementum regeneration. *J Clin Periodontol.* 2000;27:698-704.
39. Hoang AM, Oates TW, Cochran DL. In vitro wound healing responses to enamel matrix derivative. *J Periodontol.* 2000;71:1270-7.
40. Carranza FA, McClain P, Schallhorn RG. Regenerative osseous surgery. In: Newman MG, Takei HT, Carranza FA, editors. *Carranza's Clinical Periodontology*. 9th ed. Pennsylvania : W.B. Saunders; 2002 p. 804-24.
41. Schallhorn RG. Present status of osseous grafting procedures. *J Periodontol.* 1977;48:570-83.
42. Muschler GF, Nakamoto C, Griffith JG. Engineering principles of clinical cell-based tissue engineering. *J. Bone Joint Surg. AM.* 2004;86:1541-58.
43. Yannas IV. Biologically active scaffolds based on collagen-GAG copolymers. In: Ma PX, Elisseeff J, editors. *Scaffolding in tissue engineering*. New York : CRC Press; 2006 p. 3-12.
44. Neves NM, Mano JF, Reis RL. Biodegradable composites for biomedical application In: Reis R, Roman JS, editors. *Biodegradable systems in tissue engineering and regenerative medicine*. Florida : CRC Press; 2004 p. 91-113.
45. Ehrenfreund-Klienman T, Golenser J, Domb AJ. Polysaccharide scaffolds for tissue engineering In: Ma PX, Elisseeff J, editors. *Scaffolding in tissue engineering*. New York : CRC Press; 2006 p. 27-44.
46. Gallardo A, Aguilar MR, Elvira C, Peniche C, Roman JS. Chitosan-based microcomposites from biodegradable microparticles to self-curing hydrogels. In: Reis R, Roman JS, editors. *Biodegradable systems in*

- tissue engineering and regenerative medicine. Florida : CRC Press; 2004 p. 145-61.
47. Hollinger JO, Buck DC, Bruder SP. Biology of bone healing: Its impact on clinical therapy. In: Lynch SE, Genco RJ, Marx RE, editors. Tissue engineering. Application in maxillofacial surgery and periodontics. Illinois : Quintessence Publishing; 1999 p. 17-53.
 48. Eroschenko VP. Bone. In: Balado D, editor. Di Fiore's atlas of histology with functional correlations. 8th ed. Maryland : Williams & Wilkins; 1996 p. 45-62.
 49. Ross MH, Reith EJ, Romrell LJ. Bone. In: Kist K, editor. Histology: A text and atlas. 2nd ed. Maryland : Williams & Wilkins; 1989 p. 141-72.
 50. Gartner LP, Hiatt JL. Color text book of histology. Pennsylvania : W.B. Saunders 1997 p. 109-30.
 51. Donahue HJ, Siedlecki CA, Vogler E. Osteoblastic and osteocytic biology and bone tissue engineering. In: Hollinger JO, Einhorn TA, Doll BA, Sfeir C, editors. Bone tissue engineering. Florida : CRC Press; 2004 p. 44-56.
 52. Cooper GM, Hausman RE. The cell : A molecular approach. 3rd ed. Washington D.C. : ASM Press; 2004 p. 522-8.
 53. Alberts B, Bray D, Lewis J, Raff M, Robert K, Watson JD. Molecular biology of the cell. 3rd ed. New York : Garland Publishing; 1994 p. 1090-118.
 54. Spector M. Basic principles of tissue engineering. In: Lynch SE, Genco RJ, Marx RE, editors. Tissue engineering. Application in maxillofacial surgery and periodontics. Illinois : Quintessence Publishing; 1999 p. 3-16.
 55. Muschler GF, Midura RJ. Connective tissue progenitors: Practical concepts for clinical applications. Clin Orthop. 2002;395:66-80.
 56. Yang S, Leong K-F, Du Z, Chua C-K. The design of scaffolds for use in tissue engineering. Part I. Traditional factors. Tissue Eng. 2001;7:679-89.
 57. Anusaksathien O, Jing Q-M, Ma PX, Giannobile WV. Scaffolding in periodontal engineering. In: Ma PX, Elisseeff J, editors. Scaffolding in tissue engineering. New York : CRC Press; 2006 p. 437-54.

58. Capes JS, Ando HY, Cameron RE. Fabrication of polymeric scaffolds with a controlled distribution of pores. *J Mater Sci.* 2005;16:1069-75.
59. Hou Q, Grijpma DW, Feijen J. Preparation of interconnected highly porous polymeric structures by a replication and freeze-drying process. *J Biomed Mater Res Part B: Appl Biomater* 2003;67B:732-40.
60. Lazare S, Srinivasan R. Surface properties of Poly(ethylene terephthalate) films modified by Far-Ultraviolet radiation at 193 nm (Laser) and 185 nm (Low Intensity). *J Phys Chem.* 1986;90:2124-31.
61. Ellegaard B, Karring T, Listgarten M, Loe H. New attachment after treatment of interradicular lesions. *J Periodontol.* 1973;44:209-17.
62. Ellegaard B, Karring T, Davies R, Loe H. New attachment after treatment of intrabony defects in monkeys. *J Periodontol.* 1974;45:368-77.
63. Ellegaard B, Nielsen IM, Karring T. Composite jaw and iliac cancellous bone grafts in intrabony defects in monkeys. *J Periodont Res.* 1976;11:299-310.
64. Nielsen IM, Ellegaard B, Karring T. Kielbone[®] in new attachment attempts in humans. *J Periodontol.* 1981;52:723-8.
65. Karring T, Lindhe J, Cortellini P. Regenerative periodontal therapy. In: Lindhe J, Karring T, Lang NP, editors. *Clinical periodontology and implant dentistry.* 4th ed. Iowa : Blackwell Munksgaard 2003 p. 650-704.
66. Nabers CL, O'Leary TJ. Autogenous bone transplant in the treatment of osseous defects. *J Periodontol.* 1965;36:5-14.
67. Mellonig JT, Bowers GM, Bright RW, et al. Clinical evaluation of freeze dried bone allografts in periodontal osseous defects. *J Periodontol.* 1976;47:125-33.
68. Sepe W, Bowers G, Lawrence J, et al. Clinical evaluation of freeze dried bone allografts in periodontal osseous defects. Part II. *J Periodontol.* 1978;49:9-25.
69. Quattlebaum JB, Mellonig JT, Hensel NF. Antigenicity of freeze-dried cortical bone allografts in human periodontal osseous defects. *J Periodontol.* 1988;59:394-7.

70. Mellonig JT, Bowers G, Bully R. Comparison of bone graft materials. I. New bone formation with autografts and allografts determined by strontium-85. *J Periodontol.* 1981;52:291-6.
71. Schwartz Z, Mellonig JT, Carnes DL, et al. Ability of commercial demineralized freeze-dried bone allografts to induce new bone formation. *J Periodontol.* 1996;67: 918-26.
72. Becker W, Urist MR, Tucker LM, Becker BE, Ochsenbein C. Human demineralized freeze-dried bone: inadequate induced bone formation in athymic mice. *J Periodontol.* 1995;66:822-8.
73. Scopp IW, Kassouny DY, Morgan FH. Bovine bone (Boplant). *J Periodontol.* 1966;37:400-7.
74. Neilsen IM, Ellegaard B, Karring T. Kielbone in new attachment attempts in humans. *J Periodontol.* 1981;52:723-8.
75. Yukna RA. Synthetic bone grafts in periodontics. *Periodontology 2000.* 1993;1: 92-9.
76. Synder AJ, Levin MP, Cutright DE. Alloplastic implants of tricalcium phosphate ceramic in human periodontal osseous defects. *J Periodontol.* 1984;55:273-7.
77. Strub JR, Garberthuel TW, Firestone AR. Comparison of tricalcium phosphate and frozen allogenic bone implants in man. *J Periodontol.* 1979;50:624-9.
78. Yukna RA, Harrison BG, Caudill RF, Evans GH, Mayer ET, Miller S. Evaluation of durapatite ceramic as an alloplastic implant in periodontal osseous defects. II. Twelve-month reentry results. *J Periodontol.* 1985;56:540-7.
79. Yukna RA, Cassingham RJ, Caudill RF, et al. Six month evaluation of Calcitite (hydroxyapatite ceramic) in periodontal osseous defects. *Int J Perio & Rest Dent.* 1986;6:35-45.
80. Domard A. Some physicochemical and structural basis for applicability of chitin and chitosan. The Proceedings of the second Asia Pacific chitin symposium; 1996 Nov 21-23; Bangkok, Thailand.
81. Foster AB, Webber JM. Advance in Carbohydrate Chemistry and Biochemistry. 1960;15:371-92.

82. Whistler RL. Chitin. In: Whistler RL, BeMiller JN, editors. Industrial Gums: Polysaccharides and Their Derivatives. 3rd ed. California : Academic Press; 1993 p. 601-4.
83. รพีพรรณ วิทิตสุวรรณกุล, ชีรัช วิทิตสุวรรณกุล ไคติน-ไคโตซาน. ใน: ธนิต กุสุราญ (บก.), โพลีเมอร์ชีวภาพ กรุงเทพมหานคร มหาวิทยาลัยมหิดล 1993 : 53-62.
84. Bolker HI. Natural and Synthetic Polymers: An Introduction. New York : Marcel Dekker; 1974:38-40, 106-9.
85. MacLaughlin FC, Rolland AP. Chitosan. In: Mathiowitz E, editor. Encyclopedia of Controlled Drug Delivery. Vol 2. New York : Wiley; 1999 p. 881-7.
86. Baran ET, Reis RL. Use of chemically modified chitosan and other natural-origin polymers in tissue engineering and drug delivery. In: Reis R, Roman JS, editors. Biodegradable systems in tissue engineering and regenerative medicine. Florida : CRC Press; 2004:325-35.
87. Ravie kumar MNV. A review of chitin and chitosan applications. Reactive & functional polymers. 2000;46:1-27.
88. Groves MJ. Chitosan. In: Mathiowitz E, editor. Encyclopedia of Controlled Drug Delivery. Vol 2. New York : Wiley; 1999 p. 773-4.
89. Hutmacher DW, Ng KW, Khor HL. Skin tissue engineering. Part I. Review. In: Reis R, Roman JS, editors. Biodegradable systems in tissue engineering and regenerative medicine. Florida : CRC Press; 2004 p. 509-28.
90. Chen RH, Hwa HD. Effect of molecular weight of chitosan with the same degree of deacetylation on the thermal, mechanical, and permeability properties of the prepared membrane. Carbohydrate Polym. 1996;29:353-8.
91. Denkbass EB, Odabasi M. Chitosan Microspheres and Sponges : Preparation and Characterization. J Appl Polym Sci. 2000;76:1637-43.
92. Koyano T, Minoura N, Nagura M, Kobayashi K. Attachment and growth of cultured fibroblast cells on PVA / chitosan-blended hydrogels. J Biomed Mater Res. 1998;39:486-90.

93. Ko JA, Park SJ, Hwang SJ, Park JB, Lee JS. Preparation and characterization of chitosan microparticles intended for controlled drug delivery. *Int J Pharm.* 2002; 249:165-74.
94. Hu Y, Jiang X, Ding Y, Ge H, Yuan Y, Changzheng Y. Synthesis and characterization of chitosan-poly(acrylic acid) nanoparticles. *Biomaterials* 2002; 23:3193-201.
95. Sandford PA. Chitosan: Commercial uses and potential applications. In: Skjak-Braek G, Anthonsen T, Sandford P, editors. *Chitin and Chitosan: Source, Chemistry, Biochemistry, Physical Properties and Applications.* London : Elsevier Applied science; 1989 p. 51-69.
96. Denkbaz EB, Kilicay E, Birlikseven C, Ozturk E. Magnetic chitosan microsphere: preparation and characterization. *React Funct polym.* 2002;50:225-32.
97. Wang QZ, Chen XG, Liu N, Wang SX, Liu CS, Meng XH, Liu CG. Protonation constants of chitosan with different molecular weight and degree of deacetylation. *Carbohydrate Polymers.* 2006;65:194-201.
98. Prasitsilp M, Jenwithisuk R, Kongsuwan K, Damrongchai N, Watts P. Cellular responses to chitosan in vitro: The importance of deacetylation. *J Mater Sci Mater Med.* 2000;11:773-8.
99. Howling GI, Dettmar PW, Goddard PA, Hampson FC, Dornish M, Wood EJ. The effect of chitin and chitosan on the proliferation of human skin fibroblasts and keratinocytes in vitro. *Biomaterials.* 2001;22:2959-66.
100. Chatelet C, Damour O, Domard A. Influence of the degree of deacetylation on some biological properties of chitosan films. *Biomaterials.* 2001;22:261-8.
101. Hidaka Y, Ito M, Mori K, Yagasaki H, Kafrawy AH. Histopathological and immunohistochemical studies of membranes of deacetylated chitin derivatives implanted over rat calvaria. *J Biomed Mater Res.* 1999;46:418-23.
102. Varum KM, Myhr MM, Hjerde RJN, Smidsrod O. In vitro degradation rates of partially N-acetylated chitosans in human serum. *Carbohydr Res.* 1997; 299:99-101.

103. Tomihata K, Ikada Y. In vitro and vivo degradation of films of chitin and its deacetylated derivatives. *Biomaterials*. 1997;18:567-75.
104. Ono K, Saito Y, Yura H, Kurita A, Akaike T, Ishihara M. Photocrosslinkable chitosan as a biological adhesive. *J Biomed Mater Res*. 2000;49:289-95.
105. Zhu Y, Wang X, Cui FZ, Feng QL. In vitro cytocompatibility and osteoinduction of phosphorylated chitosan with osteoblasts. *J Bioactive and compatible polymers*. 2003;18:375-90.
106. Rao SB, Sharma CP. Use of chitosan as biomaterial: Studies on its safety and hemostatic potential. *J Biomed Mater Res*. 1997;34:21-8.
107. Wang X, Ma J, Wang Y, He B. Bone repair in radii and tibias of rabbits with phosphorylated chitosan reinforced calcium phosphate cement. *Biomaterials*. 2002;23:4167-76.
108. Muzzarelli RAA, Biagini G, Bellardini M, Simonelli L, Castaldini C, Fratto G. Osteoconduction exerted by methylpyrrolidinone chitosan used in dental surgery. *Biomaterials*. 1993;14:39-43.
109. Fakhry A, Schneider GB, Zaharias R, Senel S. Chitosan supports the initial attachment and spreading of osteoblasts preferentially over fibroblasts. *Biomaterials*. 2004;25:2075-9.
110. Mori T, Okumura M, Matsuura M, Ueno K, Tokura S, Okamoto Y, Minami S, Fujinaga T. Effects of chitin and its derivatives on the proliferation and cytokine production of fibroblasts in vitro. *Biomaterials*. 1997;18:947-51.
111. Ohara N, Hayashi Y, Yamada S, et al. Early expression analyzed by cDNA microarray and RT-PCR in osteoblasts cultured with water-soluble and low molecular chitooligosaccharide. *Biomaterials*. 2004;25:1749-54.
112. Ueno H, Yamada H, Tanaka I, Kaba N, Matsura M, Okumura M, Kadosawa T, Fujinaga T. Accelerating effects of chitosan for healing at early phase of experimental open wound in dogs. *Biomaterials*. 1999;20:1407-14.
113. Ueno H, Murakami M, Okumura M, Kadosawa T, Uede T, Fujinaga T. Chitosan accelerates the production of osteopontin from polymorphonuclear leukocytes. *Biomaterials*. 2001;22:1667-73.

114. Nishimura K, Nishimura S, Seo H, Nishi N, Tokura S, Azuma I. Effect of multiporous microspheres derived from chitin and partially deacetylated chitin on the activation of mouse peritoneal macrophages. *Vaccine*. 1987;5:136-40.
115. Ueno H, Nakamura F, Murakami M, Okumura M, Kadosawa T, Fujinaga T. Evaluation effects of chitosan for the extracellular matrix production by fibroblasts and the growth factors production by macrophages. *Biomaterials*. 2001; 22:2125-30.
116. Minami S, Suzuki H, Okamoto Y, Fujinaga T, Shigemasa Y. Chitin and chitosan activate complement via the alternative pathway. *Carbohydr Polym*. 1998;36:151-5.
117. Suzuki Y, Okamoto Y, Morimoto M, Sashiwa H, Saimoto H, Tanioka S, Shigemasa Y, minami S. Influence of physico-chemical properties of chitin and chitosan on complement activation. *Carbohydr Polym*. 2000;42:307-10.
118. Klokkevold PR, Vandemark L, Kenney EB, Vernard GW. Osteogenesis enhanced by chitosan(poly-N-acetyl glucosaminoglycan) in vitro. *J Periodontol*. 1996;67: 1170-5.
119. Kawakami T, Antho M, Hasegawa H, Yamagishi T, Ito M, Eda S. Experimental study on osteoconductive properties of chitosan-bonded hydroxyapatite self-hardening paste. *Biomaterials*. 1992;13:759-63.
120. Pang EK, Paik JW, Kim SK, et al. Effects of chitosan on human periodontal ligament fibroblasts in vitro and on bone formation in rat calvaria defects. *J Periodontol*. 2005;76:1526-33.
121. Azevedo HS, Reis RL. Understanding the enzymatic degradation of biodegradable polymers and strategies to control their degradation rate. In: Reis R, Roman JS, editors. *Biodegradable systems in tissue engineering and regenerative medicine*. Florida : CRC Press; 2004 p. 177-201.
122. Muzzarelli RAA. Role of lysozyme and N-acetyl- β -D-glucosaminidase in the resorption of wound dressings. In: Brine CJ, Sandford PA, Zikakis JP,

- editors. *Advances in chitin and chitosan*. London : Elsevier Applied Science; 1992 p. 25-33.
123. Mi FL, TanYc, Liang HF, Sung HW. In vivo biocompatibility and degradability of a novel injectable-chitosan-based implant. *Biomaterials*. 2002; 23:181-91.
124. Muzzarelli R, Biagini G, Pugnaroni A, Filippini O, Baldassarre V, Castaldini C, Rizzoli C. Reconstruction of periodontal tissue with chitosan. *Biomaterials*. 1989;10:598-603
125. Gerentes P, Vachoud L, Doury J, Domard A. Study of chitin-based gel as injectable material in periodontal surgery. *Biomaterials*. 2002;23:1295-1302.
126. Shu XZ, Zhu KJ. Controlled drug release properties of ionically cross-linked chitosan beads: The influence of anion structure. *Int J Pharm*. 2002;233:217- 25.
127. Gariepy ER, Chenite A, Chaput C, Guirguis S, Leroux JC. Characterization of thermosensitive chitosan gels for the sustained delivery of drugs. *Int J Pharm*. 2000;203:89-98.
128. Chandy T, Sharma CP. Chitosan matrix for ral sustained delivery of ampicillin. *Biomaterials*. 1993;14:939-44.
129. Vasudev SC, Chandy T, Sharma CP. Development of chitosan/polyethylene vinyl acetate co-matrix: controlled release of aspirin-heparin for preventing cardiovascular thrombosis. *Biomaterials*. 1997;18:375-81.
130. Gupta Kc, Kumar M.N.V. R. Drug release behaviour of beads and microgranules of chitosan. *Biomaterials*. 2000;21:1115-9.
131. Hejazi R, Amiji M. Stomach-specific anti-H. pylori therapy I: preparation and characterization of tetracycline-loaded chitosan microspheres. *Int J Pharm*. 2002;235:87-94.
132. O'Leary R, Wood EJ. A novel in vitro dermal wound-healing model incorporating a response to mechanical wounding and repopulation of a fibrin provisional matrix. *In Vitro Cell Dev Biol*. 2003;39:204-7.

133. Maeda T, Matsunuma A, Kawane T, Horiuchi N. Simvastatin promotes osteoblast differentiation and mineralization in MC3T3-E1 cells. *BioChem Biophys Res Com.* 2001;280:874-7.
134. Mosmann T. Rapid and cytotoxicity assay. *J Immunol Methods.* 1983;65:55-63.
135. Wang H-L, Miyauchi M, Takata T. Initial attachment of osteoblasts to various guided bone regeneration membranes: an in vitro study. *J Periodont Res.* 2002; 37:340-4.
136. Takata T, Wang H-L, Miyauchi M. Attachment, proliferation and differentiation of periodontal ligament cells on various guided tissue regeneration membrane. *J Periodont Res.* 2001;36:322-7.
137. Marinucci L, Lilli C, Baroni T, Becchetti E, Belcastro S, Balducci C, Locci P. In vitro comparison of bioabsorbable and non-resorbable membranes in bone regeneration. *J Periodontol.* 2001;72:753-9.
138. Bradford MM. A rapid and sensitive method for the quantitation of microgram quantities of protein utilizing the principle of protein-dye binding. *Anal Biochem.* 1976;72:248-54.
139. Gough JE, Jones JR, Hench LL. Nodule formation and mineralization of human primary osteoblasts cultured on a porous bioactive glass scaffold. *Biomaterials.* 2005;25:2039-46.
140. Coelho MJ, Cabral AT, Fernandes MH. Human bone cell cultures in biocompatibility testing. Part I: osteoblastic differentiation of serially passage human bone marrow cells cultured in α -MEM and in DMEM. *Biomaterials.* 2000;21:1087-94.
141. Coelho MJ, Fernandes MH. Human bone cell cultures in biocompatibility testing. Part II: Effect of ascorbic acid, β -glycerophosphate and dexamethasone on osteoblastic differentiation. *Biomaterials.* 2000;21:1095-102.
142. Tanabe N, Ito-Kato E, Suzuki colorimetric assay for cellular growth and survival: application to proliferative N, Nakayama A, Ogiso B, Maeno M, Ito K. 1α affects mineralized nodule formation by rat osteoblasts. *Life Sciences.* 2004;75:2317-27.

143. Hollister SJ, Taboas JM, Schek RM, Lin C-Y, Chu TM. Design and fabrication of bone tissue engineering scaffolds In: Hollinger JO, Einhorn TA, Doll BA, Sfeir C, editors. Bone tissue engineering. Florida : CRC Press; 2004 p. 44-56.
144. Martino AD, Sittinger M, Risbud MV. Chitosan: A versatile biopolymer for orthopaedic tissue engineering. *Biomaterials*. 2005;26:5983-90.
145. Park YJ, Lee YM, Park SN, Sheen SY, Chung CP, Lee SJ. Platelet derived growth factor releasing chitosan sponge for periodontal bone regeneration. *Biomaterials*. 2000;21:153-9.
146. Lee JY, Nam SH, Im SY, Park YJ, Lee YM, Seol YJ, Chung CP, Lee SJ. Enhanced bone formation by controlled growth factor delivery from chitosan-based biomaterials. *J Control Release*. 2002;78:187-97.
147. Lee YM, Park YJ, Lee SY, Ku Y, Han SB, Klokkevold PR, Chung CP. The bone regeneration effect of platelet-derived growth factor-BB delivered with a chitosan/tricalcium phosphate sponge carrier. *J Periodontol*. 2000;71:418-24.
148. Madhally SV, Matthew HWT. Porous chitosan scaffolds for tissue engineering. *Biomaterials*. 1999;20:1133-42.
149. Chow KS, Khor E. Novel fabrication of open-pore chitin matrixes. *Biomacromolecules*. 2000;1:61-7.
150. Pineda LM, Busing M, Meinig RP, Gogolewski S. Bone regeneration with resorbable polymeric membranes. III. Effect of poly(L-Lactide) membrane pore size on the bone healing process in large defects. *J Biomed Mater Res*. 1996;31:385-94.
151. O'Brien FJ, Harley BA, Yannas LV, Gibson L. Influence of freezing rate on pore structure in freeze-dried collagen-GAG scaffolds. *Biomaterials*. 2004;25:1077-86.
152. Yin Y, Ye F, Cui J, Zhang F, Li X, Yao K. Preparation and characterization of macroporous chitosan-gelatin/ β -tricalcium phosphate composite scaffolds for bone tissue engineering. *J Biomed Mater Res*. 2003;67A:844-55.

153. Khor E, Lim LY. Implantable applications of chitin and chitosan. *Biomaterials*. 2003;24:2339-49.
154. Hatmacher DW. Design and fabrication of scaffolds via solid free-form fabrication In: Reis R, Roman JS, editors. *Biodegradable systems in tissue engineering and regenerative medicine*. Florida : CRC Press; 2004 p. 67-90.
155. Taravel MN, Domard A. Collagen and its interactions with chitosan. III. Some biological and mechanical properties. *Biomaterials*. 1996;17:451-55.
156. Tan W, Krishnaraj R, Desai TA. Evaluation of nanostructured composite collagen-chitosan matrices for tissue engineering. *Tissue Eng*. 2001;7:203-210.
157. Lee JE, Kim KE, Kwon IC, Ahn HJ, Lee S-H, Cho H, Kim, Seong SC, Lee MC. Effects of the controlled-released TGF- β 1 from chitosan microspheres on chondrocytes cultured in a collagen/chitosan/glycosaminoglycan scaffold. *Biomaterials*. 2004;25:4163-73.
158. Huang Y, Onyeri S, Siewe M, Moshfeghian A, Madhally SV. In vitro characterization of chitosan-gelatin scaffolds for tissue engineering. *Biomaterials*. 2005;26:7616-27.
159. Ito M. In vitro properties of a chitosan-bonded hydroxyapatite bone-filling paste. *Biomaterials*. 1991;12:41-5.
160. Maruyama M, Ito M. In vitro properties of a chitosan-bonded self-hardening paste with hydroxyapatite granules. *J Biomed Mater Res*. 1996;32:527-32.
161. Bumgardner JD, Wister R, Gerard PD, Bergin P, Chestnutt B, Marin M, Ramsey V, Elder SH, Gilbert JA. *J Biomater Sci Polym Ed*. 2003;14:423-38.
162. Cui YL, Qi AD, Liu WG, Wang XH, Wang H, Ma DM, Yao KD. Biomimetic surface modification of poly(L-Lactic acid) with chitosan and its effects on articular chondrocytes in vitro. *Biomaterials*. 2003;24:3859-68
163. Iwasaki N, Yamane S-T, Majima T, Kasahara Y, Minami A, Harada K, Nonaka S, Maekawa N, Tamura H, Tokura S, Shiono M, Monde K, Nishimura S-I. Feasibility of polysaccharide hybrid materials for scaffolds in cartilage tissue engineering: Evaluation of chondrocyte adhesion to

- polyion complex fibers prepared from alginate and chitosan. *Biomacromolecules*. 2004;5:828-33.
164. Peng L, Cheng XR, Wang JW, Xu DX, Wang G. Preparation and evaluation of porous chitosan/collagen scaffolds for periodontal tissue engineering. *J Bioact Compat Poly*. 2006;21:207-20.
165. Arpornmaeklong P, Suwatwirote N, Pripatanont P, Oungbho K. Growth and differentiation of mouse osteoblasts on chitosan-collagen sponges. *Int J Oral Maxillofac Surg*. 2007;36:328-37
166. Beck GR, Sullivan EC, Moran E, Zerler B. Relationship between alkaline phosphatase levels, osteopontin expression, and mineralization in differentiating MC3T3-E1 osteoblasts. *J Cell Biochem*. 1998;68:269-80.
167. El-Ghannam A, Ducheyne P, Shapiro IM. Porous bioactive glass and hydroxyapatite ceramic affect bone cell function in vitro along different time lines. *J Biomed Mater Res*. 1997;36:167-80.
168. Beck GR, Zerler B, Moran E. Phosphate is a specific signal for induction of osteopontin gene expression. *PNAS*. 2000;97:8352-57.

APPENDIX

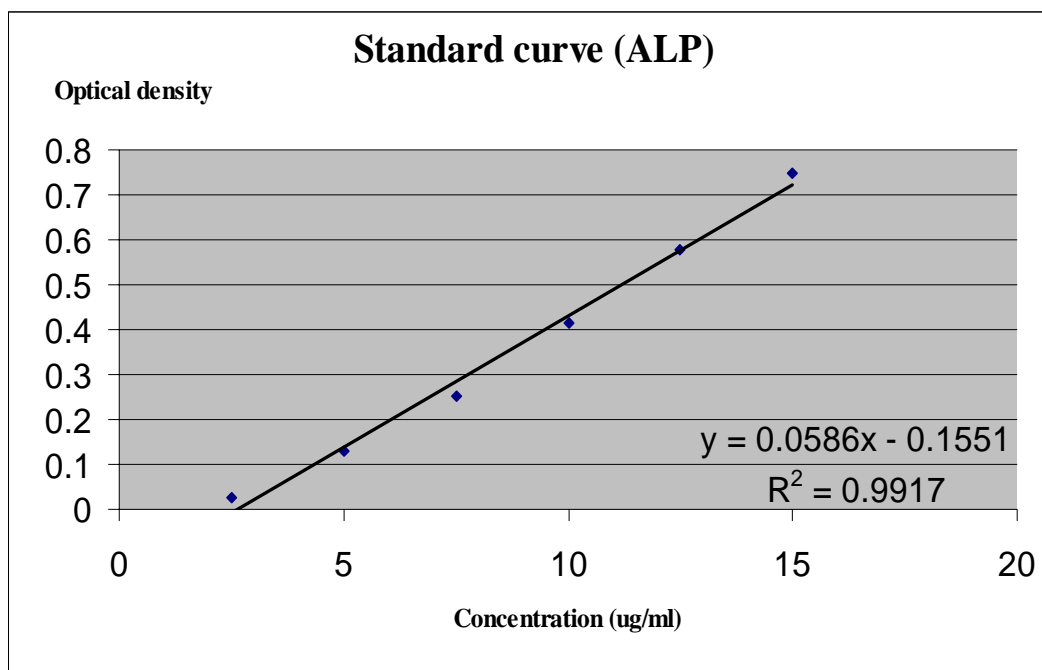


Figure 31 Standard curve of p-nitrophenol on day 4 and 6 (1st experiment)

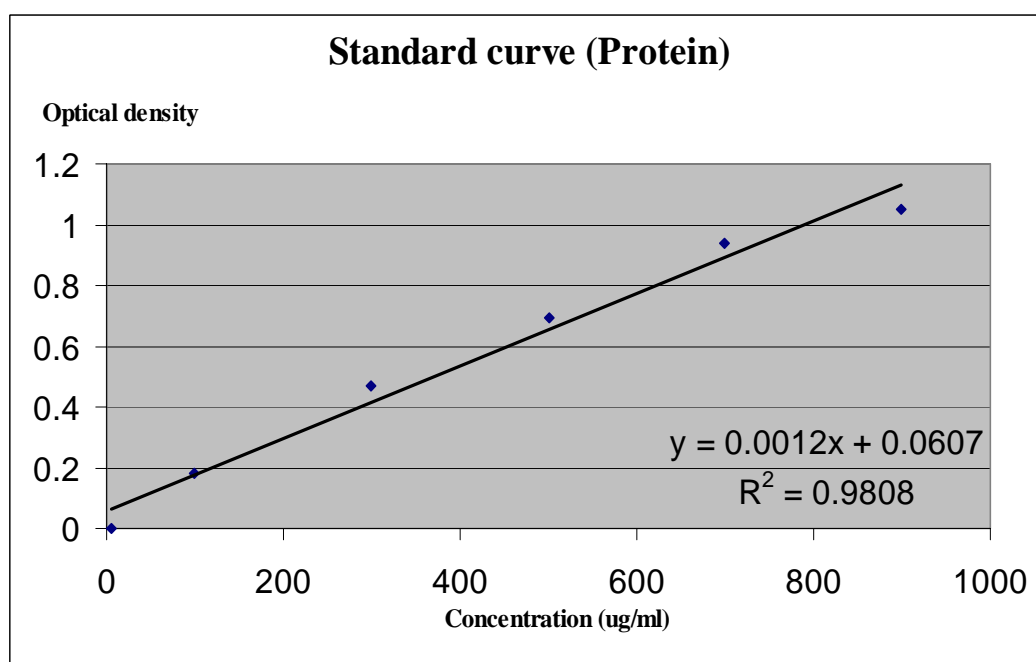


Figure 32 Standard curve of total protein on day 4 and 6 (1st experiment)

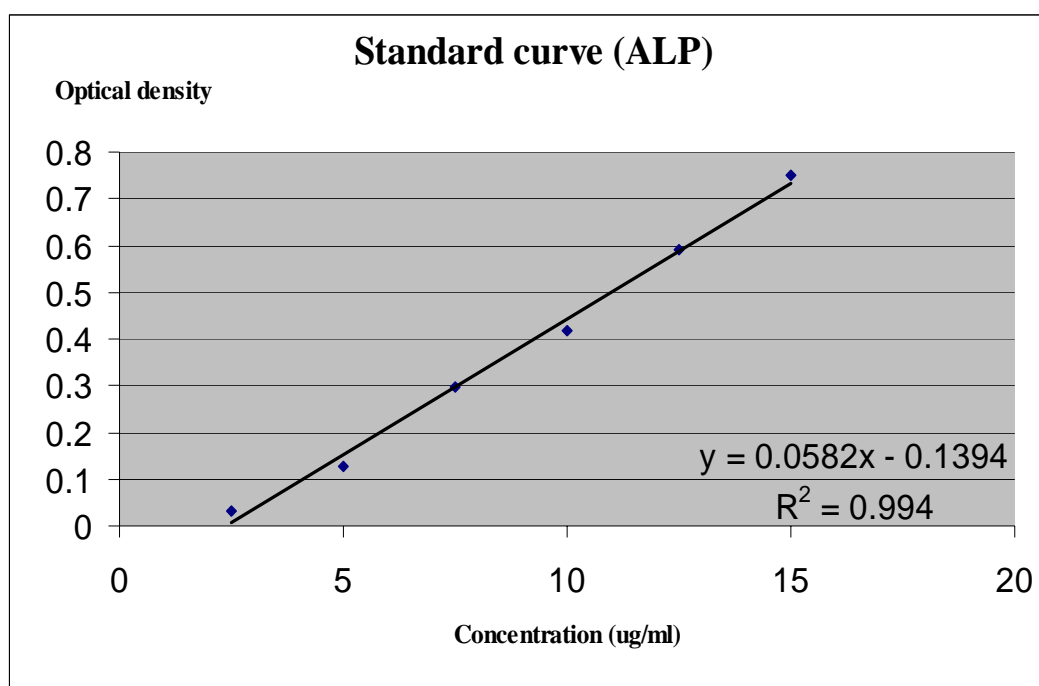


Figure 33 Standard curve of p-nitrophenol on day 10 and 14 (1st experiment)

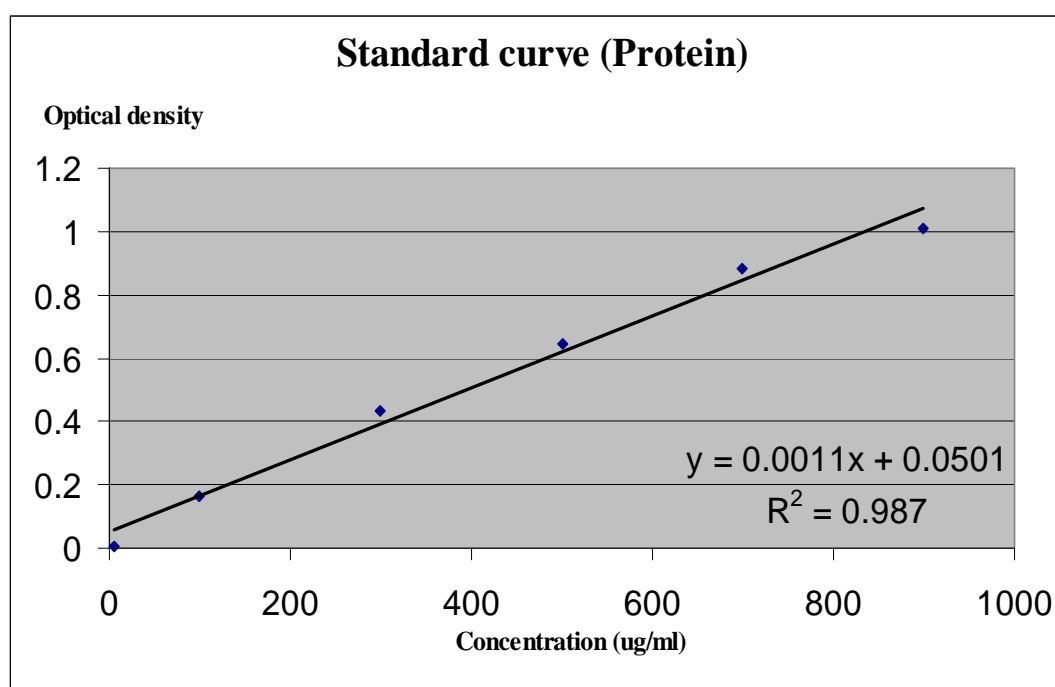


Figure 34 Standard curve of total protein on day 10 and 14 (1st experiment)

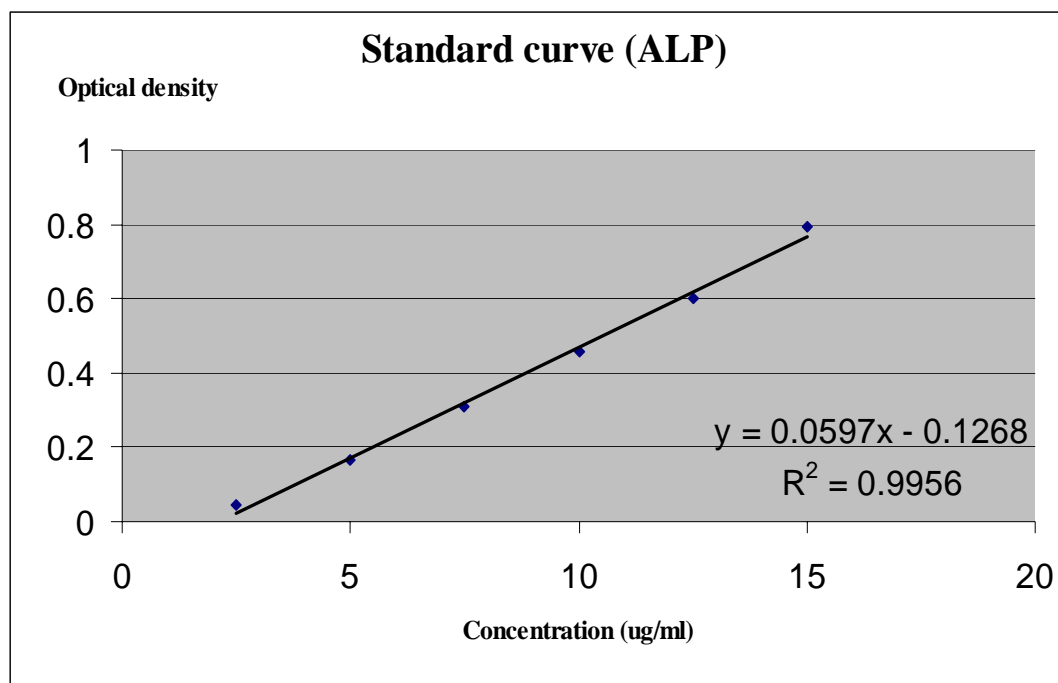


Figure 35 Standard curve of p-nitrophenol on day 18 and 22 (1st experiment)

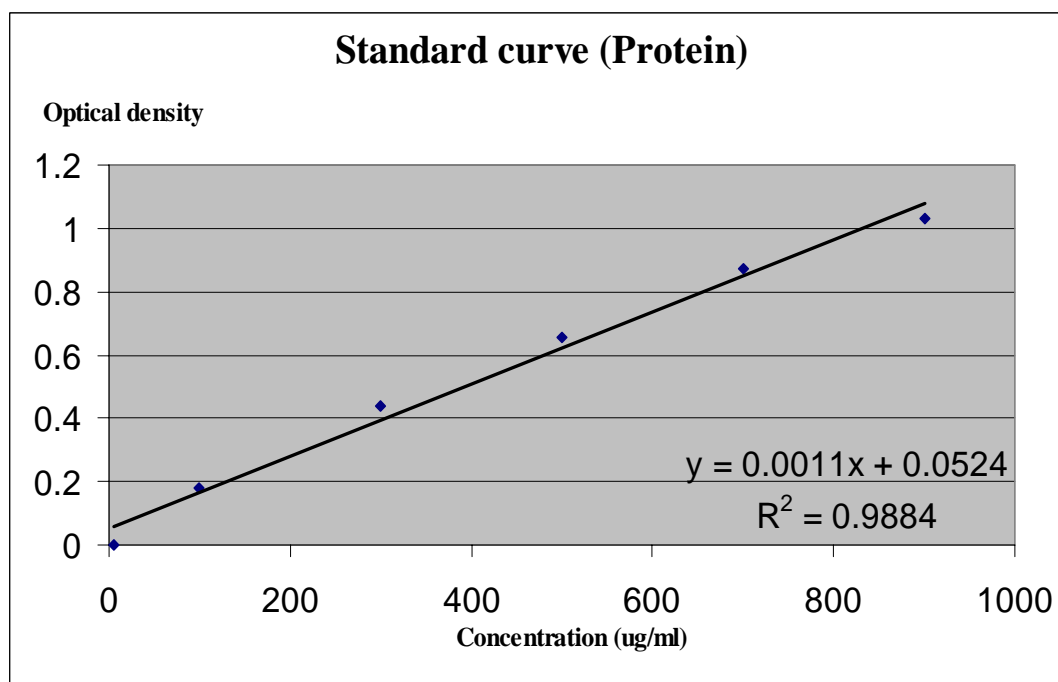


Figure 36 Standard curve of total protein on day 18 and 22 (1st experiment)

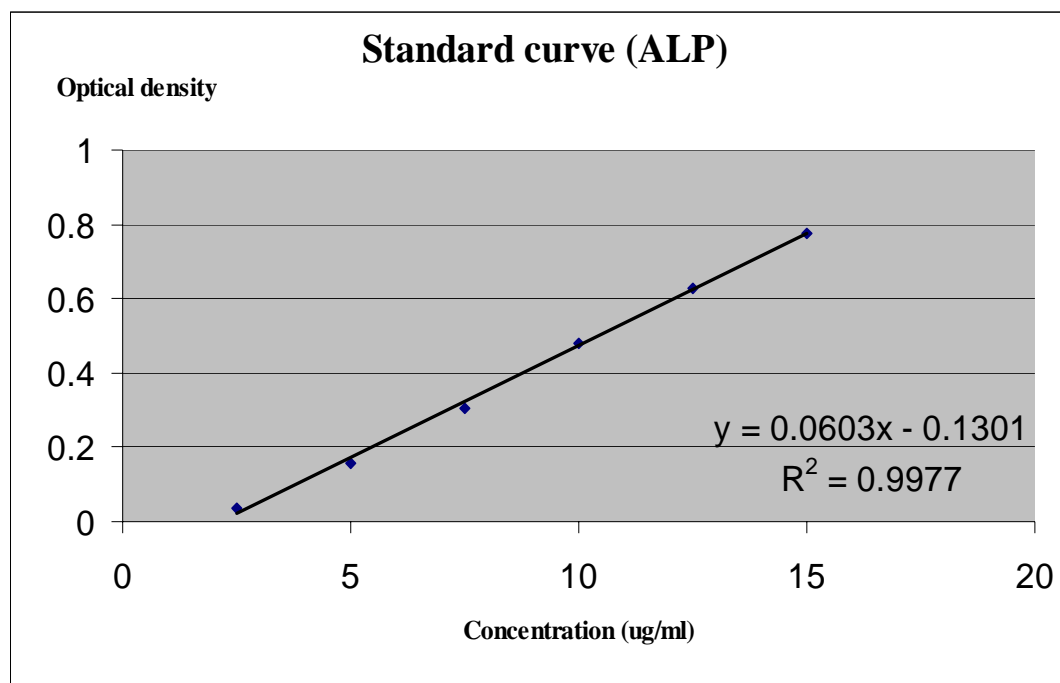


Figure 37 Standard curve of p-nitrophenol on day 26 (1st experiment)

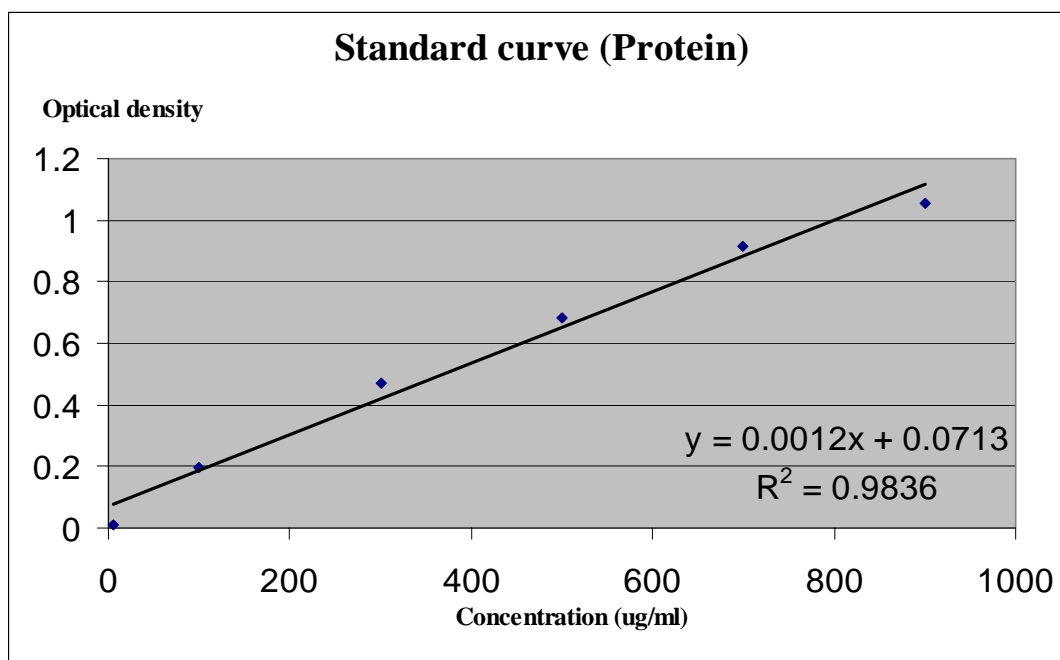


Figure 38 Standard curve of total protein on day 26 (1st experiment)

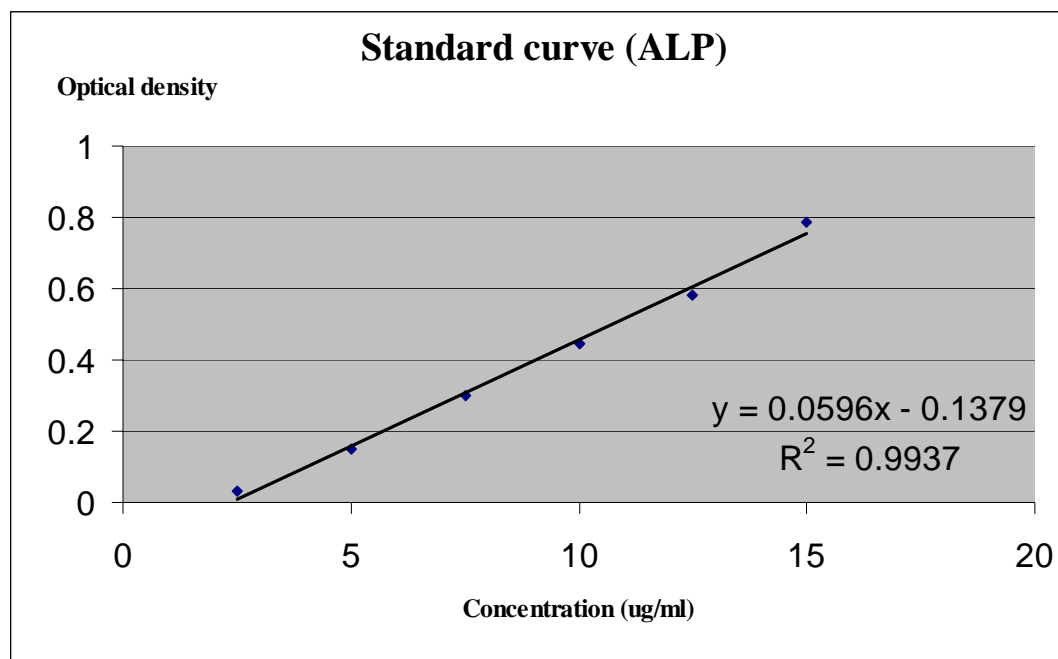


Figure 39 Standard curve of p-nitrophenol on day 4 and 6 (2nd experiment)

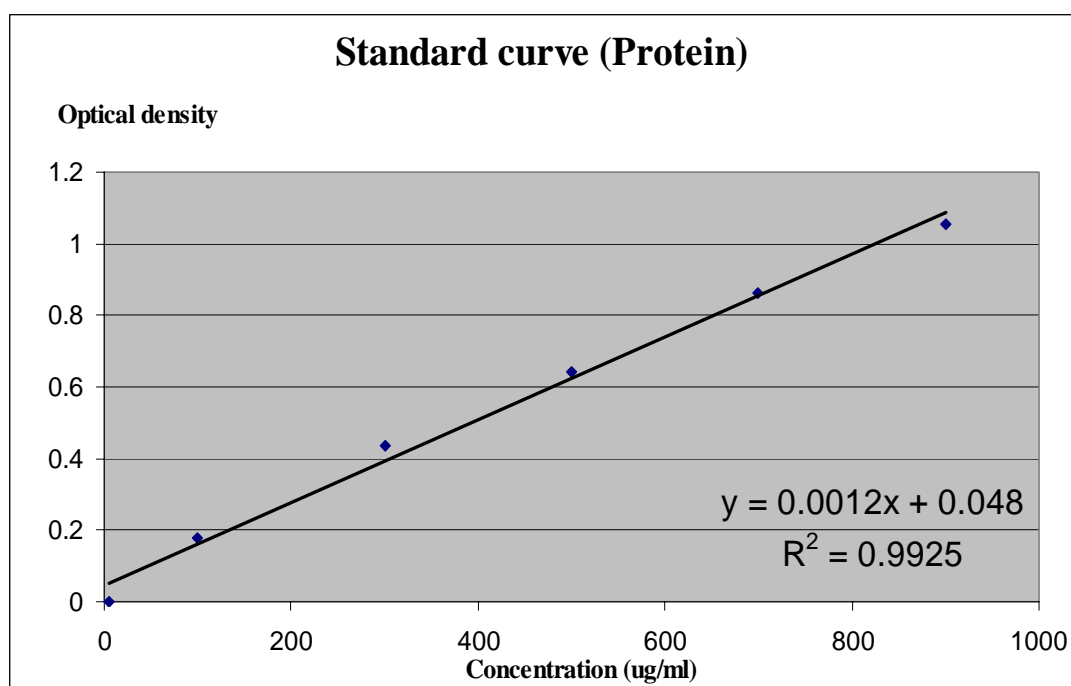


Figure 40 Standard curve of total protein on day 4 and 6 (2nd experiment)

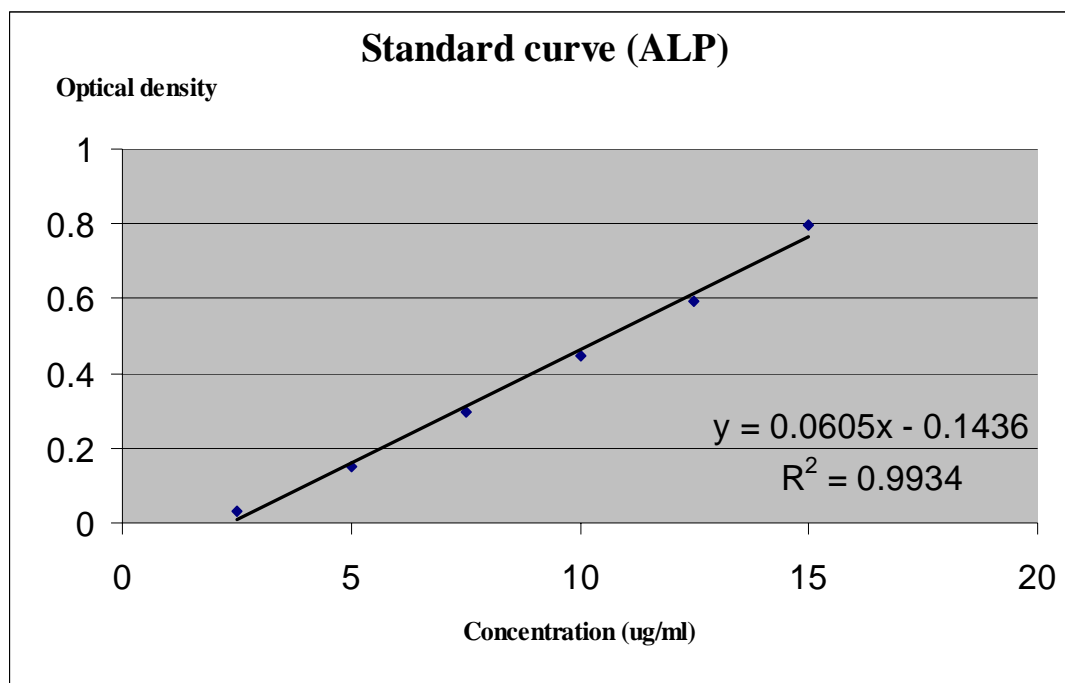


Figure 41 Standard curve of p-nitrophenol on day 10 and 14 (2nd experiment)

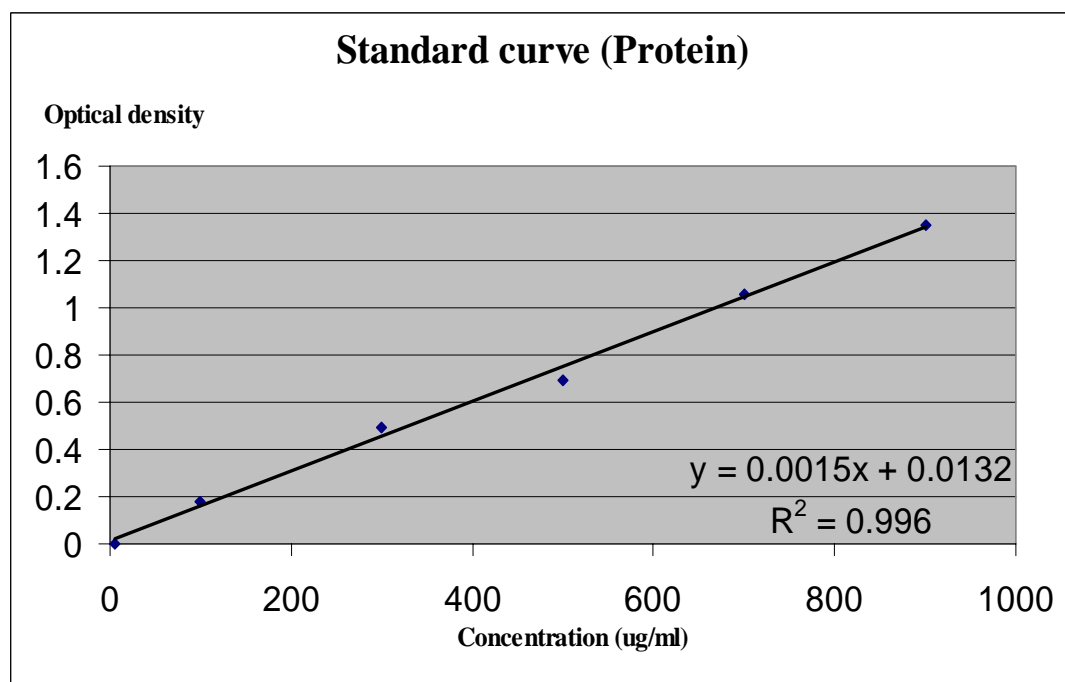


Figure 42 Standard curve of total protein on day 10 and 14 (2nd experiment)

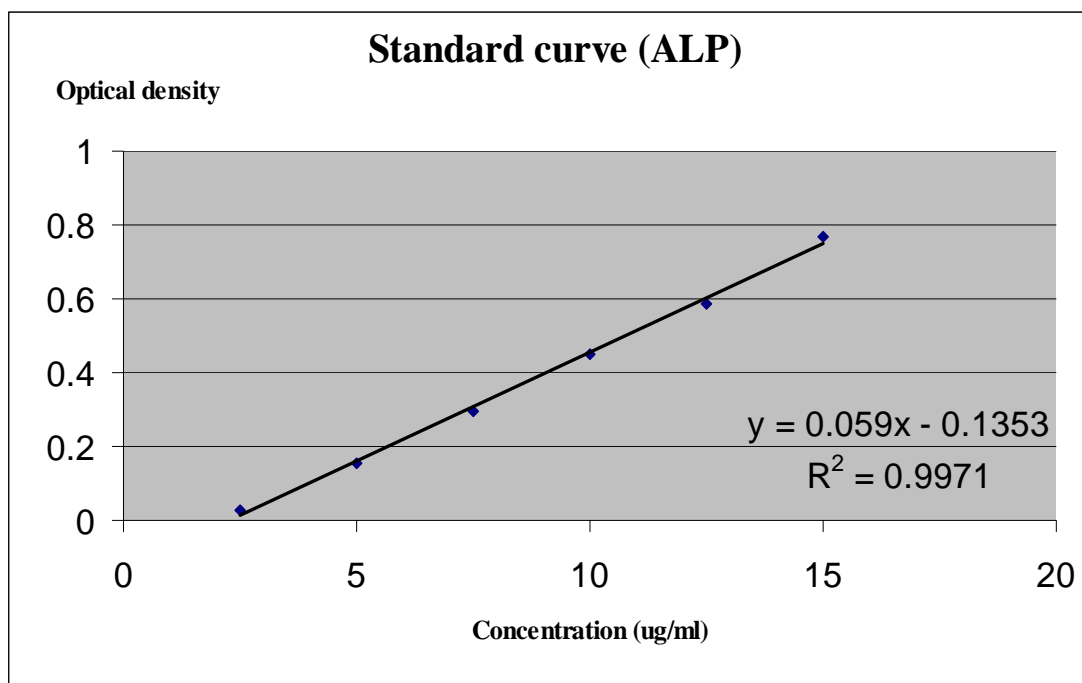


Figure 43 Standard curve of p-nitrophenol on day 18 and 22 (2nd experiment)

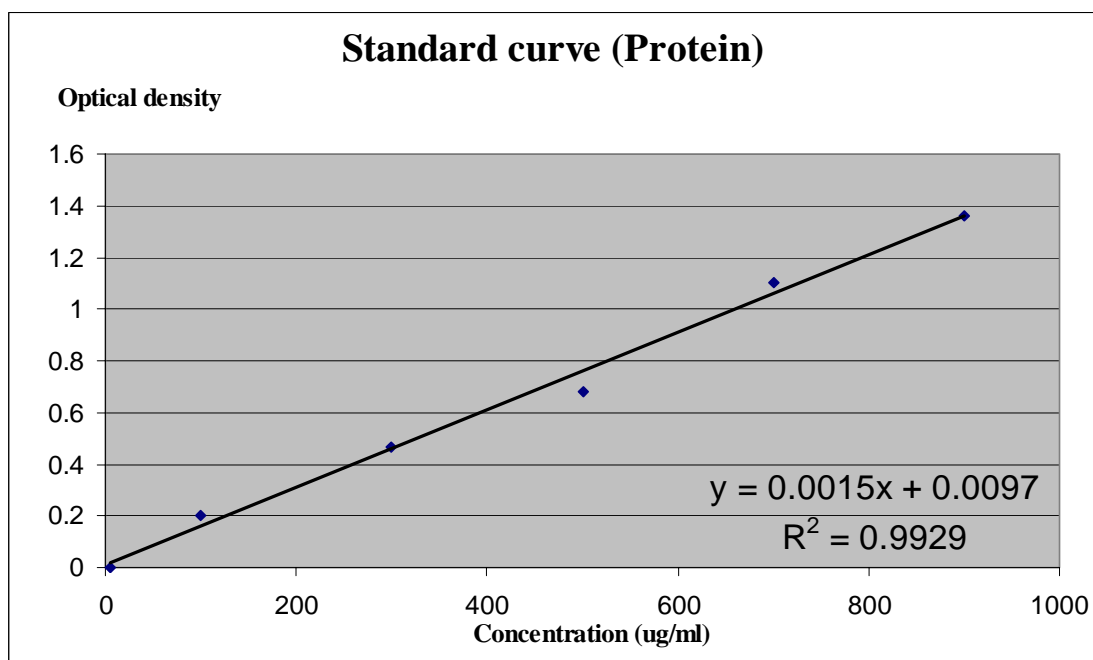


Figure 44 Standard curve of total protein on day 18 and 22 (2nd experiment)

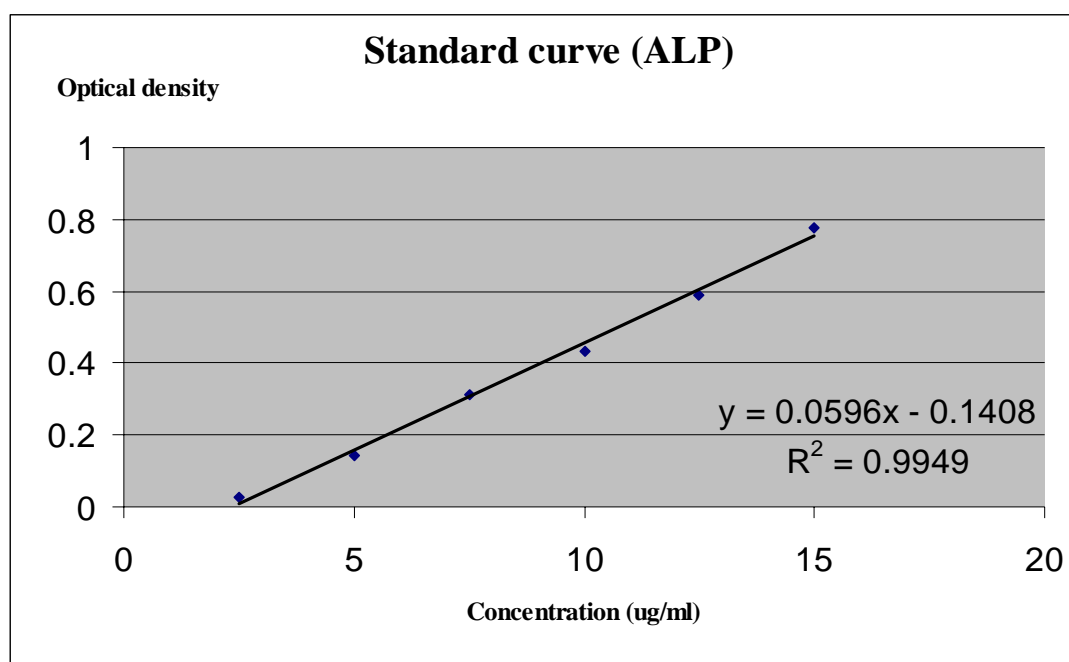


Figure 45 Standard curve of p-nitrophenol on day 26 (2nd experiment)

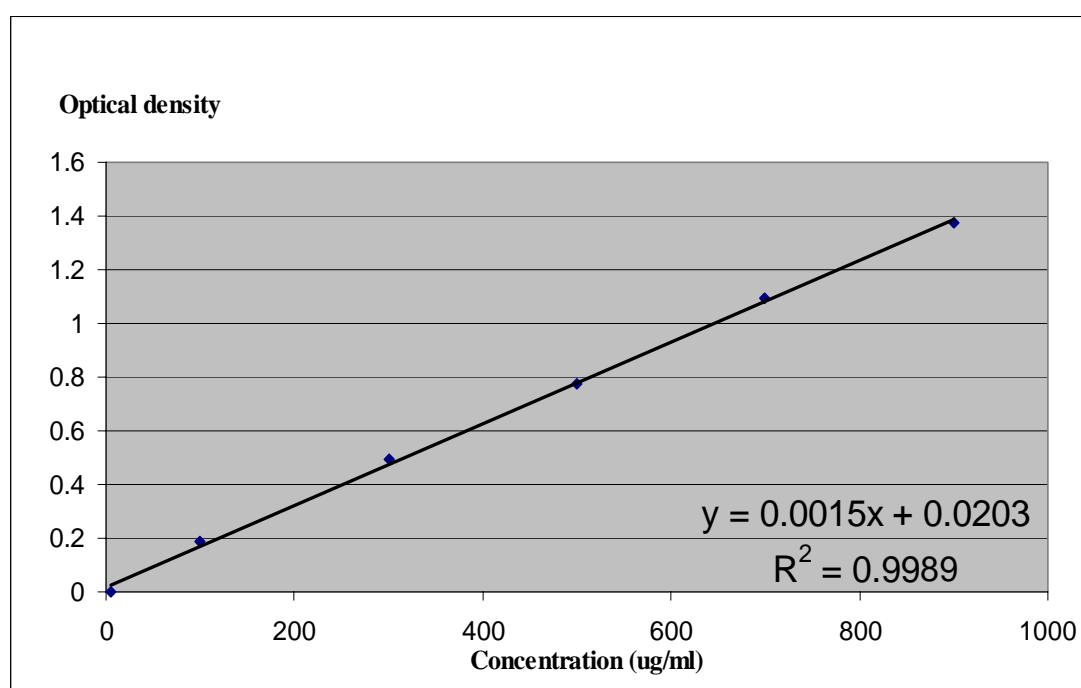


Figure 46 Standard curve of total protein on day 26 (2nd experiment)

90 : 10



70 : 30



50 : 50

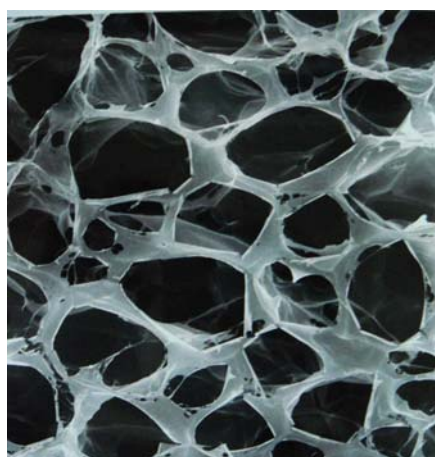


Figure 47 SEM images of chitosan-collagen scaffolds with different ratio between chitosan and collagen. A) 90 : 10 B) 70 : 30

BIOGRAPHY

NAME	Wiroj Suphasiriroj
DATE OF BIRTH	5 June 1979
PLACE OF BIRTH	Bangkok, Thailand
INSTITUTIONS ATTENDED	<p>Mahidol University, 1996-2002:</p> <p style="padding-left: 40px;">Doctor of Dental Surgery</p> <p>Mahidol University, 2004-2005:</p> <p style="padding-left: 40px;">Graduate Diploma in Clinical Science (Periodontics)</p> <p>Mahidol University, 2005-2007:</p> <p style="padding-left: 40px;">Master of Science (Periodontics)</p>
RESEARCH GRANT	Mahidol University Grant
HOME ADDRESS	<p>774 Sukhumvit Soi 50 Road, Klong-Toey,</p> <p>Bangkok, Thailand.</p>